Universidad de Valladolid

Escuela de Doctorado Universidad de Valladolid

PROGRAMA DE DOCTORADO EN INVESTIGACIÓN BIOMÉDICA

TESIS DOCTORAL:

The IRE1α-XBP1 Branch of the Unfolded Protein Response Underpins Cytokine Induction and Viral Replication in SARS-CoV-2 Infection

Presentada por
Jose Javier Fernández Rodríguez
para optar al grado de Doctor
por la Universidad de Valladolid

Dirigida por:
Dr. Mariano Sánchez Crespo
Dra. Mª Nieves Fernández García

A mi madre y abuelas

"If we knew what we were doing, it wouldn't be called research"

- A. Einstein.

Abbreviations

- 2-DG: 2-deoxyglucose
- ACE2: Angiotensin-converting enzyme 2
- ACSS2: Acyl-CoA synthetase short chain family member 2
- Ad-hACE2: Adenovirus-human ACE2
- Ad-empty: Adenovirus-empty
- ARDS: Acute respiratory distress syndrome
- ASNS: Asparagine synthetase glutamine-hydrolyzing
- ATF: Activating transcription factor
- BAAs: Bronchiolo-alveolar aspirates
- BiP: Binding immunoglobulin protein
- cDCs: Conventional dendritic cells
- chIP: Chromatin immunoprecipitation
- CHOP: CCAAT/enhancer-binding protein-homologous protein
- CP: Convalescent plasma
- CPE: Cytopathic effect
- CS: Cytokine storm
- CTH: Cystathionine γ-lyase
- DAMPs: Damage associated molecular patterns
- DMV: Double membrane vesicles
- Dpi: Days post-infection
- dsRNA: Double-stranded RNA
- E: Envelope
- EDEM1: ER degradation enhancing α-mannosidase like protein 1
- ETC: Electron transport chain
- eIF2α: Eukaryotic translation initiation factor 2α
- ER: Endoplasmic reticulum
- ERdj4: ER dnaJ family protein
- ERGIC: ER-to-golgi intermediate compartment
- FBS: Fetal bovine serum
- GADD34: Growth arrest and DNA damage-inducible protein
- GO: Gene ontology
- HERPUD1: Homocysteine inducible ER protein with ubiquitin like domain 1
- HK2: Hexokinase II
- Hpi: Hours post-infection
- Hpt: Hours post-transfection
- H&E: Haematoxylin and eosin
- Hspa5: Heat shock protein A5
- ICU: Intensive care unit
- IFN: Interferon
- IRE1: Inositol-requiring enzyme 1
- IRF: Interferon regulatory factor.
- IRG1: cis-aconitate dehydrogenase
- ISGs: Interferon stimulated genes
- M: Membrane
- MA-SARS-CoV-2: Mouse adapted-SARS-CoV-2 strain
- MDA5: Melanoma differentiation-associated protein 5
- MDDCs: Monocyte-derived dendritic cells
- MDH2: Malate dehydrogenase 2
- MHV: Mouse hepatitis virus
- MxA: Myxovirus resistance gene A
- N: Nucleocapsid
- nAbs: Neutralizing antibodies
- NSPs: Non-structural proteins
- ORF: Open reading frame
- OXPHOs: Oxidative phosphorylation
- PAMPs: Pathogen associated molecular patterns.
- pDCs: Plasmacytoid dendritic cells
- PDK4: Pyruvate dehydrogenase kinase IV
- PERK: Protein kinase RNA-like ER kinase
- PFU: Plaque forming units
- PRRs: Pattern recognition receptors
- RdRp: RNA-dependent RNA polymerase
- RIDD: Regulated IRE1-dependent decay
- RIG-I: Retinoic acid-inducible gene I
- RLR: RIG-I like receptors (RLRs)
- RTC: Replication-transcription complex
- S1/2P: Site -1/2 Protease
- S: Spike
- SARS-CoV-2: Severe acute respiratory syndrome coronavirus-2
- SDHA: Succinate dehydrogenase A
- SIR1: Sigma receptor 1
- sg-mRNA: Subgenomic-mRNA
- SLC25A11: 2-oxoglutarate-malate transporter
- ssRNA: Single-stranded RNA
- STAT: Signal transducer and activator of transcription
- TCA: Tricarboxylic acid cycle
- sXBP1: Spliced XBP1
- TLRs: Toll-like receptors
- TMPRSS2: Transmembrane serine protease 2
- UPR: Unfolded protein response
- uXBP1: Unspliced XBP1
- VOCs: Variants of concern
- WT: Wild type

Abstract

The endoplasmic reticulum (ER) is an intracellular organelle involved, among other functions, in the synthesis and secretion of proteins. These processes are tightly regulated to control the quality of protein secretion. However, excessive protein load can perturb ER homeostasis leading to accumulation of misfolded proteins resulting in the activation of the unfolded protein response (UPR). Viral infections including SARS-CoV-2, as a positive single stranded RNA (ssRNA) virus, might cause ER stress because of the exploitation of the host machinery for viral replication. Endosomal Toll-like receptors (TLR)7 and TLR8 sense ssRNA associated SARS-CoV-2 virus. Recognition of ssRNA by its cognate receptors drives transcription and translation of pro-inflammatory genes, which after release into the systemic circulation, may team up with the UPR to ignite the cytokine storm (CS) or viral sepsis observed in the severe forms of the disease. Our approach aimed to understand the connection between SARS-CoV-2 infection and the UPR, focusing on the role of the transcription factor spliced XBP1 in viral replication and cytokine overproduction. The study encompasses: i) the analysis of nasopharyngeal swabs samples and bronchiolo-alveolar aspirates of patients undergoing mechanical ventilation due to severe pneumonia hospitalized at the Internal Care Unit (ICU), ii) experiments in monocyte derived dendritic cells (MDDCs) stimulated via TLR7/8, iii) studies *in vivo* infection with SARS-CoV-2, and iv) the impact of the UPR modulation during the replication cycle in human epithelial cells infected with different variants of concern (VOCs). Taken collectively, the study has disclosed that the IRE1α-XBP1 branch of the UPR is a host-dependent factor involved in SARS-CoV-2 pathogenesis.

Index

I. Preface

During predoctoral studies, the initial project focused on mitochondrial function, since immunometabolism reached central stage in the function of the innate immune system. Immune cells metabolize a variety of carbon substrates, which allows proper adaptation to changing microenvironments, while the competition for nutrients and the adaptive advantage to change fuel sources control the states of quiescence and activation of immune cells [1, 2]. These metabolic adaptations are devoted to perform various functional outputs, where mitochondria play a key role at the core of signaling, transcription and epigenetics [3]. This explains why mitochondria, by producing metabolic intermediates have emerged as central regulators of innate sensing and gave room to new approaches for the development of therapies directed to manipulate metabolic pathways in different diseases [4, 5].

The rationale to study oxidative phosphorylation (OXPHOs) in monocyte-derived dendritic cells (MDDCs) stimulated by the fungal surrogate zymosan, stemmed from previous results where we have shown a metabolic switch characterized by concomitant increase of oxygen consumption and extracellular acidification [6]. In line with this, the main goal of the project focused on the function of mitochondria in cytokine induction by MDDCs.

The application of mass spectrometry assays disclosed a metabolic reprogramming following the activation of MDDCs by pathogen-associated molecular patterns (PAMPs) characterized by decreased levels of pyruvate, citrate, itaconate, and α-ketoglutarate, while oxaloacetate, succinate, lactate, oxygen consumption and pyruvate dehydrogenase activity showed robust increases (**Figure 1**).

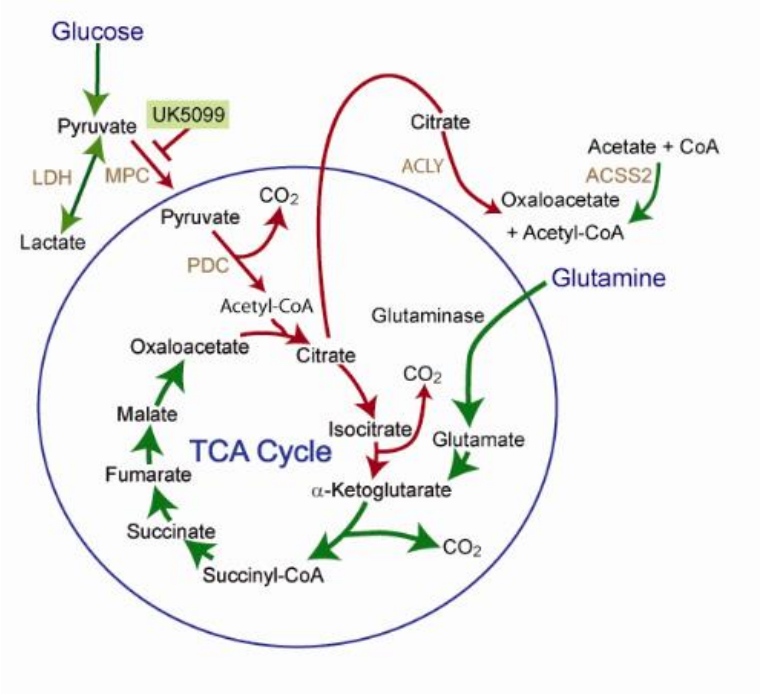

Figure 1. Energetic metabolic reprogramming in MDDCs stimulated with the fungal pattern zymosan. Intracellular metabolites downregulated are shown in red. Upregulated metabolites are shown in green. Enzymes suitable for pharmacological modulation are shown in beige. MPC indicates mitochondrial pyruvate carrier (MPC). ACLY stands for ATP citrate lyase. ACSS2 means acyl-CoA synthetase short chain family member 2. PDC, pyruvate dehydrogenase complex.

Acetyl CoA plays a key role in the TCA cycle and exerts other functions, such as the opening of chromatin structure through histone acetylation and the biosynthesis of fatty acids and the lipid mediator platelet activating factor ((PAF; 1-O-hexadecyl-2-acetyl-*sn*-glycero-3-phosphocholine) (**Figure 2**).

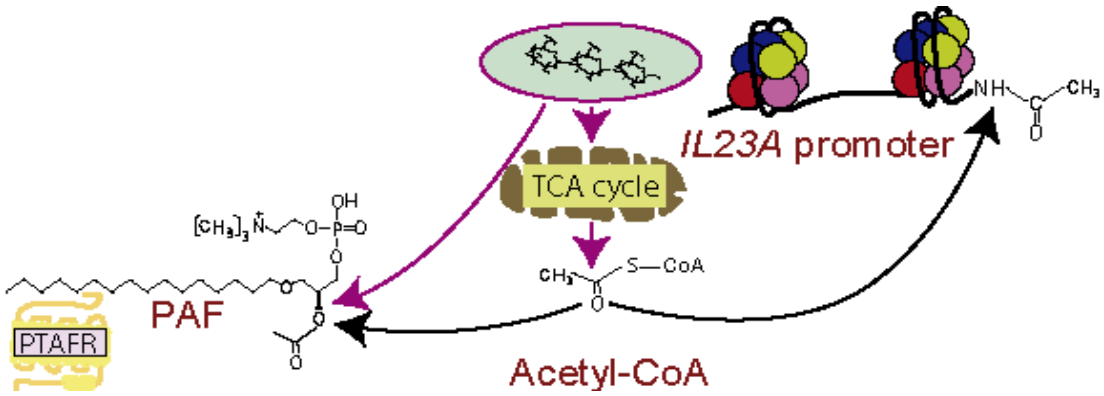

Figure 2. Schematic representation of acetyl-CoA functions disclosing the importance of this metabolite as a hub of the metabolic-epigenomic axis during the phagocytosis of fungal patterns by MDDCs. Zymosan (green) promotes TCA cycle intermediary metabolites rewiring. Acetyl-CoA allows the opening of chromatin structure through histone acetylation and is a substrate for the biosynthesis of PAF.

Mitochondrial pyruvate and the processing of acetate through acyl-CoA synthetase short chain family member 2 (ACSS2) are main sources of acetyl-CoA. Based on this, we addressed the correlation of the fluxes of these metabolites with the cytokine signature, epigenetic modifications, and lipogenesis. Special attention was paid to the regulation of the expression of the cytokines IL-23 and IL-10, which imprint the polarization of T helper lymphocytes in the TH17 and Treg phenotypes. We found that expression of *IL10* and *IL23A* (the gene encoding the p19 chain of IL-23) depended on pyruvate dehydrogenase activity. Mechanistically, pyruvate reinforced histone H3 acetylation, and acetate rescued the effect of mitochondrial pyruvate carrier inhibition, most likely because it is a substrate for the acetyl-CoA producing enzyme ACSS2. Mice lacking the receptor of the lipid mediator PAF showed a reduced production of IL-10 and IL-23 that is explained by the requirement of acetyl-CoA for PAF biosynthesis and its ensuing autocrine function. Therefore, acetyl-CoA intertwines fatty acid remodeling of glycerophospholipids and

energetic metabolism with the process of cytokine induction. These results were published in *Cell Reports*.

Due to the global COVID-19 pandemic and the expertise of our laboratory in innate immunity and inflammation, we had a unique chance to apply our expertise to the major public health challenge caused by SARS-CoV-2 infection. Recent studies disclosed that the activation of the unfolded protein response (UPR) plays a major role in the modulation of cytokine production and inflammatory response [7, 8]. The IRE1α-XBP1 system has been found to be a robust enhancer of the production of the proinflammatory cytokine IL-23 during fungal infections, as reported [6]. This background paved the way to address the pathophysiological mechanisms underlying the clinical setting of fever, immunosuppression, and cytokine storm (CS) that aggravates the clinical course of COVID-19 ailment [9]. Our working hypothesis was that sXBP1 could be involved in the pathogenesis of the severe pneumonia and the multiorgan failure characteristic of the severe forms of COVID-19 disease. For that purpose, we adapted a portion of our work to address the role of the UPR in SARS-CoV-2 infection, with special emphasis in the role of the IRE1α-XBP1 arm in the induction of the cytokine storm.

II. Introduction

The outbreak of COVID-19 pandemic

Severe acute respiratory syndrome coronavirus-2 (SARS-CoV-2) causes critical and often fatal pneumonia in numerous patients. It was declared COVID-19 pandemic by WHO in March 2020 and ever since it was associated with a widespread morbidity and mortality worldwide. Globalization has increased the likelihood of encounters with emerging and re-emerging RNA viruses. Likewise, SARS-CoV-2 caused more than 650 million cases and 6.6 million deaths in the last three years. Although vaccines are the most effective treatment to prevent the spread of infections, the propensity of mutation of SARS-CoV-2 is a challenge to immunity, even among individuals who have been vaccinated or underwent previous infection [10, 11].

The genomic structure of the ancestral SARS-CoV-2 virus (**Figure 3**) and its subsequent mutations have resulted in the variants of concern (VOCs) across time [12]. The most important VOCs reported to date, are wild type (WT) and (D614G) [13], α (B.1.1.7), β (B.1.351), γ (P.1), δ (B.1.617.2) and o (B.1.1.529). Furthermore, SARS-CoV-2 had a remarkably evolutionary plasticity of mutation and recombination [14, 15]. The new emerging VOCs of SARS-CoV-2 stand more transmissible and less pathogenic, which makes the majority of infected patients asymptomatic or showing mild symptoms, although some patients still develop severe disease [16]. The rate of developing severe pneumonia varies with age [17] and remains a serious threat for patients suffering from comorbidities and immunosuppression [18].

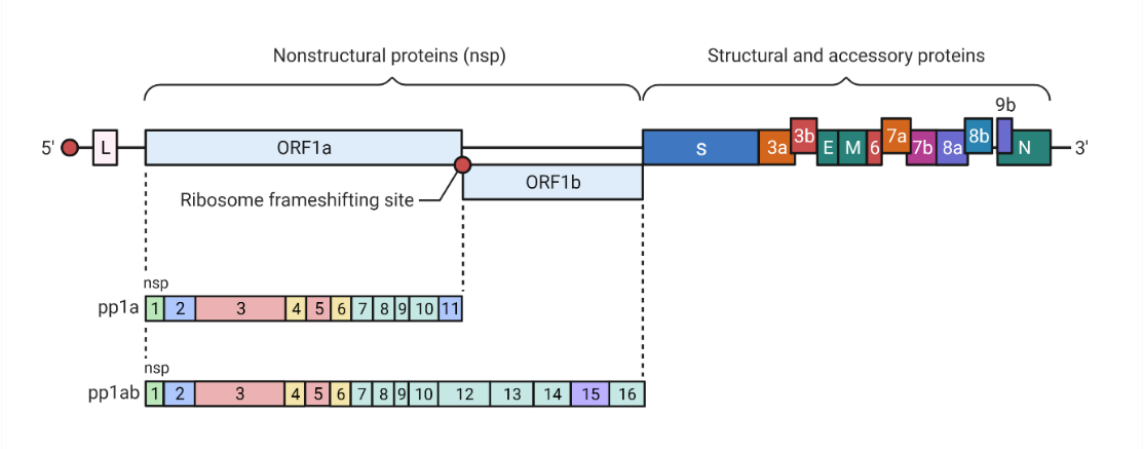

Figure 3. Coronavirus genome. Coronavirus genome consists of a positive single-strand RNA chain flanked by 3′ and 5′ untranslated regions spanning a range of 26 to 32 kilobases. The 2019 coronavirus genome contains 14 open reading frames (ORFs) encoding 27 proteins, distributed in four structural proteins: spike (S), membrane (M), envelope (E) and nucleocapsid (N). Eight accessory proteins (3a, 3b, p6, 7a, 7b, 8b, 9b and ORF14) at the 3' terminus of the genome. The first two ORFs encode non-structural proteins (NSPs). They comprised 15 NSPs, which are NSP1-NSP10 and NSP12-16, respectively [19].

SARS-CoV-2 displays several immune evasion mechanisms, not only to counteract antiviral response, but also to imbalance the cellular immune response by the overproduction of cytokines, which results in viral sepsis as a detrimental hallmark of COVID-19 pneumonia [20].

SARS-CoV-2 strategies for efficient viral replication and immune evasion

SARS-CoV-2 virus primarily infects lung cells by interaction with the angiotensin-converting enzyme (ACE)2 receptor. The ACE2 protein is most abundant in lung alveolar epithelial cells, small intestine enterocytes and endothelial cells [21]. Other receptors could also mediate viral entry, including CD147, neuropilin-1, AXL, DC-SIGN and FcγR after forming immune complexes with antibodies [22-25]. After ACE2 binding, the S protein of SARS-CoV-2 promotes host membrane fusion and proteolytic cleavage with the cooperation of host proteases such as furin, the cellular transmembrane serine protease (TMPRSS)2 and cathepsins. This process is followed by the release of viral RNA into the host cytoplasm, where viral RNA uses the host machinery to replicate and assemble new viral particles [26, 27]. The interaction of coronavirus with the host creates an optimal environment for replication using different strategies to counter host's antiviral response.

During the invasion phase, coronavirus infection displays high viral replication, followed by an inflammatory response of the host directed to counter disease progression. SARS-CoV-2 proliferates, without any associated specific symptoms, mainly in type II pneumocytes, ciliated epithelium of nasopharynx, upper respiratory tract, and endothelial cells. Only certain types of cells maintain an effective viral replication and release of virions. The vast majority of those cells locate in the respiratory tract [28, 29].

Upon disease progression, virus induce cell damage and release of PAMPs as well as damage-associated molecular patterns (DAMPs), which may activate neighbour epithelial cells and macrophages [30]. The presence of viral components in other cell types can be the result of phagocytic processes, abortive infections, or binding of viral antigens to cell surface receptors [31]. Although ACE2 and TMPRSS2 expression were higher in epithelial

cells from human nasal exudates of SARS-CoV-2 patients, viral transcripts of SARS-CoV-2 have also been found in neutrophiles and macrophages [32].

Plasmacytoid dendritic cells (pDCs) infiltrating the lung sense SARS-CoV-2 and activate macrophages through the production of IFN-I [33]. This drives an inflammatory milieu optimal to produce cytokines and chemokines by macrophages and paves the way for the attraction of T cells to the niche of infection, which enhance the inflammatory response by recruiting IFN-γ production [34]. Although the primary goal of these responses is the blockade of viral proliferation hyperactivation of innate immune cells could induce an unintended CS that increases disease severity.

Endoplasmic reticulum as a central hub of coronavirus replication

Coronavirus are enveloped virus with positive-sense, non-segmented, single-stranded RNA genome, the replication of which takes place in close association with intracellular membrane structures mainly provided by the ER [35]. The formation of viral replication-transcription complexes (RTC) and double membrane vesicles (DMVs), the massive production and posttranslational modifications of viral proteins, as well as virion budding during the replication life cycle (**Figure 4**), overload the ER folding capacity, assembly, and secretion of proteins triggering ER stress response.

Since only properly folded proteins should exit from the ER to maintain homeostasis, cells arrange a response directed to retain and degrade defective proteins. This involves an intracellular signaling pathway termed the UPR [36-38]. The UPR includes a down regulation of global protein synthesis, the degradation of some proteins, and the transcriptional induction of specific genes associated with the activity of its three branches. Various studies have documented the activation of one or more of the three arms of the UPR during coronavirus replication [39].

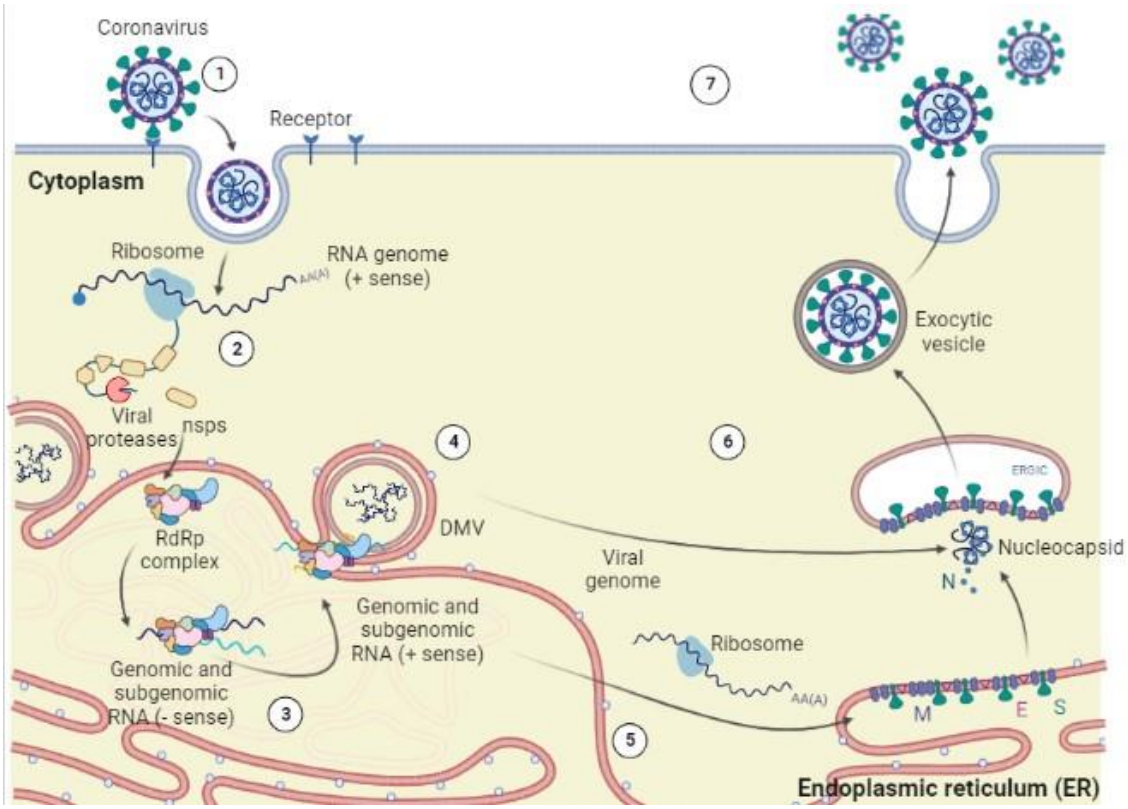

Figure 4. Coronavirus life cycle. Coronavirus infection begins when the viral S protein attaches to its cognate host receptor. This allows virus entry into the host cell by endocytosis or direct fusion of the viral envelop with the cell membrane. (1) Process of SARS-CoV-2 virus entry and uncoating. (2) Translation of the viral positive-sense RNA. (3) Viral genomic RNA replication and the transcription of subgenomic mRNAs (sg mRNAs). (4) Virus-induced massive rearrangement of the intracellular membrane network for the biogenesis of viral replication organelles consisting of characteristic perinuclear DMVs create a protective micro-environment for sg mRNAs encoding structural and accessory proteins. (5) Coronavirus replication occurs within DMVs and transmembrane structural proteins (S, M and E) and accessory proteins are synthesized in the ER. (6) Translated structural proteins translocate into ER membranes and transit through the ER-Golgi intermediary compartment (ERGIC), where they interact with the viral nucleocapside (N) protein to encapsidate newly produced genomic RNA. (7) New viral particles result in budding into the lumen of secretory vesicular compartments which are transported to the ERGIC for assembly and exported through secretory pathway in smooth-wall vesicles, which ultimately fuse with the plasma membrane to release the mature virus.

Replication and transcription of the coronavirus genome occurs within the RTC anchored in rearranged internal host membranes. These membranes act as a framework for viral genome replication by localizing and concentrating the necessary factors, as well as for providing protection from host cell defences. In coronavirus, the host membranes required for the RTC formation emerge from the ER membranes. The hallmark membrane rearrangements observed in coronavirus are DMVs, so named for their distinctive double-lipid bilayer structure observed in electron micrographs. A recent report indicates that such DMVs are the primary site of RNA replication [40]. Such a high demand for host membranes formation represents an additional burden on the ER that contributes to trigger ER stress.

UPR activation is associated with certain coronaviral proteins that have previously been investigated [41-43]. Recent reports demonstrated that expression of the SARS-CoV-2 S or ORF8 proteins is sufficient to induce the three major signalling pathways of the UPR [44]. In contrast, E protein of SARS-CoV has been reported to protect from ER stress [45]. Coronavirus proteins, especially the S protein, are modified by a variety of post-translational modifications that affect viral replication and pathogenesis [46]. Translated structural proteins S, M and E translocate into the ER membranes and transit through the ERGIC, where they interact with the N protein-encapsidated newly produced genomic RNA. This results in budding into the lumen of secretory vesicular compartments. Finally, virions are secreted from infected cells by exocytosis. This virion budding-related ER membrane depletion overloads the folding capacity of the ER and, therefore, might be another mechanism whereby SARS-CoV-2 trigger ER stress and the UPR.

Given the various mechanisms involved in viral proliferation that impinge on the ER function, it seems likely that SARS-CoV-2 might divert the UPR from its purported role devoted to restoring ER homeostasis and take advantage of it for its own benefit.

The unfolded protein response

The accumulation of misfolded proteins activates three sensors of the UPR. The response starts by the detachment of the chaperone binding immunoglobulin protein (BiP), also called GRP78 and heat shock protein A5 (HSPA5), from the three transmembrane ER stress sensors: Inositol-requiring enzyme (IRE) 1α, protein kinase RNA-like ER kinase (PERK) and activating transcription factor (ATF) 6. Each sensor initiates an arm of the UPR [37, 47]. In case these responses fail to restore homeostasis, autophagy, apoptosis, and dysregulated mitochondrial bioenergetics may occur [48-50]. Mechanistically, when misfolded proteins accumulate in the ER lumen, BiP is detached from the luminal domains of the three sensors where it is bound. This allows the formation of homodimers by PERK and IRE1 and full length ATF6 translocate from the ER to the Golgi.

ATF6 is cleaved by site-1 protease (S1P) and site-2 protease (S2P). This releases a cytosolic fragment (ATF6p50), which then transits to the nucleus and contributes to restore homeostasis. PERK phosphorylates the α-subunit of eukaryotic translation initiation factor 2A (eIF2α), resulting in a global reduction of protein synthesis, while the translation of a few key proteins is maintained, including, ATF4, which induces expression of the transcription factor C/EBP homologous protein (CHOP), as well as genes involved in redox homeostasis, amino acid metabolism, protein synthesis, autophagy, and apoptosis. Protein synthesis is restored when eIF2α is dephosphorylated by a negative feedback loop of growth arrest and DNA damage-inducible protein (GADD34). IRE1 auto-phosphorylates to switch on its RNase activity, inducing a process known as regulated IRE1-dependent decay (RIDD), in which IRE1 cleaves and leads to the selective degradation of a small set of mRNAs and miRNAs. IRE1 also excises a short 26-nucleotide intron from the mRNA encoding transcription factor X-box binding protein 1 (uXBP1), generating the spliced

XBP1 (sXBP1) mRNA, which is ultimately translated into the transcription factor sXBP1 that, like ATF4 and ATF6 upregulates genes involved in multiple signaling pathways. (**Figure 5**).

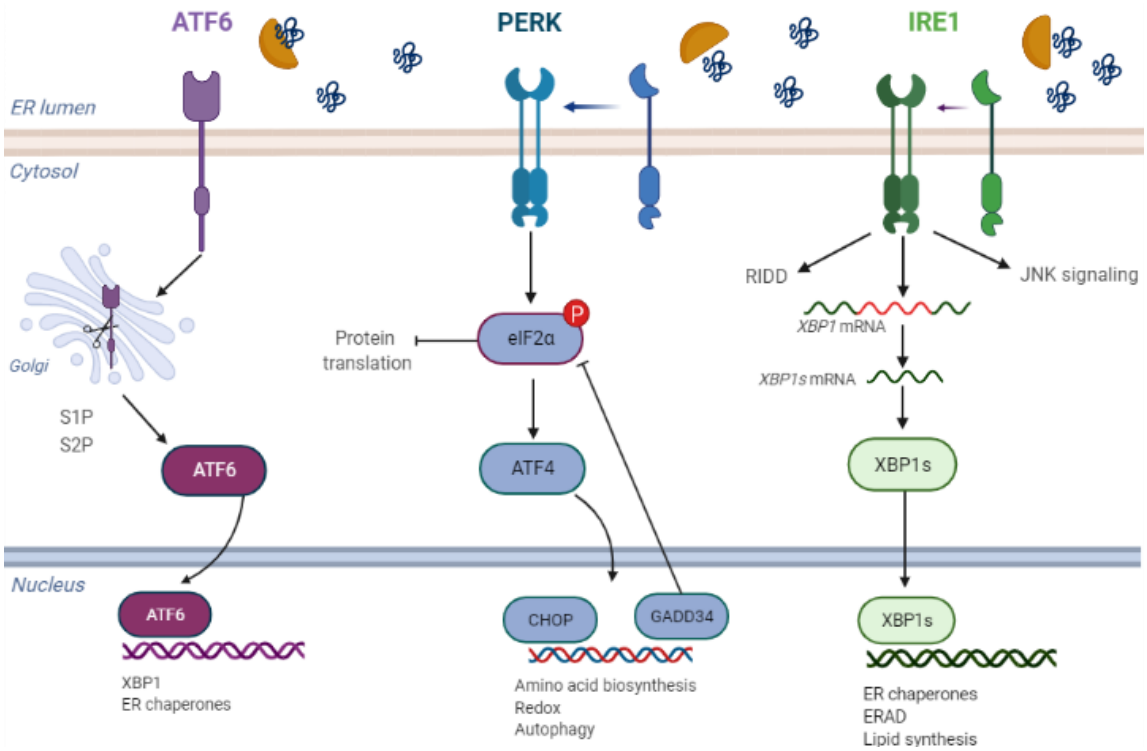

Figure 5. The three branches of the UPR. (Left) ATF6, (middle) PERK and (right) IRE1 arms. Upon ER stress, the ATF6 branch is activated when ATF6 translocate from the ER to the Golgi, where it is cleaved. After cleavage, the amino-terminus of ATF6 (ATF6-Nt) translocate to the nucleus to upregulate ER chaperones and XBP1. PERK oligomerises and auto-phosphorylates. Activated PERK phosphorylates the α-subunit of eIF2 resulting in a general shutdown of protein synthesis. However, translation of ATF4 is increased under these conditions leading to the induction of its target genes CHOP and GADD34. Finally, a negative feedback loop of GADD34 dephosphorylates eIF2α when homeostasis is recovered. Activated IRE1α removes a 26-nt intron from uXBP1 mRNA leading to a translational reading frame shift and a longer protein sXBP1, which is an active transcription factor that upregulates ER chaperones, endoplasmic-reticulum-associated protein degradation (ERAD) pathway and lipid biosynthesis.

The IRE1α-XBP1 branch of the UPR

The IRE1α-XBP1 branch is the most conserved one and is activated by direct interaction of misfolded proteins with IRE1α, while BiP acts as a sensitive adjustor for stressors [51, 52]. Upon ER stress, IRE1α endoribonuclease domain excides a 26-nucleotide fragment of the *uXBP1* immature mRNA to allow the translation of the potent transcription factor sXBP1 [53].

sXBP1 promotes rapid expression of chaperones, glycosylases, quality control proteins, and ERAD components. In addition, sXBP1 regulates the adaptative UPR target genes to restore homeostasis, sXBP1 also affects host responses to pathogens since it behaves as a transcription factor involved in the regulation of inflammatory proteins, including prostaglandin-producing enzymes and cytokines, as well as controlling cell viability during ER stress [54, 55], the ubiquitin-like modifier ISG15, and the cytokines IL-6, IL-23, and TNFα [6, 56, 57]. Although the goal of the UPR is alleviating ER-stress, the IRE1α-XBP1 branch contributes to the pathogenesis of many ailments, i.e., cancer, infections, and autoimmune diseases [58-60].

When ER homeostasis is recovered because of UPR activity, UPR branches promote the degradation of misfolded proteins and a global reduction of protein synthesis and translation through ERAD. Under conditions of excessive ER stress and independently of XBP1, hyperactivated IRE1α can also cleave a specific subset of mRNAs connected to the translocon of the ER to inhibit further influx of proteins into the ER. These mRNAs encode proteins involved in ER homeostasis, cell-to-cell contact, antigen processing and in addition to their nearby location, the mRNAs of which contains an expression of cleavage sites with a consensus sequence (CUGCAG) and a secondary structure mimicking the IRE1 recognition stem-loop of XBP1 mRNA by the process termed RIDD.

Innate immune sensing of viral components of SARS-CoV-2 by TLRs

Innate immunity is the first line of antiviral defence and is essential to control virus infections. SARS-CoV-2 derived molecules can bind Toll like receptors (TLRs) and activate the innate immune response, wherein the IFN system is crucial for controlling viral infection. Innate immune response often contributes to viral clearance and disease resolution, while dysregulated immune signaling may lead to the detrimental production of proinflammatory cytokines and chemokines driving immunopathology.

Immune cells are characterized by their array of pattern recognition receptors (PRRs). They are located on the cell membrane, inside the cell and even secreted. PRRs recognize PAMPs and DAMPs and activate inflammatory cascades to produce IFNs and other cytokines [61]. TLRs, retinoic acid-inducible gene I (RIG-I)-like receptors (RLRs) and melanoma differentiation-associated protein 5 (MDA5) recognize viral particles and non-self RNA molecules [62-64].

When viruses invade the host, cell surface TLRs recognise viral components to induce immune response. *In silico* studies on SARS-CoV-2 glycoproteins disclosed its ability to bind ACE2 receptor as well as cell surface TLRs [65]. The recognition of the SARS-CoV-2 S protein by TLR4 increased ACE2 expression, thus enhancing viral entry, aberrant signaling, and hyperinflammation [66]. Other structural proteins such as, S, E and N protein, triggers TLR2 and upregulate the production of proinflammatory cytokines [67-70].

As regards intracellular recognition of PAMPs, the tandem TLR7/8 detects viral singled-stranded RNA (ssRNA), TLR3 detects viral double-stranded RNA (dsRNA), while TLR9 detects viral deoxyribonucleic acid [71]. The plausible involvement of the tandem TLR7/8 in COVID-19 disease stems from its ability to bind positive-sense, ssRNA like

SARS-CoV-2 RNA, and from clinical reports showing that loss-of-function variants in X-chromosomal TLR7 driving impaired type I and II IFN responses associate with severe COVID-19 disease in young patients [72].

The purpose of this study has been addressing whether TLR7/8 engagement and sXBP1 may contribute to viral sepsis in COVID-19 disease, given that dysregulated TLR responses may lead to persistent inflammation and tissue damage [73-75] and intracellular TLRs may recognize viral RNA during the replication life cycle of SARS-CoV-2. In addition, TLR7/8 involvement in COVID-19 pathogenesis was postulated as a target with potential therapeutics [76].

Cytokine storm and global immune dysregulation in SARS-CoV-2 disease

Hyperinflammation was soon recognized as a mechanism driving mortality that could proceed after the end of viral proliferation. This resembled the state of immune cell hyperactivation observed in various clinical conditions and this explains why the term CS was selected to refer to this phase of the disease. In fact, CS has been reported to be more damaging than viral infection itself [77] and drives lung damage that causes hypoxemia, as well as disseminated intravascular coagulation, and multiorgan failure [78]. Cytokines recruit immune cells into the site of infection and pave the way for the activation of the adaptative immune response. The purported function of this sequence of mechanisms is the cooperation of innate and adaptive immune responses to elicit viral clearance and a gradual decay of virus-induced inflammation.

While CS was simply considered a sudden release of cytokines [79], current views stress that the CS is the outcome of the confluence of genetic and physiological conditions [80, 81], as well as the result of the concomitant imbalance between proinflammatory and anti-inflammatory cytokines [82], further nuanced by the redundant and pleiotropic actions of cytokines, which upon activation of different cell populations can produce a distinct spectrum of biological effects [83].

Proinflammatory cytokines, chemokines, and immune mediators lead to the recruitment of macrophages, T and B cells to the lung [84]. T cells can become depleted when high levels of IL-10, TNF, and IL-6 compromise T cell survival and proliferation [85]. In fact, lymphopenia has been detected in 60-70% of severe infections [86] and in patients requiring treatment in internal care unit (ICU) patients [87]. In early studies, IL-6 levels was considered an archetypal cytokine increased in bronchoalveolar lavage fluid of deceased patients as compared to the surviving ones [88]. Drugs targeting innate immunity

and inflammation are promising since excessive inflammation is a critical sign of poor outcome. Several single-centre studies have used IL-6 inhibitors to treat patients with COVID-19 with some clinical benefits [89-91] and reported failures in patients receiving CAR T cells treatment [92].

The hyperinflammation of viral sepsis may lead to immune paralysis, when innate immune cells become unresponsive to immune stimulation [93-95]. Since proinflammatory cytokines exert key roles in SARS-CoV-2 infection and can be used as biomarkers of disease progression, they may also be targets for therapies, and this notion has guided the design of biological therapies and the repurposing of drugs well-known for their anti-inflammatory effects [96, 97].

COVID-19 therapeutic options

COVID-19 pandemic put an unprecedented pressure to the health systems. A cogent point of view suggests the use of antivirals as the first strategy to counter viral load. Some antivirals may target viral entry or the replication machinery of coronavirus, while the array of immunomodulators includes corticosteroids, cytokine blockers, neutralizing antibodies (nAbs), and convalescent plasma (CP) from recovered patients. Despite this, safe and effective therapeutics to treat hospitalised patients remain an unmet clinical need, even though many cohorts and clinical trial studies demonstrated that the timely administration of antivirals at the beginning of the disease, and the use of immunomodulatory drugs on severe COVID-19 patients mitigate disease severity, hospital stay and mortality.

Remdesivir, is an antiviral which target the RNA dependent RNA polymerase (RdRp), block the synthesis of viral RNA and counteract viral replication [98-100]. Macaques treated with remdesivir showed a reduction in lung viral loads and pneumonia symptoms but no reduction in virus shedding. This study disclosed that timely administration of remdesivir may be an effective treatment of SARS-CoV-2 infection [101]. The 3C-like protease, which hydrolyses viral polyproteins, is indispensable for coronavirus replication and has been considered a therapeutic target for COVID-19 pandemic [102]. In keeping with this fact, nine existing HIV protease inhibitors (nelfinavir, lopinavir, ritonavir, saquinavir, atazanavir, tipranavir, amprenavir, darunavir, and indinavir) have been evaluated for their antiviral activity in Vero cells infected with SARS-CoV-2 [103]. Nirmatrelvir, molnupiravir, and remdesivir have shown robust antiviral activities against the omicron variant [104].

Because of their anti-inflammatory activity, steroids have taken central stage as an adjuvant therapy for acute respiratory distress syndrome (ARDS) and CS. However, the

broad immunosuppression mediated by corticosteroids entails the possibility of blunting a proper anti-viral response. A meta-analysis of SARS-CoV-2 infection assessed 2,636 patients and found no mortality difference associated with steroid treatment, including a subset of patients with ARDS [105]. Other studies have reported associations with delayed viral clearance and increased complications in SARS and MERS patients [106]. Another retrospective analysis found that patients who received steroids were more likely to either being admitted to the ICU or perished. As a caution to a proper construal of these data, the corticosteroid-treated group also had significantly more comorbidities [107]. A smaller observational study of 31 patients found no association between corticosteroid treatment and time to viral clearance, length of hospital stays or symptom duration [108]. Others have published perspectives in support of early (K.-Y. Lee, Rhim, & Kang, 2020) and short-term, low-dose administration [109].

Vaccines are being developed to educate a person's immune system to make their own nAbs against SARS-CoV-2. However, there is interest in using adoptive transfer of nAbs as a therapeutic approach. The adoptive transfer of nAbs has been found effective against SARS-CoV-1 [110-115]. Patients who recovered from SARS-CoV-2 infection are one potential source of nAbs [116, 117]. Although recombinant nAbs could provide an effective treatment, they will require a significant time investment to develop and escalate production before becoming available for widespread use. A faster strategy consists of transferring CP from previously infected individuals that have developed high nAbs targeting SARS-CoV-2.

Despite the current lack of appropriately controlled trials, some studies and case reports on CP therapy for COVID-19 have evaluated the safety and the potential effectiveness of CP therapy in patients with severe disease [118-122]. However, with the new emerging VOCs, only CP from donors who recovered from COVID-19 infection and are vaccinated provides

substantial antibody protection [123]. Nevertheless, SARS-CoV-2 new variants has demonstrated a clever evasion from antibody neutralization in vaccinated people [124, 125].

Repurposing fluvoxamine in SARS-CoV-2 clinical trials

The global impact of COVID-19 pandemic accelerate drug repurposing efforts to manage SARS-CoV-2 infection. This strategy led to the use of approved medicaments to fight severe outcomes of COVID-19. SIGMA receptor 1 (SIR1) is a multifunctional inter-organelle signaling chaperone that plays various roles in cellular survival. Extensive studies demonstrate its ubiquitous expression throughout the body tissues [126, 127]. Among their pleiotropic functions, SIR1 ligands have been recently explored as therapeutic target in COVID-19 [128-130]. The cardioprotective role of SIR1 was associated with the regulation of the UPR [131] and more recently was identified as a functional host-dependent factor for SARS-CoV-2 disease [132].

Subsequent studies showed that fluvoxamine, a potent agonist of SIR1, could protect from CS through inhibition of the UPR, as demonstrated in a lethal septic shock mice model [133]. Fluvoxamine an antidepressant currently used in several mental disorders [134] alleviates ER stress via induction of SIR1 [135]. This view has been confirmed in several clinical trials showing a beneficial effect in COVID-19 disease [136-138]. Specifically, the TOGETHER randomised platform clinical trial disclosed that treatment with fluvoxamine of high-risk outpatients reduced the need of hospitalisation [139].

III. Rationale of the study

The purpose of this study has been the investigation of COVID-19 pathogenesis, focusing on the innate immune response and the role of the UPR as a reinforcing mechanism of the inflammatory response and viral replication. The study stems from previous work on the role of sXBP1 in the transcriptional regulation of proinflammatory cytokines and enzymes involved in the biosynthesis of lipids mediators [6, 55]. In addition, sXBP1 is activated by the encounter of PAMPs with TLRs [7, 56] and enhances the expression of the IL-23, while concomitantly inhibits the expression of the anti-inflammatory cytokine IL-10 [6, 140]. This displays an optimal scenario for the CS to occur. Previous reports support the notion that modulation of the UPR might be beneficial to counteract viral replication in coronavirus infected cell lines [44, 141, 142]. Therefore, the possible activation of the UPR during virus-host-cell interactions prompted us to investigate the role of the UPR in COVID-19 illness. New SARS-CoV-2 variants show increasing infectiveness and a lower ability to induce severe illness, which can be treated with new antivirals [143, 144]. Current approaches for the treatment of severe pneumonia include the use of immunomodulators, cytokine blockade, and antibody-rich plasma from recovered patients, including existing drugs have been repurposed during SARS-CoV-2 infection. A better understanding of the pathophysiology of SARS-CoV-2 may lead to the design of treatments acting on selected targets with a wider scope of application than current biological therapies [108, 145].

IV. Hypothesis

The hypothesis is that the UPR is involved in COVID-19 pathogenesis contributing to the replication of coronavirus and underpins the transcriptional activation of cytokines. This might contribute to the production of the CS/viral sepsis associated with the severe forms of COVID-19 disease.

V. Objectives

The principal aim of this work is the analysis of the ER stress response during SARS-CoV-2 infection, focusing on the IRE1α-XBP1 branch to identify host-dependent factors involved in the CS and viral replication. The following specific objectives were designed:

1. **Assaying the presence of *XBP1* splicing in nasopharyngeal swab samples of patients with COVID-19 symptoms.**
2. **The investigation of the transcriptomic profile of BAAs from patients under mechanical ventilation at ICU due to severe SARS-CoV-2 pneumonia.**
   - This includes the assay of the arms of the UPR, the cytokine-signature, immunometabolic enzymes and markers of the differentiation of the monocyte-macrophage lineage.
3. **The study of the effect of different ligands of the TLR7/8 system on XBP1 splicing in MDDCs.**
   - The assay of the role of sXBP1 in the transactivation of pro-inflammatory cytokines.
4. **Assessing the presence of the UPR during SARS-CoV-2 infection in different *in vivo* models.**
   - Studies in the Ad-hACE2 and K18-hACE2 mice models.
   - Analysis of the UPR and the inflammatory response in Syrian hamster.
   - Testing the effect of fluvoxamine during SARS-CoV-2 infection, focusing on viral replication and cytokine production.
5. **Addressing the role of the UPR in the viral replication cycle.**
   - Mechanistic analysis of different SARS-CoV-2 VOCs triggering the UPR and specific inhibition of XBP1 splicing during infection.

VI. Material and Methods

Patients and Ethic Statements

Nasopharyngeal swab samples

Nasopharyngeal samples were obtained from patients studied in different medical departments for symptoms consistent with SARS-CoV-2 infection at *Hospital Clínico Universitario de Valladolid* between July and November 2020. Patients were stratified according to the results of SARS-CoV-2 RT-PCR positive or negative tests and the correlation of *sXBP1* and clinical outcome addressed.

Bronchiolo-alveolar aspirates

In the case of patients with mechanical ventilation and endotracheal intubation, samples were obtained by endotracheal aspirations to remove respiratory secretions as part of clinical care by the attending staff at ICU. Brochiolo-alveolar aspirate (BAA) samples were collected from September 2020. Samples were obtained as soon as the patients underwent endotracheal intubation and pulmonary secretions aspirated.

BAAs were directly transferred to the DNA/RNA extraction kit MagMAXTM Pathogen RNA/DNA (Applied Biosystems) for the automated extraction machine Kingfisher Flex (Thermo Fisher Scientific). Infection diagnosis was carried out using the TaqPath™ COVID-19 CE-IVD RT-PCR Kit from Applied Biosystems, which targets ORF-1ab, S protein and N protein regions selected with the purpose of having specificity and reducing the risk for overlooking mutations. A representative sequence of the SARS-CoV-2 RNA prevalent at the time of study can be obtained at NCBI using accession PRJNA894347 to the SRA database and temporary submission ID SUB12205626. Resolution of infection was confirmed by the analysis of samples collected four days after a positive test. BAAs

from patients with infections with other pathogens were obtained from samples collected for microbiological diagnosis in patients suffering from bacterial pneumonia requiring ventilatory support and endotracheal intubation at ICU. Lung protective ventilation of both COVID-19 and non-COVID-19 patients was performed according to the current guidelines on mechanical ventilation of ARDS in adult patients, which makes it unlike the induction of cytokine expression by mechanical ventilation [146]. The clinical part of the study was approved by the Ethics Committee of *Area de Salud Valladolid Este* (ref. PI-GR-20-2011 COVID).

Cells, Viruses and Reagents

ACE2-A549, A549-ACE2-TMPRSS2, Vero E6 and HEK-293T

ACE2-A549 recombinant cells [147] and A549 ACE2-TMPRSS2 [148] were kindly gifts from the referred laboratories. Vero E6 cells (ATCC, CRL-1586) and HEK-293T cells (ATCC, CRL-11268) were maintained in DMEM (Corning) supplemented with 10% fetal bovine serum (FBS) (Peak Serum), 1% non-essential amino acids (Corning, 25-025-CI) and penicillin/streptomycin (Corning) at 37ºC and 5% CO_2 atmosphere. All cell lines used in this study were regularly screened for mycoplasma contamination using MycoStrip™ - Mycoplasma Detection Kit (InvivoGen).

Monocyte-derived dendritic cells

For *in vitro* experiments, MDDCs were obtained from human mononuclear cells collected from pooled buffy coats of healthy donors provided by *Centro de Hemoterapia y Hemodonación de Castilla y León Biobank*. The study was approved by the Bioethical Committee of the Spanish Council of Research (CSIC) and the written informed consent of all healthy donors was obtained at *Centro de Hemoterapia y Hemodonación de Castilla y León Biobank*. The researchers received the samples in an anonymous way. The process is documented by the Biobank authority according to the specific Spanish regulations. The ethics committee approved this procedure before starting the study.

The differentiation of monocytes was carried out in the presence of GM-CSF and IL-4 for 5 days. Culture was carried out in RPMI 1640 medium containing 11.1 mM D-glucose and 4 mM L-glutamine. 10% FBS was maintained during the differentiation process and reduced to 2% at the start of experiments (**Figure 6**).

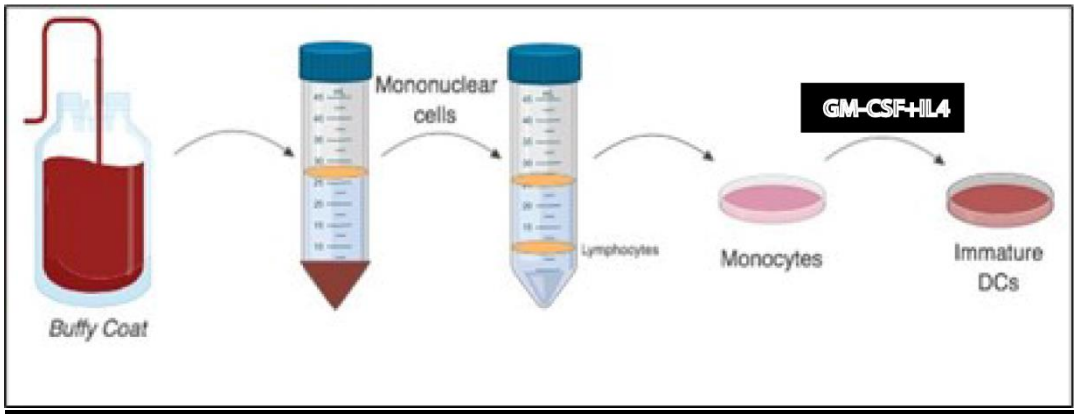

Figure 6. Isolation of monocytes from buffy coat and differentiation to MDDCs. Monocytes were isolated from pooled buffy coats by centrifugation in Ficoll. The differentiation from monocytes to dendritic cells was carried in the presence of GM-CSF and IL-4 for 5-7 days.

Viruses

SARS-CoV-2, isolate USA-WA1/2020 (BEI Resources NR-52281) termed as (WA1); (lineage B SARS-CoV-2/human/Liverpool/REMRQ0001/2020), was a kind gift from Ian Goodfellow, previously isolated by Lance Turtle (University of Liverpool), David Matthews and Andrew Davidson (University of Bristol) termed as (UK). Alpha variant (B.1.1.7; SARS-CoV-2 England/ATACCC 174/2020) was a gift from G. Towers [149]. Lineages B.1.1.617.2 (Delta, GISAID: EPI_ISL_1731019) and B.1.1.529 (Omicron UK isolate, G. Screaton) [150, 151] were received as part of the work conducted by G2P-UK National Virology Consortium. The mouse adapted (MA-SARS-CoV-2) [152], was also used for *in vivo* experiments (**Figure 7**). Viruses were used under biosafety level 3 (BSL3) containment in accordance with the biosafety protocols developed by the Icahn School of Medicine at Mount Sinai and University of Cambridge.

Viruses were grown in Vero-TMPRSS2 cells (BPS Bioscience; Catalog #78081) for 4-6 d. The supernatant was clarified by centrifugation at 4,000 x g for 5 min and aliquots were

frozen at -80°C for long term use. Expanded viral stocks were sequence-verified to be the identified SARS-CoV-2 and titered on Vero-TMPRSS2 cells before use in all assays.

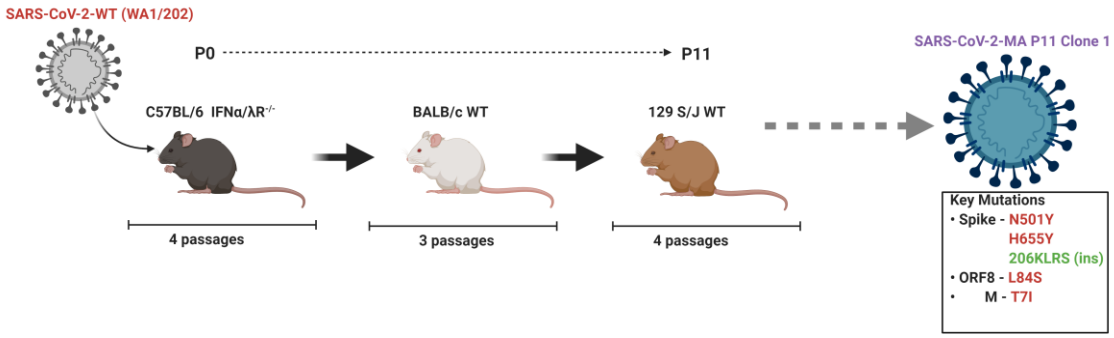

Figure 7. Mouse adapted SARS-CoV-2 strain. Protocol of MA-SARS-CoV-2 strain generation as described by [152].

Reagents

Imiquimod (Sigma-Aldrich), ssRNA40/LyoVec™, and its negative control ssRNA41/LyoVec™ (InvivoGen) were used as TLR7 and TLR8 as selective ligands in MDDCs. The inhibitors MKC8866, KIRA8 IXA4 and CU-CPT9a were from MedChemExpress. Fluvoxamine was from Sigma Aldrich.

Animal models of SARS-CoV-2 infection experiments

Hemizygous 6-week-old female K18-hACE2 mice on the C57BL/6J background (Jax strain 034860), were compared to age and sex-matched WT C57BL/6J (Jax strain 000664) and WT BALB/cJ (Jax strain 000651) mice. Golden Syrian hamsters 10-12 weeks old (Envigo RMS, LLC) and the 129S1/SvImJ mice (Strain #002448 from Jackson Laboratories) were used for mouse-adapted SARS-CoV-2 infection and treatment with 150 mg/kg subcutaneous fluvoxamine daily. All animal studies were performed in animal BSL3 facility at the Icahn school of Medicine in Mount Sinai Hospital, New York City. Animal studies were approved by the Institutional Animal Care and Use Committee (IACUC) of Icahn School of Medicine at Mount Sinai (ISMMS).

***In vivo* delivery of virus**

Mice were housed in a BSL-2 facility for intranasal instillation of non-replicating adenoviral vectors before being transferred to a BSL-3 facility at ISMMS for challenge with SARS-CoV-2. Mice were housed under specific pathogen-free conditions in individually ventilated cages and fed using irradiated food and filtered water. Mice were infected with 1×10^4 Plaque forming units (PFU). Viral seed stocks for non-replicating E1/E3 deleted viral vectors based on human adenovirus type-5 (HAdV-C5, referred to as Ad throughout without an antigen (Ad-Empty), or expressing the human ACE2 receptor (Ad-ACE2) under the control of a CMV promoter, were obtained from Iowa Viral Vector Core Facility.

For *in vivo* delivery of Ad vectors to the lung, mice were anesthetized by intraperitoneal (i.p) injection of ketamine and xylazine diluted in water for injection (WFI; Thermo Fisher Scientific, Waltham, MA). Ad-Empty at 2.5×10^8 PFU, or Ad-hACE2 at a dose of 2.5×10^8

PFU, were instilled intranasally in a final volume of 50 μL sterile PBS. Untreated control mice received the same volume of sterile PBS. Mice were transferred to the BSL3 facility on day 3 post-Ad for subsequent challenge with SARS-CoV-2 virus on day 5. For SARS-CoV2 challenge, mice were anesthetized as above and infected with 1×10^4 PFU in 50 μL of PBS. Mice were sacrificed at day 2 and day 5 post-infection by i.p. injection of pentobarbital. Lungs were homogenized in 1 ml PBS using ceramic beads. Golden Syrian hamsters 10-12 weeks old were infected i.n. with SARS-CoV-2 WA1 in a 50 μl suspension containing a targeted dose of 100 PFU and compared to a Mock group.

Methods

Real-time RT-PCR

Total RNA was obtained by TRIzol/chloroform extraction and used for RT reactions. RNA was reverse transcribed using maxima reverse tanscriptase and oligo-dT (Thermo). The resulting cDNA was amplified in a LightCycler 480 equipment using SYBR Green I mix containing Hot Start polymerase. Cycling conditions were adapted to each set of primers. *GAPDH* and *ACTB* was used as a housekeeping gene to assess the relative abundance of the different mRNA using the comparative cycle threshold method.

Quantitative RT–PCR was performed on cDNA using Light-Cycler 480 SYBR Green I Master Mix (Roche) on a LightCycler 480 II. For the analysis of Syrian hamster gene expression, we use taqman probes *Hspa5* (Cg01333324_g1), *Ddit3/Chop* (Cg04519311_g1), *Atf4* (Cg04423842_g1), *Actb* (Cg04424027_gH) and mice probes *Herpud1* (Mm00445600_m1), *Edem1* (Mm00551797_m1), *Pdia3* (Mm004333130_m1) and *Actb* (Mm02619580_g1) from (Thermo). Quantitative RT-PCR with probes was performed using Light-Cycler 480 TaqMan Real-time master mix (Thermo).

Protein assay by ELISA and Western Blot

IL-6 and TNFα proteins were assayed in supernatants of MDDCs stimulated with ssRNA40 using kits from Elabscience. Protein extract concentration was quantified using the Pierce BCA Protein Assay, according to the manufacturer's instructions. 10 µg of protein extracts were resolved in 10% Mini-PROTEAN® TGX Stain-Free™ Protein Gels (Biorad), then transferred to nitrocellulose membranes (0.45 µm, Bio-Rad). These lysates were used for Western blotting to determine the protein expression of CHOP, GADD34, XBP1,

HERPUD1 and viral protein S. Briefly, membranes were incubated with rabbit mAb anti-XBP-1s (E9V3E, #40435) mouse mAb anti-CHOP (L63F7)mAb β-actin (13E5, #2895,), rabbit mAb anti-HRP conjugated from Cell Signaling (#5125), mouse mAb anti-GADD34 (ab9869), rabbit mAb anti-HERPUD1 (ab150424), and SARS-CoV-2 viral glycoprotein Spike (S) (ab272504) were from abcam and diluted at 1:1000. The HRP-conjugated anti-mouse IgG antibody (GTX26820, Genetex) and the HRP-conjugated anti-rabbit IgG antibody (GTX26802, Genetex) were used to detect the primaries antibodies at 1:10000. HRP was detected using Clarity™ Western ECL Substrate (Biorad). Each protein band was quantified by ImageJ and normalized to GAPDH or β-actin levels. IRDye 800CW donkey anti-rabbit IgG (H+L), IRDye 680RD goat anti-mouse IgG (H+L), and IRDye 680RD goat anti-mouse IgM (μ chain specific) were from Licor.

XBP1 Splicing Assay

This was carried out by RT-PCR reactions using primers spanning the unspliced regions (Figure X). The PCR conditions were 5 min at 95°C (hot start), 45 cycles of denaturation at 95°C for 15 s, annealing at 60°C for 20 s and elongation at 72°C for 1 min. Final extension was carried out at 72°C for 5 min. Gel electrophoresis was carried out in 3% agarose and spliced XBP1 and unspliced XBP1 bands visualized by GelRed™ staining and quantified using GelDoc Go Image System (Bio-Rad). The position of the primers and the spliced region in human samples is shown in **Figure 8**. These correspond to GenBank sequence NM_001079539.2, which differs from *uXBP1* sequence NM_005080.4 by the deletion of 26 nucleotides. For Syrian hamster, PCR product *uXBP1* (XM_040746756.1) were digested with PstI restriction enzyme (NEB #R040S), for 24 h at 37ºC, following manufacturer's instructions.

Figure 8. Sequences of XBP1 mRNA and primers designed for the study of human samples. The splicing of 26 nucleotides in NM_005080.4 sequence generates the sequence in NM_001079539.2. The position of primers, including the reverse primer spanning the spliced sequence is shown.

Chromatin Immunoprecipitation (ChIP) assay

Chromatin immunoprecipitation assays were conducted using a rabbit mAb (Cell Signaling Technology) against sXBP1. DCs were fixed with 1% formaldehyde and cross-linking was finished by 0.125 M glycine. Chromatin sonication was carried out using a Bioruptor™ device. The chromatin solution was precleared by adding Protein A/G PLUS-Agarose. After preclearing, anti-sXBP1 Ab or irrelevant Ab were added for overnight incubation at 4°C, and then Protein A/G PLUS-Agarose was added and incubated for an additional period of 2 hours at 4°C. Cross-links were reversed by heating and the DNA bound to the beads isolated by extraction with phenol/chloroform/isoamylalcohol. Irrelevant Ab and sequences of the *IL12A* promoter were used as control of binding specificity. Results are expressed as percentage of input.

Whole lung RNA and protein extraction

Approximately, 25% of lung tissue was homogenized in Trizol (Thermo) and RNA extracted using Direct-zol RNA Miniprep Plus kit (Zymo Research). For protein extraction, the remaining material was homogenized in PBS with silica glass beads and the supernatant mixed 1:1 with RIPA for 15 minutes in the BSL3 facilities prior to UV inactivation followed by 10 min centrifugation to eliminate de debris.

Bioinformatic Analysis

For the analysis in Golden hamster, the reads from the Illumina paired-end sequencing were processed with the Trimmomatic v0.36 program to filter out low-quality reads and to trime the adapters. Then, a check of the Trimmomatic results was carried out using FastQC v0.11.9 and MultiQC v1.11 was conducted. It was verified that the mean value of the Phred Score for all the samples was greater than Q30 and that the rest of the parameters were within the normal values for RNA samples. The available assembled genomes of *Mesocricetus auratus* were studied to verify that their corresponding annotation files contained the genes of interest for the study. It was concluded that the best assembled and annotated genome for our purposes was that of the Baylor College of Medicine Human Genome Sequencing Center (RefSeq assembly accession GCF_017639785.1). With said reference genome and using the HISAT2 v2.2.1 program, the mapping of the cleaned reads was carried out. Using SAMtools v1.12 the SAM files produced in the mapping were transformed into ordered BAM files and indexed in a later step. In order to count the reads that map against each of the *Mesocricetus auratus* genes, it was necessary to make a small modification to the GTF annotation file. The original GTF file has no gene identifier for some gene id in the 9th column. Seeing that in the "product" field it was indicated that these

entries were tRNA, and that they were not relevant for our research, it was decided to eliminate these entries to carry out the analysis. With the fixed GTF file, the mapping BAM files, and the featureCounts v2.0.1 program, the count of the reads that map against each of the genes was carried out. When the table of counts was obtained, the differential expression analysis was carried out using the DESeq2 and EdgeR programs. Finally, volcano plots of the significant genes object of study were represented using the library EnhancedVolcano v1.14.0 of R v4.2.0. For further gene sets analysis, Gene onthology (GO) enrichment pathways derived from *Mus musculus* and *Rattus norvegicus* genome were identified instead of *Mesocricetus auratus* genome, which was not annotated. Thus, CAMERA (Correlation Adjusted Mean Rank) method [153] was employed (implemented by the R package "Enrichmentbrowser" v2.2.2). We selected differential biological processes according to ER function, viral process, inflammation, and cytokines with an FDR<0.05, represented as bubble colour, and the number of genes within the GO pathway was represented as bubble size using Prism software (GraphPad v 9.0.0).

Lung viral titres

129S1/SvImJ female mice 4-week-old specific pathogen-free were used. These mice were anesthetized with a mixture of ketamine/xylazine before each intranasal infection with MA-SARS-CoV-2 and compared to a group treated with 150 mg/Kg fluvoxamine. At day 3 post-infection, animals were humanely euthanized. Weight data were transformed into body weight percentage. Lungs were harvested for viral titration and histopathology. Whole lung was homogenized and then frozen at -80°C for viral titration via TCID50. Briefly, infectious supernatants were collected at 48 h post-infection and frozen at -80 °C until later use. Infectious titres were quantified by limiting dilution titration using Vero TMPRS2 cells. Briefly, Vero-TMPRS2 cells were seeded in 96-well plates at 20,000 cells/well. Next

day, SARS-CoV-2-containing supernatant was applied at serial 10-fold dilutions ranging from 10^{-1} to 10^{-8} and, after 4 d, viral cytopathic effect was detected by staining cell monolayers with crystal violet.

Immunohistopathology

Mice were euthanized with pentobarbital and death confirmed by exsanguination following severing of the femoral artery. After death, the trachea was exposed, and lungs inflated with 1.5 mL of 10% formalin using a 21G needle fitted to a 3 mL syringe. Lungs were removed intact, trimmed carefully, and loaded into a tissue embedding cassette. Tissue was fixed overnight in 10% formalin, transferred to PBS after 24 h and sent for processing and paraffin embedding at the Biorepository and Pathology Core at ISMMS. Paraffin-embedded lung tissue blocks for mouse lungs were cut into 5 μm sections, which were stained with H&E and analyzed by Histowiz (Brooklyn, NY). Digital light microscopic scans of whole lung processed were examined by an experienced veterinary pathologist. H&E-stained sections from 129S1 mice were examined by implementing a semi quantitative, 5-point grading scheme (0 - within normal limits, 1 - mild, 2 - moderate, 3 - marked, 4 - severe), which considered four different histopathological parameters: 1) perivascular inflammation, 2) bronchial or bronchiolar epithelial degeneration or necrosis, 3) bronchial or bronchiolar inflammation, and 4) alveolar inflammation.

Analysis of peripheral blood cytokines

Cytokine levels in serum of mice infected with MA-SARS-CoV-2 were measured in samples inactivated as described [154]. Sera were collected after centrifugation at 3000 x g for 5 minutes, deactivated by UV, and stored at -80°C. Cytokine analysis was performed

at Eve Technologies (Calgary, AB) using the Mouse Cytokine Array/Chemokine Array 44-Plex (MD44) immunoassay.

ACE2-A549 viral RNA and protein extraction

A549 cells were seeded at 1×106 cells per well in BSL2 in DMEM supplemented with 10% FBS, 1% non-essential amino acids, and penicillin/streptomycin at 37ºC and 5% CO_2 atmosphere. The day of the experiment, cells were transferred to BSL3 and media were replaced by complete DMEM with 2% FBS containing SARS-CoV-2 WA1 at 0,1 and 1 MOI. Cells were harvested at 4, 8, 16 and 24 h post infection using RIPA lysis and extraction buffer (Thermo) with protease inhibitor cocktail (P8340, Sigma). RNA extracted from 1×10*6 A549 cells were used for retro transcription (150-500ng total RNA input). Quantitative PCR was run as described below. Then, viral RNA was calculated by quantification of *N* gene expression normalized to *GAPDH*.

siRNA knockdown of *TLR8, CHOP, GADD34* and *XBP1*

To knockdown TLR8, MDDCs were transfected with ON-TARGETplus human TLR8 (Dharmacon 51311, J-004715- 05) using Dharmafect reagent (Horizon, T.2001.02) according to the manufacturer's protocol and as described in [155]. Ambion Silencer™ Select Negative control siRNA (Ambion, 4390844) was used as negative control siRNA.

ACE2-A549 cells were transfected with 20 nM siRNA against human *CHOP* (J-004819-06-0002), human *GADD34* (J-004442-05-0002) and human *XBP1* (J-009552-07-0002), Dharmacon™. A negative control siGENOME non-targeting siRNA (D-001206-13-05, Dharmacon™) was used at the same concentrations of the siRNA described above. Gene knockdown was performed using 1×10^6 cells per well using Lipofectamine RNAiMAX

Transfection Reagent following manufacturer's protocol for A549 cells (Invitrogen). Tunicamycin 10 µM was used as a positive control of UPR activation for 6 h. After 24 h post-transfection, plates were transferred into the BSL3 facility, transfection media was removed, and cells were infected with SARS-COV2 at MOI of 1 for 2 h, infectious media was removed and replaced to a new media and cells were harvested at 16 h post infection for Western blot analysis and supernatants used for plaque assay.

Plaque assay

Plaque assays were performed using Vero E6 cells as previously described [156]. Briefly, Vero E6 cells seeded in 12-well plate format were infected with serial ten-fold dilutions of supernatants from ACE2-A549 cells used in siRNA experiments. Virus absorption was carried out for 1 h using an inoculum of 200 µL and rocking the plates every 10-15 min. After 1 hour, the inoculum was removed and the cells incubated with an overlay composed of MEM with 2% FBS and 0.7% Oxoid^{TM} agar for 72 hours at 37°C with 5% CO_2 atmosphere. The plates were subsequently fixed using 5% formaldehyde and immuno-stained using a monoclonal anti-SARS-CoV-NP antibody (Creative-Biolabs; NP1C7C7). In brief, plates were blocked (3% skim-milk TBS with 0.1% 591 Tween20 for 1 h), stained for 90 min with anti-NP antibody (mAb 1C7, diluted 1:1000 in 1% skim592 milk TBS with 0.1% Tween20), and finally secondary-stained with anti-mouse-HRP (antibody diluted 1:5000 in 1% skim-milk TBS with 0.1% Tween20 for 45 min). Plates were incubated for 10 min with KPL TrueBlue peroxidase substrate (Seracare) to reveal staining.

Plate-based cytometer image

Two thousand ACE2-A549 cells (BPS Bioscience) were seeded into 96-well plates in DMEM (10% FBS) and incubated for 24 hours at 37°C in 5% CO_2 atmosphere. Gene

knockdown was performed using 20 nM siRNA using Lipofectamine RNAiMAX Transfection Reagent following manufacturer's protocol for A549 cells (Invitrogen). After 24 h, plates were transferred into the BSL3 facility and 0,1 or 0,2 MOI were added in 50 μL of DMEM supplemented with 2% FBS. After 2 hours, the inoculum was removed and plates incubated for 24 and 48 hours at 37°C. After infection, supernatants were removed, and cells were fixed with 4% formaldehyde for 24 hours before being removed from the BSL3 facility. The cells were then immunostained for the viral N protein (an in house mAb 1C7, provided by Dr. Thomas Moran) with DAPI counterstain. Infected cells and total cells were quantified using the Celigo (Nexcelcom) imaging cytometer. Infectivity was measured by the accumulation of viral N protein. Percent infection was quantified as (Infected cells/Total cells – Background) and the DMSO control was set to 100% infection for analysis.

Plasmids and transfection

All SARS-CoV-2 S protein VOCs plasmids (a kind gift of Dr. Thomas Peacock and Prof. Wendy Barclay, Imperial College London) were human codon-optimised with the Δ19 mutation (K1255*stop codon), which increases cell surface expression. To express the full-length protein, the stop codon was corrected by standard site-directed mutagenesis using the following primers (5´- GGCAGCTGCTGCAAGTTCGACGAGG and 5´-CCTCGTCGAACTTGCAGCAGCTGCC).

HEK-293T cells were transiently transfected with full-length pcDNA3.1-SARS-CoV-2-S protein VOCs plasmids, namely WT (D614G), beta (B1.351), gamma (P.1), delta (B1.617.2), and omicron (BA.1 and BA.2) using a commercial liposome method (TransIT-LT1, Mirus). Transfection mixtures containing plasmid DNA, serum-free medium (Opti-MEM; Gibco-BRL), and liposomes were set up as recommended by the manufacturer and

added dropwise to the tissue culture growth medium. Cells were harvested at 36 h post-transfection.

A549-ACE2/TMPRSS2 VOCs infection experiments

A549 cells were seeded at $5x10^5$ cells per well in DMEM supplemented with 10% FBS, 1% non-essential amino acids and penicillin/streptomycin at 37ºC, at 5% CO_2 atmosphere in a BSL2 containment laboratory. The day of the experiment, cells were transferred to a BSL3 containment laboratory and infected with SARS-CoV-2 WT, B.1.1.7 (alpha), B.1.617.2 (delta), and B.1.1.529 (omicron) VOCs at MOI 0.1. After the adsorption hour, media were replaced with complete DMEM supplemented with 10% FBS. 10 µM KIRA8 (MedChemExpress) was added to the DMEM-10% FBS immediately after the virus adsorption period and maintained in the medium. Cells were harvested at 16 h post infection using Laemmli's buffer for protein extraction and RNeasy kit (Qiagen) for RNA extraction. Viral RNA in SARS-CoV-2 infected cells was quantified by *N* gene expression normalized to *RPL19*. SARS-CoV-2 viral titres were assessed using a TCID50 assay in Vero E6 cells. Supernatant derived from infected A549-ACE2/TMPRSS2 cells was subjected to 10-fold serial dilutions. At 72 hours post-infection (hpi), cells were fixed and stained. Wells showing any sign of cytopathic effect (CPE) were scored as positive.

Quantification and Statistical Analysis

Data are represented as the mean ± SEM and were analysed with the Prism 9.0 statistical program. Repeated-measures one-way and two-way ANOVA analyses were performed. When data did not follow normal distribution nor had equal variances, log-transformation was applied before analysis. Comparison between experimental groups was carried out using unpaired or paired two-tailed Student's t test, Wilcoxon signed-rank test, and Mann-

Whitney. Kruskal-Walli's test and Friedman tests were used for multiple comparison in the case of non-normally distributed samples. Differences were considered significant for $p < 0.05$. Data is shown as relative expression ($2^{-\Delta Ct}$ relative to *Actb*). sXBP1 was measured by the equation $sXBP1/XBP1^{T}(uXBP1+sXBP1)$. $TCID_{50}$/ml were calculated using the method of Reed and Muench).

Table I. Sequences of primers used for RT-PCR and ChIP assays in human samples and experiments in MDDCs

GENE	Forward primer	Reverse primer
XBP1	5'- TGAGCTGGAACAGCAAGTGG -3'	5'- ATACCGCCAGAATCCATGGGGA -3'
sXBP1	5'- TGAGCTGGAACAGCAAGTGC -3'	5'- CTGCACCTGCTGCGGACTCA -3'
DDIT3	5'- GCAGAGATGGCAGCTGAGTC -3'	5'- AGCCAAGCCAGAGAAGCAGGGT -3'
ERDJ4	5´-AGCAAAATTCAGAGAGATTGCAGA-3´	5´-ACTTCCACTACCTCTTTGTCCT-3´
EDEM1	5´-TGACTCTTGTTGATGCATTGGA-3´	5´-CTCAAAGACTTGGACGGTGGA-3´
HERPUD1	5´- CGGCATGTTTTGCATCTGGT-3´	5´- CCTCAGGATACTGTCCCCGA-3´
HSPA5	5´-ACGTGGAATGACCCGTCTG-3´	5´-CTTTGTTTGCCCACCTCCAAT-3´
ASNS	5´-TGTGGCTCTGTTACAATGGTG-3´	5´-ACAAATGCAAACACACCATCCA-3´
CTH	5´-GCTTCAGGTTTAGCAGCCAC-3´	5´-TGCCACTTGCCTGAAGTACC-3´
IL1B	5'- ATGATGGCTTATTACAGTGGCAA -3'	5'- GTCGGAGATTCGTAGCTGGA -3'
TNF	5`-GTTGTAGCAAACCCTCAAGC-3´	5`-TTGAAGAGGACCTGGGAGTA-3´
IL6	5'- TTCGGTACATCCTCGACGGC -3'	5'- TCTGCCAGTGCCTCTTTGCT -3'
CXCL8	5'- ATTTCTGCAGCTCTGTGTGAA -3'	5'- AACTTCTCCCGACTCTTAAGT -3'
IL10	5´-GAGAACAGCTGCACC CAC TT-3´	5´-GGCCTTGCTCTTGTT TTCAC-3´
IL23A	5`- GTTCCCCATATCCAGTGTGG -3'	5'- TTAGGGACTCAGGGTTGCTG -3'
IL12B	5'- CATGGGCCTTCATGCTATTT -3'	5'- TTTGCATTGTCAGGTTTCCA -3'
IFNB1	5'- TCTAGCACTGGCTGGAATGAG- 3'	5'- GTTTCGGAGGTAACCTGTAAG-3'
IFNG	5'-CCAACGCAAAGCAATACATGA-3'	5'-CCTTTTTCGCTTCCCTGTTTTA-3'
N Gene	5'- CAATGCTGCAATCGTGCTAC -3'	5'- GTTGCGACTACGTGATGAGG -3'
COX2	5'- TTCAAATGAGATTGTGGGAA -3'	5'- AGATCATCTCTGCCTGAGTA -3'
GLUT1	5'- GAAGAGAGTCGGCAGATGAT- 3'	5'- AATAGAAGACAGCGTTGATGC -3'
HIF1A	5´-AGTGTACCCTAACTAGCCGA-3´	5´-GTGCAGTGCAATACCTTCC-3´
HK2	5'- TAGGGCTTGAGAGCACCTGT -3'	5'- CCACACCCACTGTCACTTTG -3'
PDK4	5'- CCCGCTGTCCATGAAGCAGC -3'	5'-CCAATGTGGCTTGGGTTTCC-3'
MDH2	5'- TCGGCCCAGAACAATGCTAAA -3'	5'- GCGGCTTTGGTCTCGATGT -3'
SDHA	5'- CAGCATGTGTTACCAAGCT -3'	5' -GGTGTCGTAGAAATGCCAC -3'
SLC25A11	5'- ACACCGTCCTCACCTTCATC -3'	5'- CAGGGGGTAGAACAGACCAA -3'
IRG1	5'- GTTCCTGGGAACCACTACG -3'	5'- GATGTCTGGCTGACCCCAA -3'
TLR7	5´-CTTGGCACCTCTCATGCTCT-3'	5`-GTCTGTGCAGTCCACGATCA-3'
TLR8	5' -GCTGACCTGCATTTTCCTGC-3`	5`-CCGTTTGGGGAACTTCCTGT-3´
HLA-DRB1	5' -TTCCTGTGGCAGCCTAAGAG-3'	5' -AACCCCGTAGTTGTGTCTGC-3'
CD300E	5' -AGAGAAGGTGGAGAGGAATGG-3'	5' -AGGAAGATGGGAGGTGTGG-3'
CCR2	5'- CCCCAACGAGGCATAGA -3'	5'- AAGAGTCTCTGTCACCTGCG -3'
MMP9	5' -CGTCTTCCCCTTCACTTTCC-3	5' -CCCCACTTCTTGTCGCTGT-3'
BATF3	5' -AGGAAGGTCCGAAGGAGAGA-3'	5' -GAGGCACTGGCACAAAGTTC-3'
MX1	5' -CTGGGATTTTGGGGCTTT-3'	5' -GGGATGTGGCTGGAGATG-3'
OAS1	5' - TCAGAAATACCCCAGCCAAA-3'	5' -GAGCCACCCTTTACCACCTT-3'
ACTB	5`-CTGTCTGGCGGCACCACCAT-3'	5'-GCAACTAAGTCATAGTCCGC-3'
	ChIP Assays Primers	
PROMOTER	**Forward Primer**	**Reverse Primer**
IL1B Proximal	5`-TAGTTTGCTACTCCTTGCCCT-3´	5`-AGGAAAGGGGAAAAGAGTATTGGT-3´
IL1B Medial	5`-TGAATGAAGAAAAGTATGTGCATGT-3´	5`-AAATACTGGATTTTCCCACGTTAG-3´
IL6 Proximal	5`-AGCCTCAATGACGACCTAAGC-3	5`-GGGTGGGGCTGATTGGAAA-3`
IL6 Medial	5`-ACCTTCTTCATAATCCCAGGC-3´	5´-AGGCTAGAATTTAGCGTTCCAGT-3´
TNF Proximal	5`-ATGCTTGTGTGTCCCCAACT-3´	5`-CAGCGGAAAACTTCCTTGGTG-3´
TNF Medial	5`-GACCCAAACACAGGCCTCA-3`	5`-ACTAGAACTGGGAGGGGCTT-3´
TNF Distal	5`-GTCCAGGGCTATGGAAGTCG-3´	5`-CCCAGTGTGTGGCCATATCTT-3´

Table II. Sequences of primers used for RT-PCR in animal samples and experiments in HEK293T and ACE2-A549

Species	Transcript	Primer direction	Sequence 5'-3'	Purpose
mouse	*Xbp1*	Forward	ACACGCTTGGGAATGGACAC	Splicing assay
		Reverse	CCATGGGAAGATGTTCTGGG	
mouse	*Actb*	Forward	CTCAGGAGGAGCAATGATCTTGAT	RT-qPCR
		Reverse	TACCACCATGTACCCAGGCA	
mouse	*Gapdh*	Forward	AGGTCGGTGTGAACGGATTTG	RT-qPCR
		Reverse	TGTAGACCATGTAGTTGAGGTCA	
mouse	*sXbp1*	Forward	AAGAACACGCTTGGGAATGG	RT-qPCR
		Reverse	CTGCACCTGCTGCGGAC	
mouse	*Ddit3/Chop*	Forward	GTCCCTAGCTTGGCTGACAGA	RT-qPCR
		Reverse	TGGAGAGCGAGGGCTTTG	
mouse	*Hspa5/BiP*	Forward	TCATCGGACGCACTTGGAA	RT-qPCR
		Reverse	CAACCACCTTGAATGGCAAGA	
mouse	*Dnajb9/ERdj4*	Forward	TAAAAGCCCTGATGCTGAAGC	RT-qPCR
		Reverse	TCCGACTATTGGCATCCGA	
mouse	*Sec61a1*	Forward	CTATTTCCAGGGCTTCCGAGT	RT-qPCR
		Reverse	AGGTGTTGTACTGGCCTCGGT	
mouse	*Atf4*	Forward	GAGCTTCCTGAACAGCGAAGTG	RT-qPCR
		Reverse	TGGCCACCTCCAGATAGTCATC	
mouse	*Erp44*	Forward	GCTGAAACGACACCAGTCAG	RT-qPCR
		Reverse	CAGATGCTCCTTGCTGCTC	
mouse	*Rpn1*	Forward	GTTTCCACAACGACCGAGAT	RT-qPCR
		Reverse	CCTAGGCGTGCAGATAAAGG	
mouse	*Hgsnat*	Forward	CTGATGACTGTTACCAATGCACC	RT-qPCR
		Reverse	GCACCAAAAGGGAATAGTTTCCA	
mouse	*Tapbp*	Forward	GGAGGGTGTCTACCTGGCTA	RT-qPCR
		Reverse	AACGGGTGCTGGTGTTAGAG	
mouse	*Bloc1s1*	Forward	GAAGCGTTGGTGGATCACCT	RT-qPCR
		Reverse	TCACCTCATGGTCCAGCTTTC	
mouse	*Tnf*	Forward	ACGGCATGGATCTCAAAGAC	RT-qPCR
		Reverse	AGATAGCAAATCGGCTGACG	
mouse	*Il10*	Forward	GCTCTTACTGACTGGCATGAG	RT-qPCR
		Reverse	CGCAGCTCTAGGAGCATGTG	
mouse	*Il1β*	Forward	GCAACTGTTCCTGAACTCAACT	RT-qPCR
		Reverse	ATCTTTTGGGGTCCGTCAACT	
mouse	*Ifnβ*	Forward	GAGGAAAGATTGACGTGGGA	RT-qPCR
		Reverse	CTGAAGATCTCTGCTCGGAC	
mouse	*Il12a*	Forward	ATGACCCTGTGCCTTGGAC	RT-qPCR

		Reverse	TCTCCCACAGGAGGTTTCTG	
mouse	*Il23a*	Forward	AGGGAACAAGATGCTGGATT	RT-qPCR
		Reverse	AGTAGATTCATATGTCCCGCT	
mouse	*Cxcl9*	Forward	GTTCGAGGAACCCTAGTGAT	RT-qPCR
		Reverse	TTTGTAGTGGATCGTGCCTC	
Syrian hamster	*Xbp1*	Forward	CAGAGTCCAAGGGAAATGGA	Splicing assay
		Reverse	AGATCGGCAGATTCTGGGGA	
Syrian hamster	*sXbp1*	Forward	CAGAGTCCAAGGGAAATGGA	RT-qPCR
		Reverse	CTGCACCTGCTGCGGACTCA	
Syrian hamster	*Gadd34*	Forward	TGTGGAAGTTTGCATGCGTG	RT-qPCR
		Reverse	CAGCCCTGTCAAGACTCCTG	
human	*Rpl19*	Forward	ATGTATCACAGCCTGTACCTG	RT-PCR
		Reverse	TTCTTGGTCTCTTCCTCCTTG	
human	*Xbp1*	Forward	TGAGCTGGAACAGCAAGTGG	Splicing assay
		Reverse	ATACCGCCAGAATCCATGGGGA	
SARS-CoV-2	*N*	Forward	TCACCGCTCTCACTCAACAT	RT-PCR
		Reverse	CTGGCCCAGTTCCTAGGTAG	

VII. Results

PART I

Expression of *XBP1* in nasopharyngeal swabs of patients with symptoms of COVID-19 illness

Initial assays were conducted in nasopharyngeal samples from patients receiving medical assistance for symptoms consistent with COVID-19 disease. 119 samples of nasopharyngeal swabs were randomly collected from different medical departments at Hospital Clínico Universitario of Valladolid. The demographic analysis of patients with SARS-CoV-2 RT-PCR positive assays showed older distribution than those with a negative assay. The same trend was observed when the analysis was carried out in cohorts stratified by sex; however, statistical significance was not observed in this case, what can be explained by the lower number of patients included in each cohort (**Figure 9**).

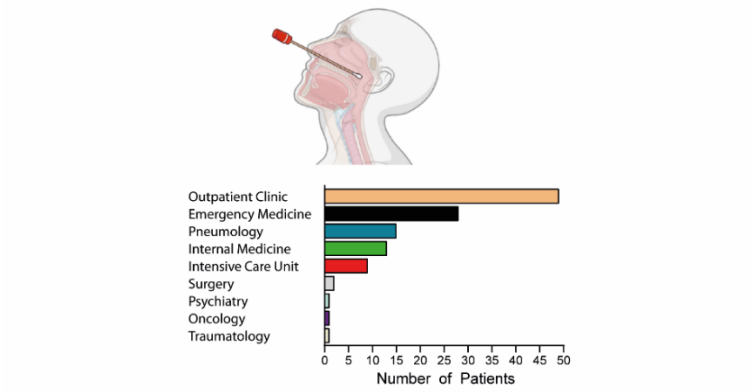

COVID-19 +	Age (mean ±SEM)	Age Range (years)	n	COVID-19 -	Age (mean ± SEM)	Age Range (years)	n	P value
Total	62.07±2.381	11-92	60	Total	55.54±2.679	18-91	59	n.s.
Females	60.31±3.877	11-92	26	Females	55.61±3.492	18-89	36	n.s.
Males	63.41±3.008	22-88	34	Males	55.43±4.263	21-91	23	n.s.

FIGURE 9. Stratification of patients involved in the analysis of nasopharyngeal swabs. (Upper panel) Medical departments involved in the obtention of nasopharyngeal swabs and (lower panel) demographic data.

The extracted RNA used for the diagnosis of SARS-CoV-2 infection by RT-PCR assay in the Microbiology Department, was also utilized for the assay of *sXBP1* by PCR. This entails the separation of the PCR products by electrophoresis in agarose gel and

densitometric analysis of GelRed stained bands. *sXBP1* is distinguished from *uXBP1* by its faster migration due to the loss of 26-nucleotide. The presence of *uXBP1* and *sXBP1* is shown in a random selection array of RT-PCR negative and positive samples (**Figure 10A**). The presence of three bands in some cases is explained by the formation of heteroduplexes [157]. The splicing was confirmed by separate sequencing of the bands on both strands, which showed the GenBank sequences NM_001079539.2 and NM_005080.4, for *sXBP1* and *uXBP1* respectively. The former sequence differs from the later by the deletion of 26 nucleotides (**Figure 10B**).

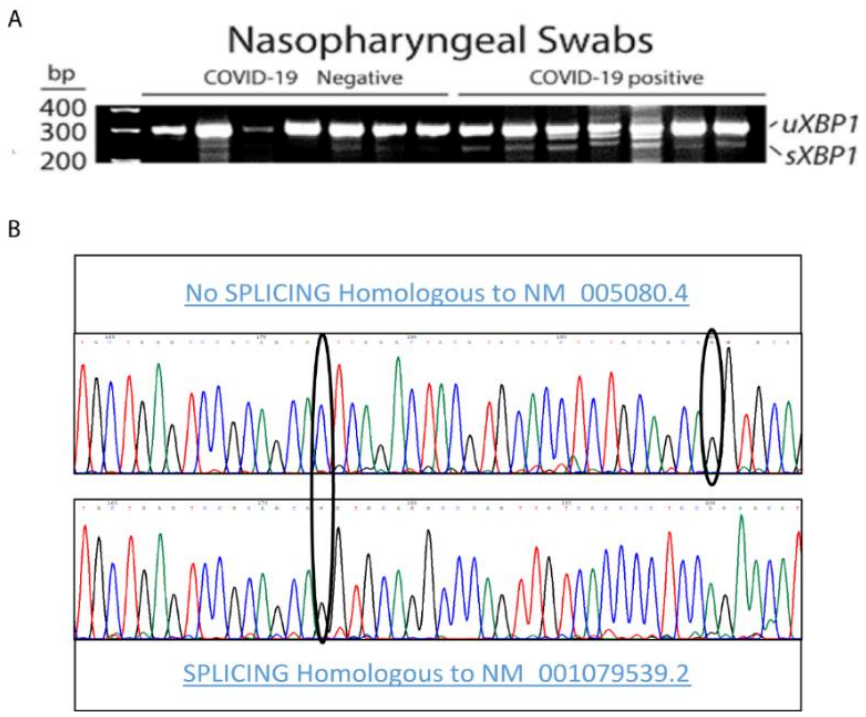

FIGURE 10. Analysis of RT-PCR products and sequences of *XBP1* mRNA transcripts in nasopharyngeal samples. (A) Agarose gel electrophoresis of *XBP1* showing the *sXBP1* and *uXBP1* products in a series of samples from COVID-19 negative and positive patients. The presence of three bands in some cases is due to the formation of heteroduplexes. (B) Amplicon sequencing showing the splicing of 26 nucleotides in NM_005080.4 sequence that generates the sequence in NM_001079539.2.

The extent of *sXBP1* was quantitated by the ratio (*sXBP1/XBP*^{T}) and showed higher values in COVID-19 positive patients than in those showing negative tests (**Figure 11**).

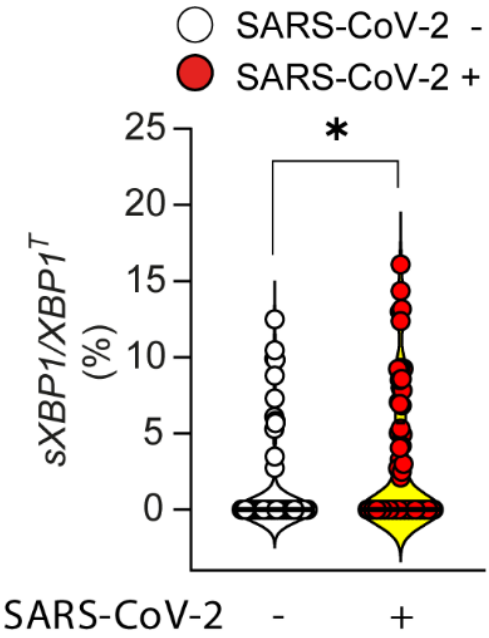

Figure 11. Densitometry quantification of *XBP1* PCR products in nasopharyngeal swab samples. Quantification of *sXBP1* in COVID-19 positive and negative samples. *p < 0.05 paired (two tail).

RT-PCR infection tests showed negative results in 59 patients and positive in 60 patients. *sXBP1* was detected in 17.91% of SARS-CoV-2 negative and in 40.32% of SARS-CoV-2 positive patients (**Figure 12A**). A demographic survey showed that the presence of *sXBP1* was higher in older SARS-CoV-2 positive patients (**Figure 12B**), while no significant difference was observed between female and male patients (**Figure 12C**). Mortality was observed in four patients who showed a degree of splicing above 10% of total *XBP1* (**Figure 12D**).

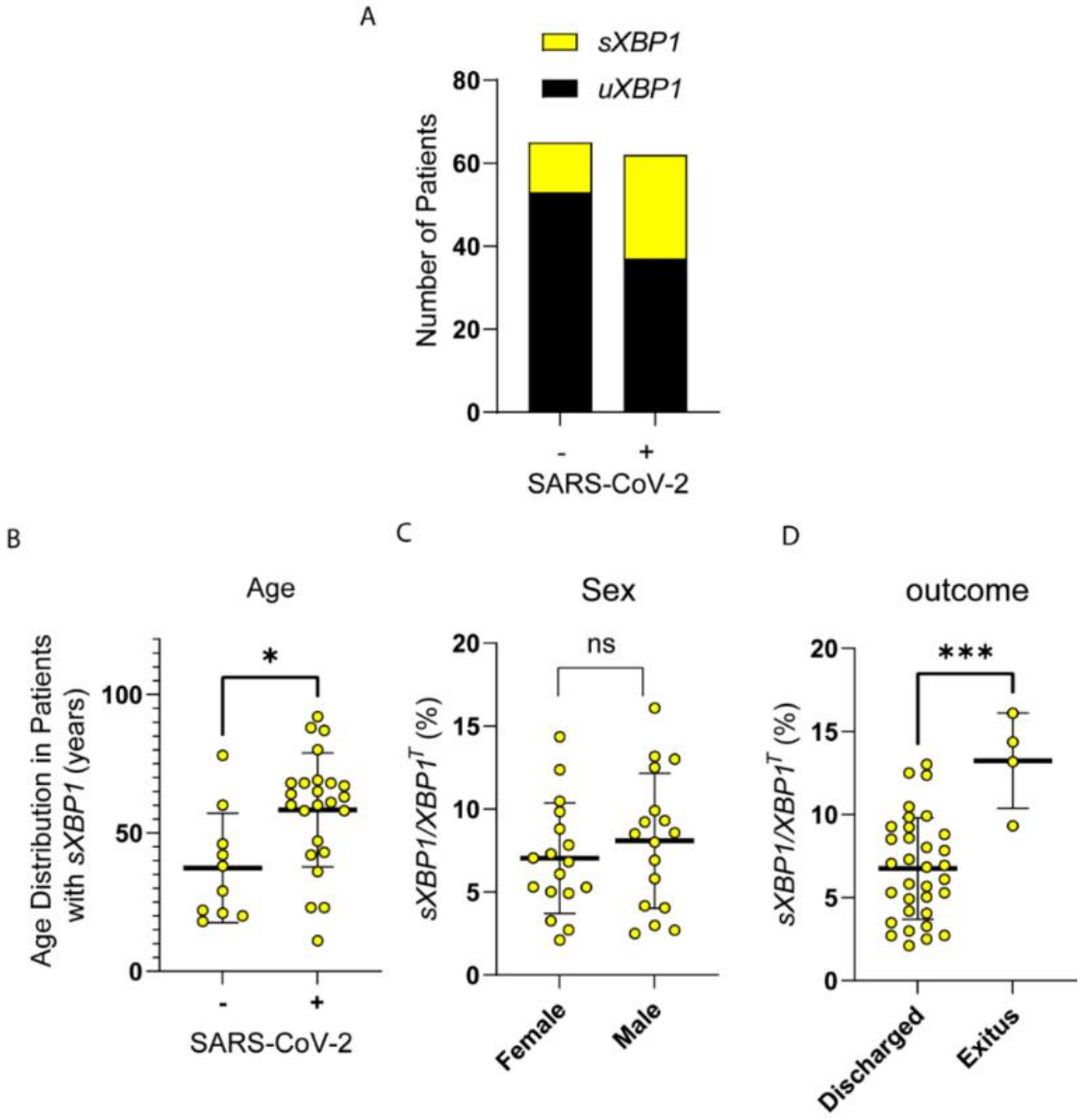

<u>Figure 12.</u> Demographic results of patients with *sXBP1*. (A) Distribution of patients according to the presence or absence of *sXBP1* in SARS-CoV-2 positive and negative patients. (B) Age distribution of patients with *sXBP1*. (C) Quantitation of *sXBP1* in males and females. (D) Quantitation of *sXBP1* according to the outcome in SARS-CoV-2 positive and negative patients. *$p < 0.05$, ***$p< 0.005$ paired (two tail).

These findings show a higher incidence of *sXBP1* in nasopharyngeal exudates from patients with active SARS-CoV-2 infection, particularly in dying patients.

Transcriptomic profile of BAA samples in patients under mechanical ventilation due to severe SARS-CoV-2 pneumonia

In view of the previous results in nasopharyngeal swabs, further studies were carried out using RNA extracted from BAAs of patients under mechanical ventilation and endotracheal intubation. Ventilatory support and endotracheal intubation were indicated because of acute hypoxemic respiratory failure despite high-flow nasal oxygen therapy or non-invasive ventilation at the ICU. BAA samples were collected according to the protocol shown in **Figure 13A**. Patients were assigned to the different cohorts as indicated (**Figure 13B**). The study involved 85 patients and demographic data showed older distribution in non-COVID patients, while mortality was found higher in post-COVID patients showing *sXBP1* and non-COVID patients with *uXBP1*. COVID-19 patients received a standard and proved useful treatment for the hyperinflammatory state consisting of 6 mg dexamethasone daily or 50 mg of IV hydrocortisone every 8 hours for up to 10 days, while this protocol was not routinely used in non-COVID-19 patients.

A

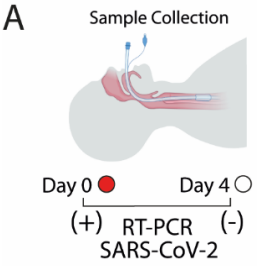

B

Pneumonia	Age (mean± SEM)	*sXBP1* % mortality	*uXBP1* % mortality	Steroid treatment
COVID-19 RT-PCR +	69.90 ± 2.006	22.72	22.22	Mandatory
Post-COVID RT-PCR -	70.92 ± 2.995	33.33	22.66	Mandatory
Non-COVID	75.59 ± 1.561	16.66	40.33	Occasional

Figure 13. Stratification of patients involved in the study of BAAs. (A) Scheme of sample collection. Day 0 indicates the time at which the last RT-PCR SARS-CoV-2 positive test was recorded. Day 4 indicates that the sample was RT-PCR SARS-CoV-2 negative and is referred as post-COVID. (B) Patient were assigned to the different cohorts according to SARS-CoV-2 RT-PCR test diagnosis, including active COVID-19 infection, post-COVID-19 infection and non-COVID infection. Demographic data of the different cohorts showing age, mortality and steroid treatment.

Analysis of the UPR genes in BAAs

The evolution of XBP1 splicing and viral load in a patient under respiratory control for 16 days is shown in **Figure 14A**. The extent of *sXBP1* was higher in SARS-CoV-2 pneumonia patients than in those with respiratory failure due to other conditions and decreased after COVID-19 tests turned negative (**Figure 14B**). Moreover, *sXBP1* rate showed higher values than those observed in nasopharyngeal swabs.

The PERK-eIF2α-ATF4-CHOP branch of the UPR was explored assaying *DDIT3*/CHOP gene expression. *DDIT3*/CHOP expression decreased after SARS-CoV-2 tests turned negative, while there was no significant difference of expression between non-COVID-19 and COVID-19 pneumonia patients (**Figure 14C**).

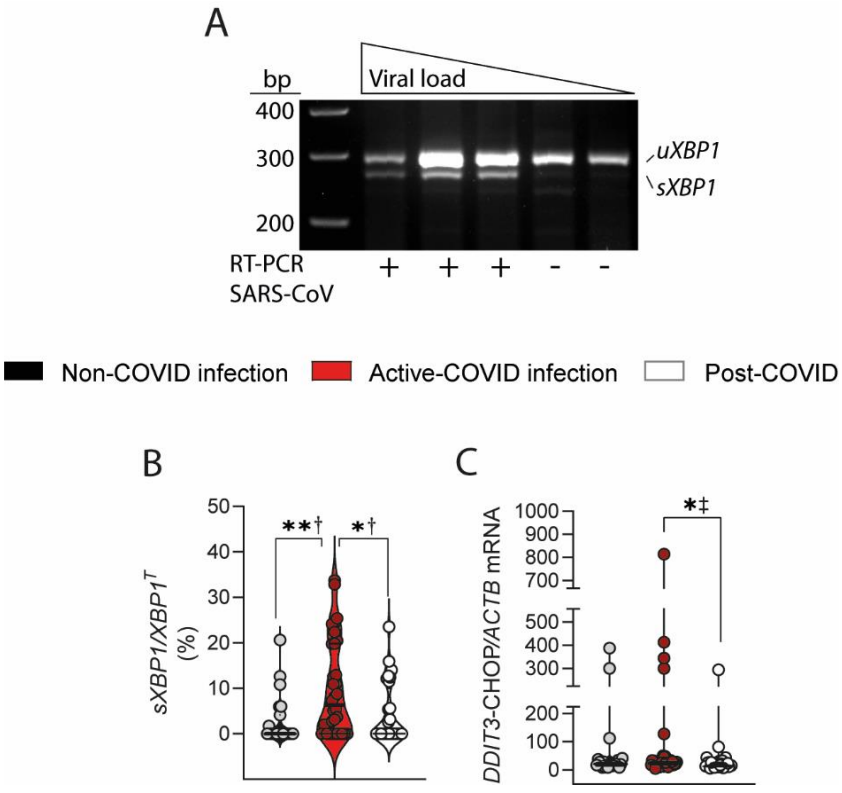

Figure 14. Expression of *XBP1* and *DDIT3*/CHOP in BAAs. (A) Evolution of *XBP1* splicing and viral load in BAAs of a patient with SARS-CoV-2 infection under respiratory control for 16 days. (B-C) *sXBP1* quantification and *DDIT3*/CHOP expression in the different cohorts. Results are expressed as mean ± SEM. *p < 0.05, **p < 0.01. †Ordinary one-way ANOVA with the Tukey's multiple comparisons test. ‡Kruskal-Wallis *U* test.

Next, we evaluated different UPR-target genes. The higher values of *sXBP1* observed in active COVID-19 infection was accompanied by an increased expression of the sXBP1 downstream gene ER DNAJ family-4 (*ERDJ4).* Moreover, the expression of ER degradation enhancing α-mannosidase like protein 1 (EDEM1) did not reach statistical significance as compared to non-COVID-19 pneumonia, although it decreased after infection turned negative (**Figure 15A**).

The expression of the ATF4-dependent genes asparagine synthetase (glutamine-hydrolyzing) (*ASNS*) and cystathionine γ-lyase (*CTH*) was higher in COVID-19 patients than in non-COVID-19 infection (**Figure 15B**), which agrees with early reports on the activation of PERK branch by coronavirus [158, 159]. The ATF6 target genes homocysteine inducible ER protein with ubiquitin like domain 1 (*HERPUD1*) and *HSPA5* did not show significant difference between non-COVID-19 and COVID-19 pneumonia (**Figure 15C**).

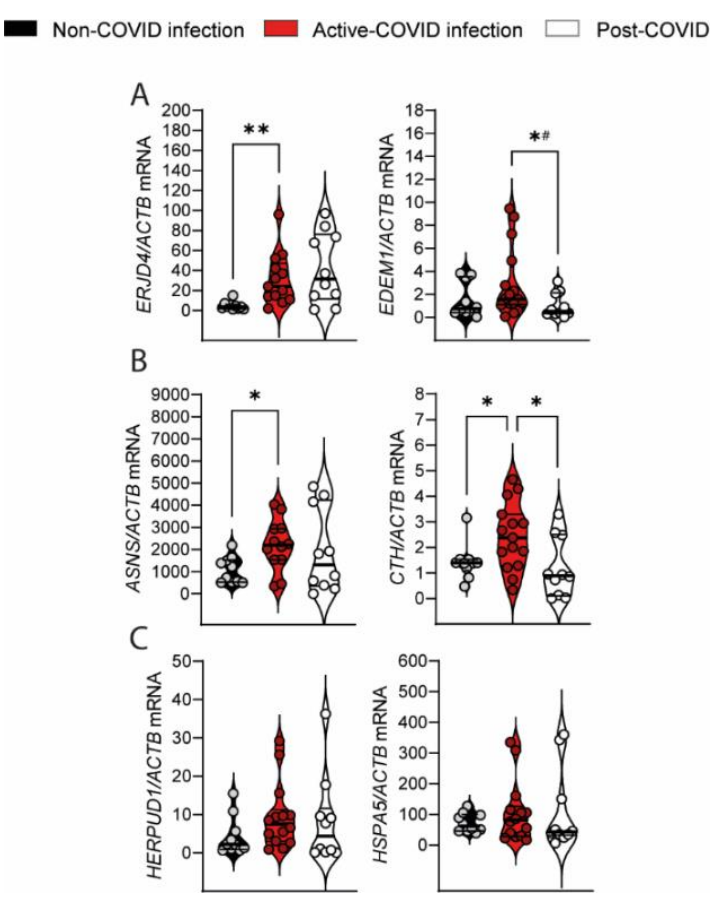

Figure 15. UPR target genes expression in BAAs samples. (A) mRNA expression of the sXBP1-dependent genes *ERJD4* and *EDEM1* in the different cohorts. (B) mRNA expression of the ATF4-dependent genes *ASN* and *CTH*. (C) mRNA expression encoding the AT6-dependent genes *HERPUD1* and *HSPA5*. Results are expressed as mean ± SEM. *p < 0.05, **p < 0.01. #Welch's test.

Analysis of the cytokine signature in BAAs

Given the role assigned to the CS in SARS-CoV-2 infection (**Figure 16A**), the expression of cytokine mRNAs was assayed in BAAs. During viral proliferation, *IL1B* and *IL6* mRNA levels were significantly lower than those detected in non-COVID-19 patients. Cytokine mRNA did not show a trend to decrease after SARS-CoV-2 tests were negative (**Figure 16B-C**). In contrast, *IL10* expression was higher in SARS-CoV-2 infection than in non-COVID pneumonia and continued elevated after COVID-19 tests turned negative (**Figure 16D**).

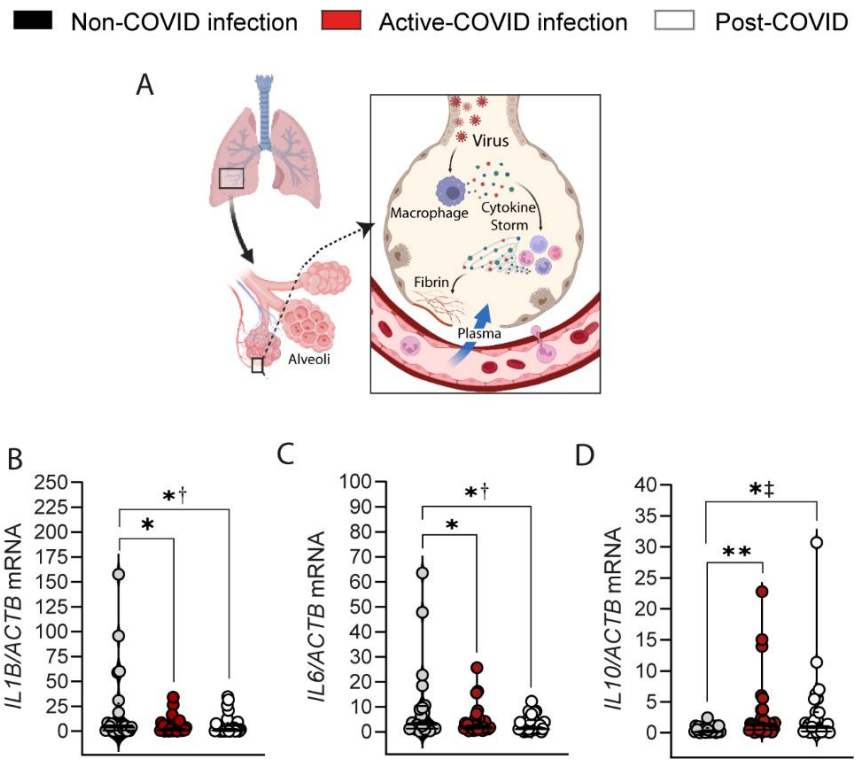

Figure 16. Cytokine profile in BAAs from ICU patients. (A) Scheme showing the mechanism leading to SARS-CoV-2 induced pneumonia and CS after viral invasion of the alveoli. (B-D) Expression of the mRNA encoding *IL1B*, *IL6*, and *IL10* in BAAs. Data are presented as mean ± SEM. *p < 0.05, **p < 0.01. †Ordinary one-way ANOVA with the Tukey's multiple comparisons test. ‡Kruskal-Wallis U test.

However, *TNF*, *IL8*, *IL12B* and *IL23A* mRNA expression did not reach any statistical significance difference between cohorts (**Figure 17A-D**).

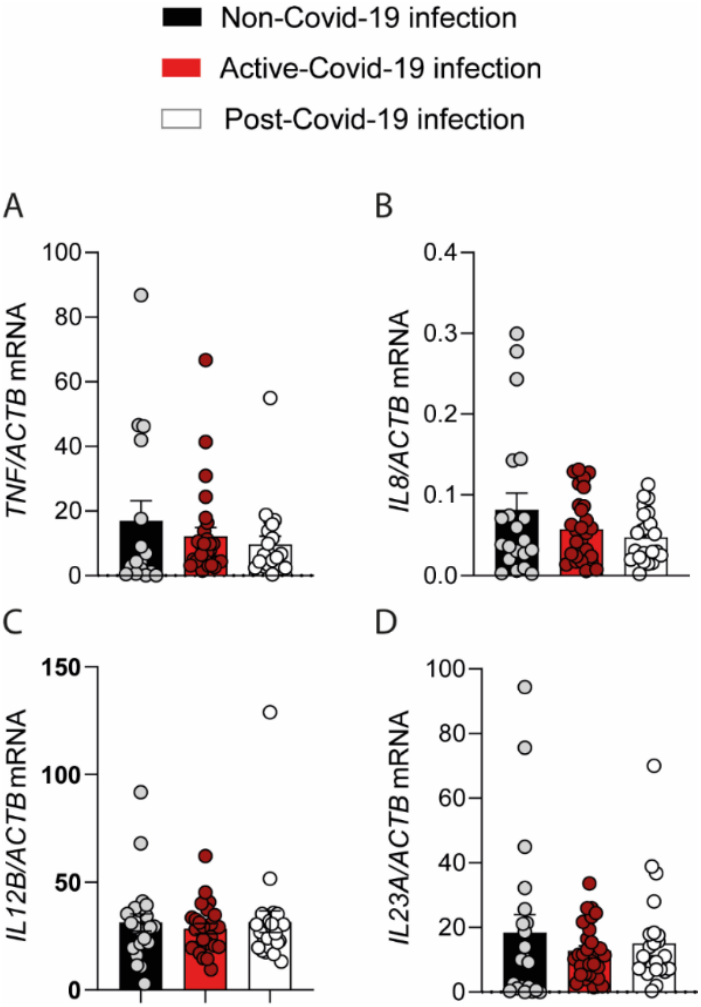

Figure 17. Cytokine profile in BAAs from ICU patients. (A-D) Expression of the mRNA encoding *TNF*, *IL8*, *IL12B* and *IL23A* in BAAs.

The analysis of IFNs and IFN stimulated genes (ISGs) showed a trend of *IFNB* to increase during COVID-19 pneumonia as compared to non-COVID infection. *IFNG* showed a trend to be increased in COVID-19, although statistical significance was not observed (**Figure18A-B**). The assay of ISGs showed decreased levels of *MX1* and *OAS1* mRNA during COVID-19 active infection, and their recovery after resolution of viral infection (**Figure 18C-D**).

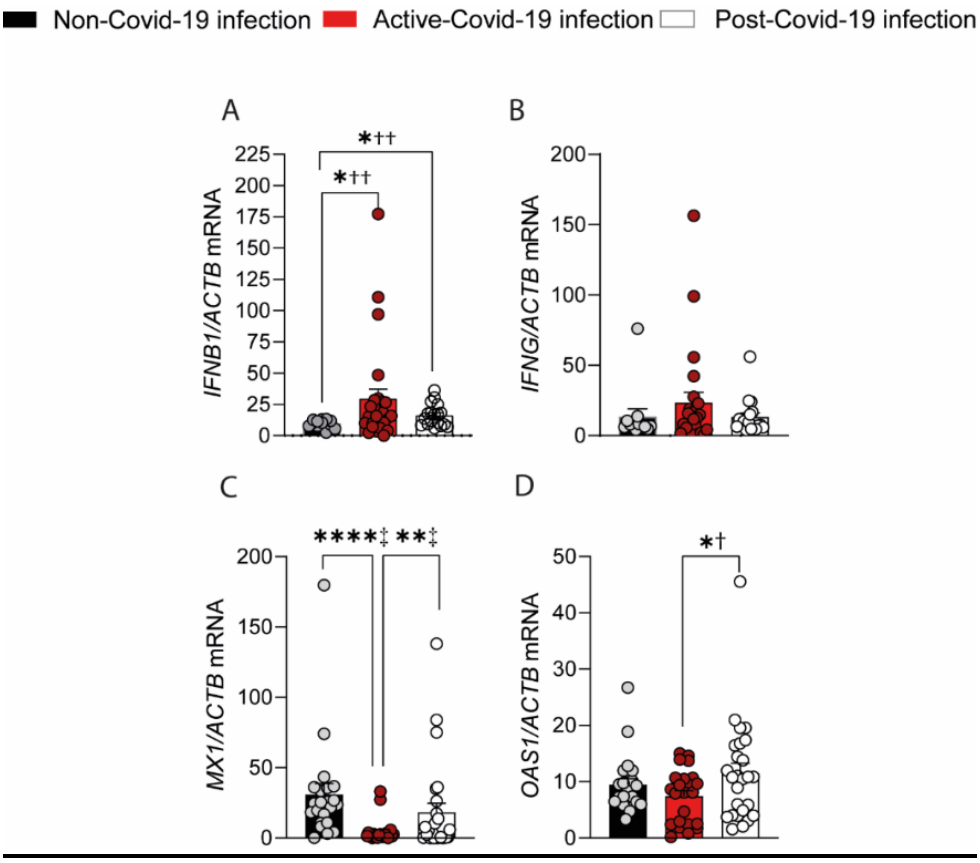

<u>Figure 18.</u> Expression of IFNs and ISGs in BAAs from ICU patients. (A-D) mRNA expression of *IFNB*, *IFNG*, *MX1*, and *OAS1*. Data are presented as mean ± SEM. *p < 0.05, **p < 0.01, ****p < 0.001. ‡Kruskal-Wallis U test. ††Welch and Brown-Forsythe ANOVA test.

Overall, these results show that the levels of cytokine expression were higher in non-COVID-19 pneumonia compared to COVID-19 pneumonia. The high expression of *IL10* mRNA suggests a parallel activation of an archetypal anti-inflammatory cytokine that might counter the inflammatory response. The increased expression of *IFNB1* mRNA is consistent with its involvement in viral sepsis. The low expression of *MX1* agrees with the reported association of single nucleotide polymorphisms within *TMPRSS2* and near *MX1* gene with severe COVID-19 disease [160]. A cogent explanation for the low *MX1* expression could be an evasive strategy of SARS-CoV-2 to avoid and/or shut down type I IFN signaling [161].

To further analyse the involvement of sXBP1 in CS, SARS-CoV-2 patients were stratified according to the presence or absence of both active infection and *sXBP1*. **Figure 19A** shows viral load in samples collected during SARS-CoV-2 infection and four days after recording the last RT-PCR COVID-19 positive test. *PTGS2, TNF* and *IL1B* mRNAs were higher in patients with *sXBP1* both during infection and after negativization of the RT-PCR test (**Figure 19B-D**). *IL6* mRNA increased in patients with *sXBP1* and active infection (**Figure 19E**). *CXCL8* mRNA was expressed at lower levels than those encoding other cytokines and showed lower values after RT-PCR tests turned negative in patients without *sXBP1,* which suggests some contribution of sXBP1 to *CXCL8* expression and agrees with the low induction of *CXCL8* mRNA observed upon infection of primary nasal epithelial cells and pluripotent stem cell-derived alveolar type II cells by SARS-CoV-2 [159] (**Figure 19F**). *IL10* mRNA was higher in SARS-CoV-2 positive patients who did not show *sXBP1* and remained elevated in patients showing *sXBP1* after resolution of the infection. (**Figure 19G**). In contrast, *IL12B* and *IL23A* were not influenced by either *sXBP1* or viral load (**Figure 19H-I)**.

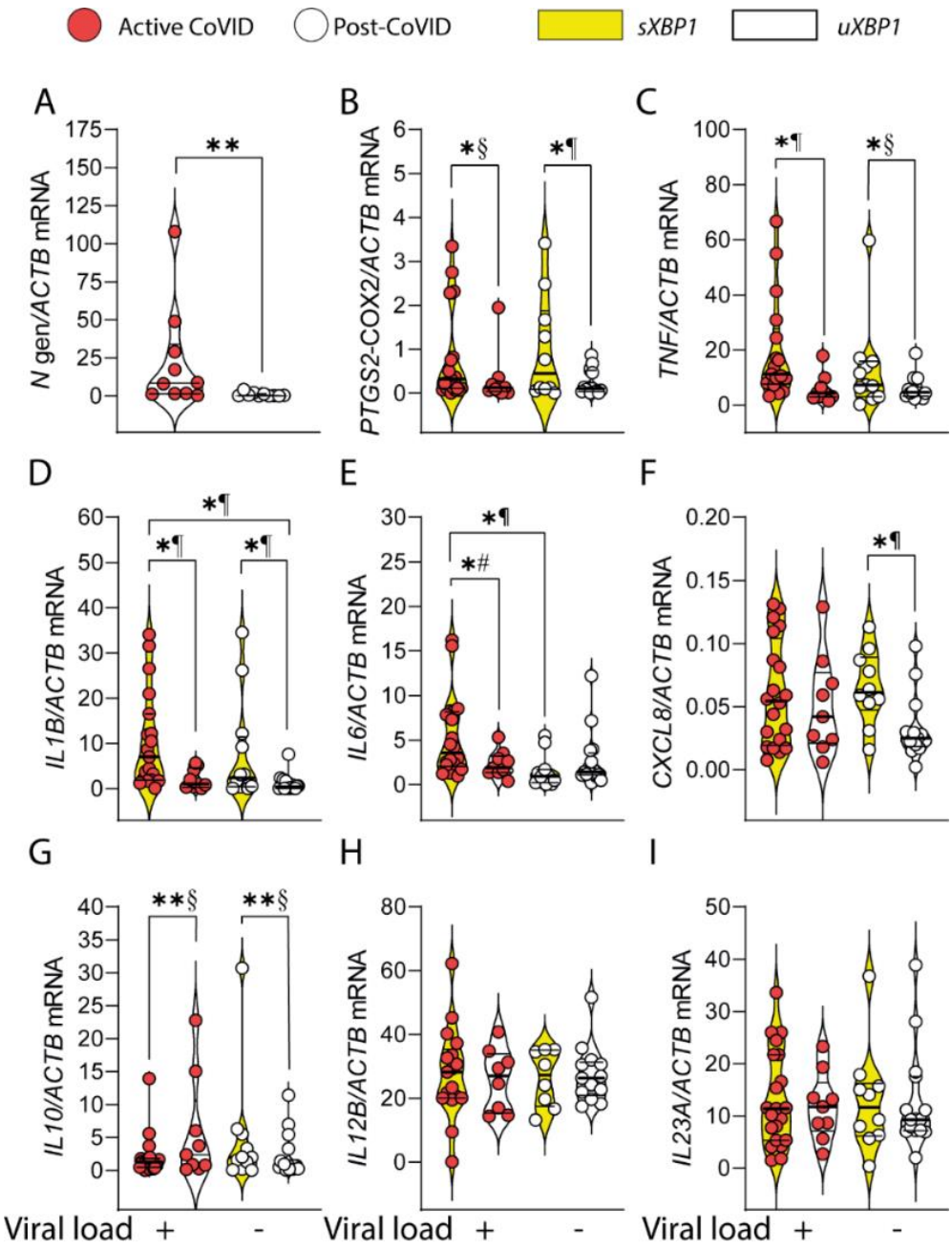

Figure 19. Association of *sXBP1* with cytokine expression in BAAs. (A) Viral load in samples obtained at the time of SARS-CoV-2 positive and negative tests (B-I) Patients were stratified in cohorts according to the presence of *sXBP1* and the presence or absence of viral load as deemed from RT-PCR test for SARS-CoV-2 infection. The mRNA of *PTGS2* and various cytokines was assayed in the extracted RNA and the statistical significance of the results was assayed using ordinary one-way ANOVA with Tukey´s post-hoc multiple comparison test. Data are presented as mean ± SEM. *p<0.05, **p<0.01, ***p<0.005. §One-sample Wilkoxon signed rank test. ¶Unpaired (two-tail) *t* test. #Welch's test.

These results show a high expression of the mRNA of *PTGS2* and several proinflammatory cytokines in patients with *sXBP1*, which may persist after SARS-CoV-2 test become negative. Together, the results agree with the reported role of sXBP1 in the transcriptional activation of COX2, TNFα, IL-1β and IL-6.

Analysis of enzymes involved in immunometabolic reprogramming in BAAs

Lymphocytes and myeloid cells respond to PAMPs with a robust rewiring of their energetic metabolism, characterized by a reinforcement of glycolysis (**Figure 20A**). The impairment of O_2 supply due to pneumonia further explains the resort to glycolysis and agrees with reports showing that SARS-CoV-2-induced metabolic reprogramming enhances the production of proinflammatory cytokines and IFNs by monocytes, and concomitantly inhibits T cell function [162, 163]. Consistent with this notion, the expression of *GLUT1* mRNA, a glucose transporter and *HIF1A* mRNA, which encodes a subunit of a transcription factor involved in the regulation of glycolytic enzymes, were increased during active infection. However, there was no difference as compared to non-COVID-19 pneumonia (**Figure 20B-C**). The mRNA encoding hexokinase II (HK2), pyruvate dehydrogenase kinase IV (PDK4) and malate dehydrogenase (MDH) 2 increased during active infection as compared to both non-COVID-19 pneumonia and post-COVID infection (**Figure 20D-F**). Proteins involved in mitochondrial function also increased during active COVID-19 pneumonia, including, succinate dehydrogenase (SDH) subunit A, the 2-oxoglutarate-malate transporter (SLC25A11), and *cis*-aconitate dehydrogenase (*IRG1* gene) (**Figure 20G-I**).

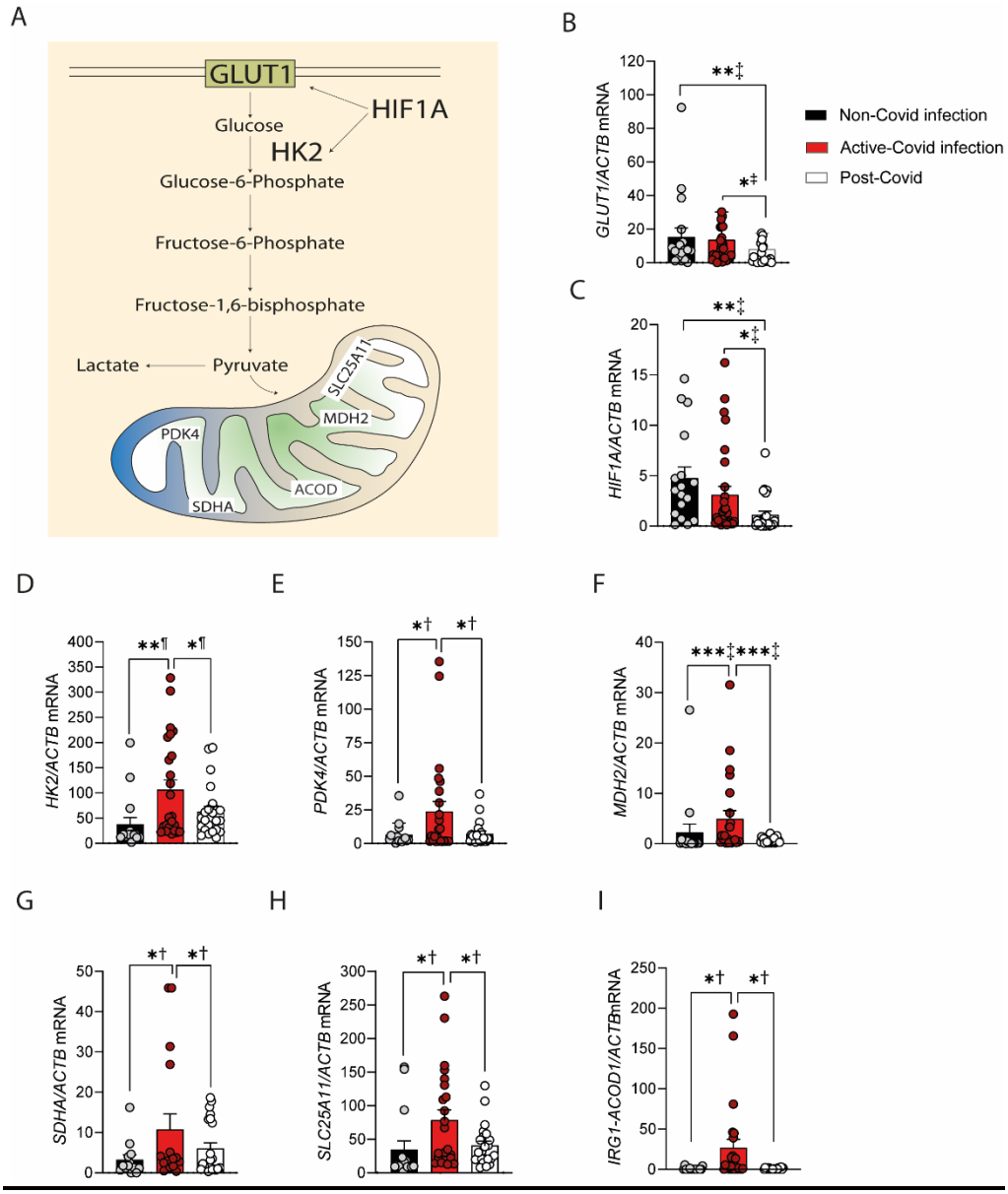

<u>Figure 20.</u> Expression of enzymes involved in glycolysis and mitochondrial proteins. (A) Diagram of glycolytic and mitochondrial proteins assayed in BAAs. (B-I) BAAs of patients with controlled respiration were used for RNA extraction and RT-PCR assay of mRNA expression of genes encoding for proteins involved in glycolysis, response to hypoxia, and mitochondrial function. *GLUT1*, glucose transporter 1. *HIF1A*, hypoxia-inducible factor 1α. *HK2*, hexokinase 2. *PDK4*, pyruvate dehydrogenase kinase. *MDH2*, malate dehydrogenase 2. *SDHA*, succinate dehydrogenase protein subunit A. *SLC25A11*, mitocondrial 2-oxoglutarate-malate carrier. *IRG1*/ACOD1, immunoresponsive gene 1-aconitate decarboxylase. Data are presented as mean ± SEM. *p < 0.05, **p < 0.01, ***p < 0.005. ‡Kruskal-Wallis *U* test. †Ordinary one-way ANOVA. ¶Paired or unpaired (two-tail) *t* test.

Together, these data show a resort to glycolysis during active SARS-CoV-2 infection that seems supported by the activity of HIF1 and elements of the malate-aspartate shuttle such as MDH2 and SLC25A11, which buttress the NAD^+/NADH redox balance necessary for the progression of glycolysis at the glyceraldehyde 3-phosphate-dehydrogenase step.

Analysis of monocyte-macrophages differentiation markers in BAAs

The characterization of the monocytic-macrophage lineage was addressed assessing the expression of several well-known differentiation markers. *HLA-DRB1*, which encodes a protein involved in antigen presentation, and *BATF3* showed a reduced expression during active COVID-19 infection (**Figure 21A-B**). *CD300E* a gene associated with survival signals, the chemokine receptor *CCR2*, and the migration receptor *MMP9* showed a reduced expression associated with the detection of SARS-CoV-2 RT-PCR positive tests (**Figure 21C-E**).

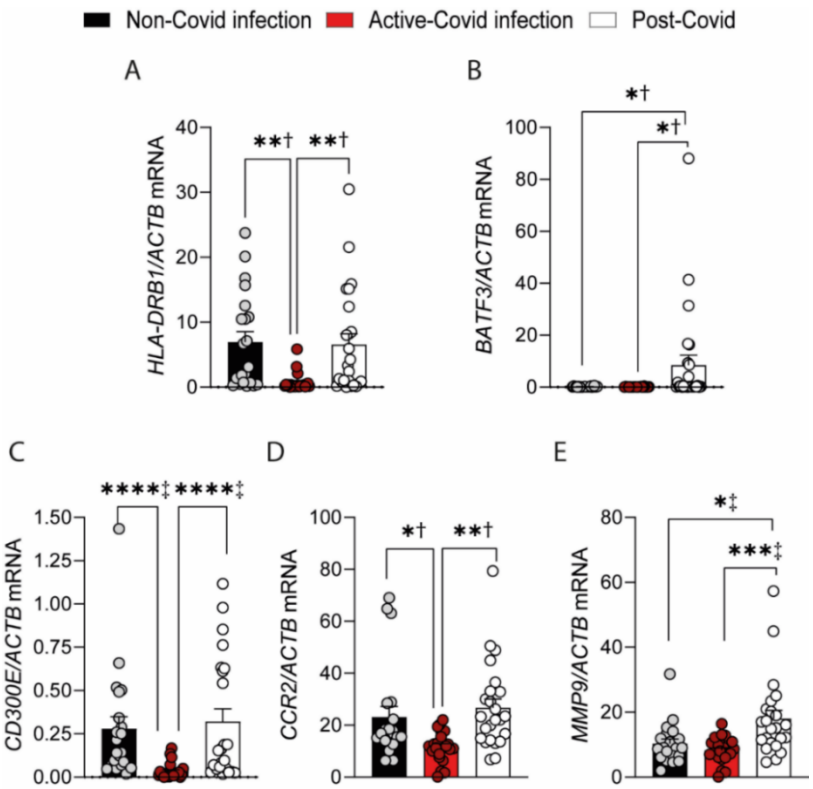

Figure 21. Expression of markers involved in the differentiation of the monocyte-macrophage lineage. (A-E) mRNA expression of *HLA-DRB1*, *BATF3*, *CD300E*, *CCR2* and *MMP9*. Data are presented as mean ± SEM. *p < 0.05, **p < 0.01, ***p < 0.005, ****p < 0.001. †Ordinary one-way ANOVA. ‡Kruskal-Wallis *U* test.

These results disclose a differentiation profile during COVID-19 infection characterized by a low expression of markers associated with antigen presentation and survival signals, as well as *CCR2* and *MMP9* involved in chemotaxis and migration functions.

TLR7/8 expression in BAAs and MDDCs

TLR7 and TLR8 expression were assayed given their involvement in the recognition of viral RNA. *TLR8* mRNA was expressed to a far greater extent than *TLR7* mRNA both in BAAs and in MDDCs (**Figure 22A-B**), which agrees with the decay of *TLR7* expression during the differentiation of monocytes to MDDCs [162].

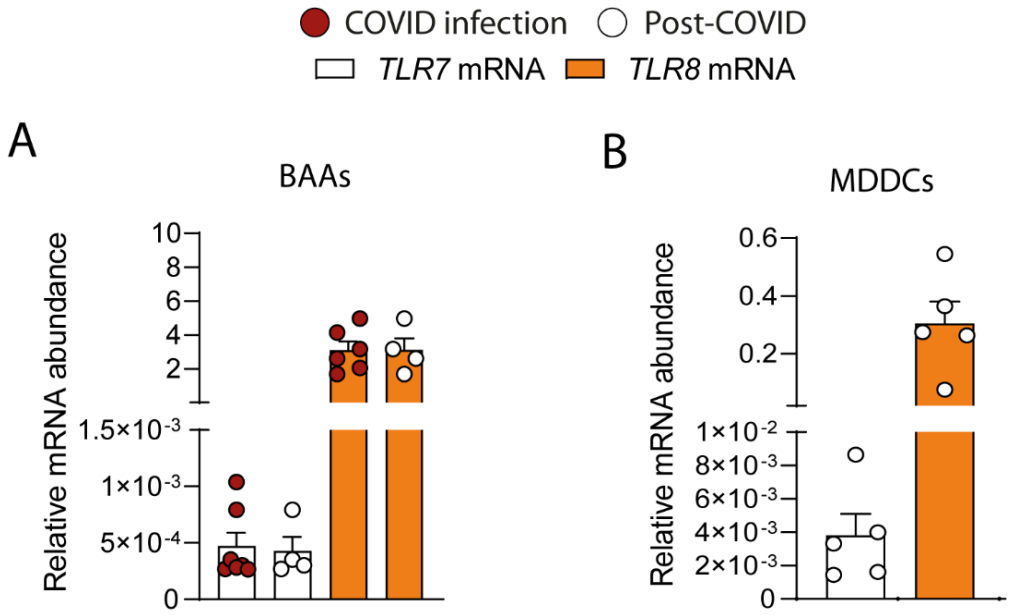

Figure 22. Expression of *TLR7* and *TLR8* mRNA in BAAs from ICU patients and MDDCs. (A) Expression of *TLR7* and *TLR8* mRNA in patients with active SARS-CoV-2 infection and after negative tests. (B) Expression of the mRNA encoding *TLR7* and *TLR8* in MDDCs.

Because SARS-CoV-2 is a positive ssRNA virus, we posited that TLR7/8 might shape the innate immune response, given their endosomal location and accessibility to intracellular viral RNA.

PART II

Effect of TLR7 and TLR8 ligands in MDDCs

The high expression of *TLR8* and the low expression of *TLR7* mRNA singles out TLR8 as the main receptor involved in the recognition of ssRNA by MDDCs. The morphology of MDDCs stimulated with the TLR7 agonist imiquimod and the TLR8 ligand ssRNA40 (20-mer phosphorothioate protected single-stranded RNA oligonucleotide containing a GU-rich sequence) was assessed using conventional microscopy after four hours of stimulation. An overt elongated phenotype was observed in ssRNA40 stimulated MDDCs. This morphological change was construed as the spreading required for MDDC migration following activation [164]. In contrast, this phenotype was not found in imiquimod-treated MDDCs (**Figure 23**), which agrees with the notion that recognition of ssRNA by TLRs in MDDCs is mediated by TLR8 and may play a role in viral recognition.

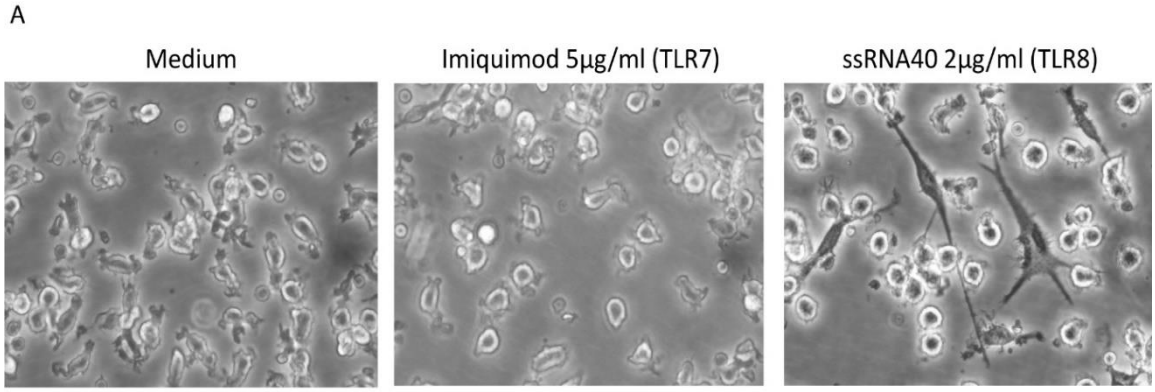

Figure 23. Effect of imiquimod and ssRNA40 in MDDCs. MDDCs were stimulated at the concentration indicated with the different ligands for 4 hours before analysis of the morphologic phenotype by conventional microscopy. Unstimulated cells (left panel), imiquimod (medium panel) and ssRNA40 (right panel) stimulated cells.

The activation of the UPR by imiquimod and ssRNA was assayed by measuring *XBP1* mRNA in agarose gel electrophoresis and qPCR using specific oligonucleotides flanking the splicing regions of s*XBP1*. Imiquimod showed a low extent of *XBP1* splicing,

even in real-time RT-PCR assays (**Figure 24A-B**). Consistent with the potentiating effect of palmitate on the splicing of *XBP1* reported in mice [165] and the enhancing effect of 2-deoxyglucose [6], combination of imiquimod with these compounds induced *sXBP1* to a higher extent (**Figure 24A-B**). In contrast to the limited effect of imiquimod, the TLR8 agonist ssRNA40, induced a robust degree of *XBP1* splicing, which in turn was blocked by the IRE1α RNase inhibitors MKC8866 (**Figure 24C-D**).

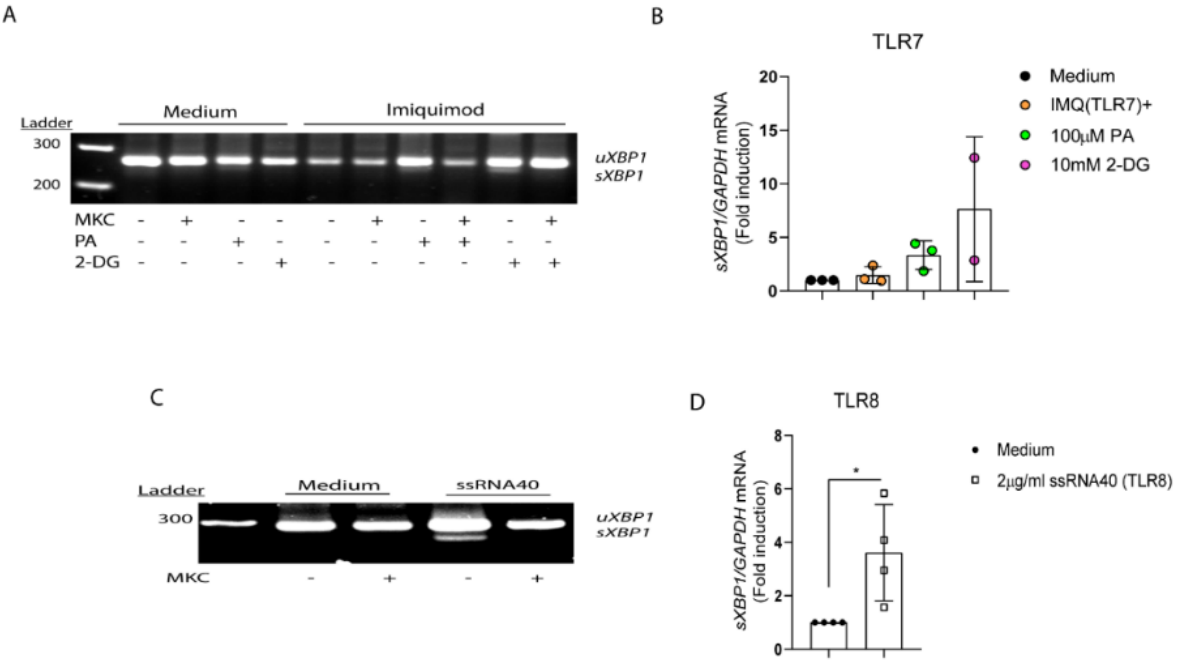

<u>Figure 24.</u> Assay of *XBP1* in MDDCs stimulated by imiquimod and ssRNA40. (A-D) MDDCs were stimulated with imiquimod and ssRNA40 for 4 hours, and then RNA was collected for the assay of *XBP1* splicing by RT-PCR followed by agarose analysis and qPCR. The palmitate and 2-DG priming experiments were conducted adding the priming agents 1 hour before imiquimod. Data are presented as mean ± SEM. *p < 0.05 paired *t* test.

Given that IFN teams up with TNF to induce mortality in mice during SARS-CoV-2 infection [166] and IFN has been associated with the development of CS [167-170], the expression of type I IFNs and ISGs was assayed in MDDCs, in the presence of MKC8866 and the SIR1 agonist fluvoxamine [133]. MKC8866 and fluvoxamine did not influence the

expression of IFNs and the ISGs *MX1* and *OAS1* mRNA in imiquimod stimulated MDDCs (**Figure 25A**), while the expression of *MX1* and *OAS1* mRNA decreased in ssRNA40 treated MDDCs (**Figure 25B**). Thus, suggesting a direct effect of sXBP1 on *MX1* and *OAS1* expression, rather than an indirect effect mediated by IFNs.

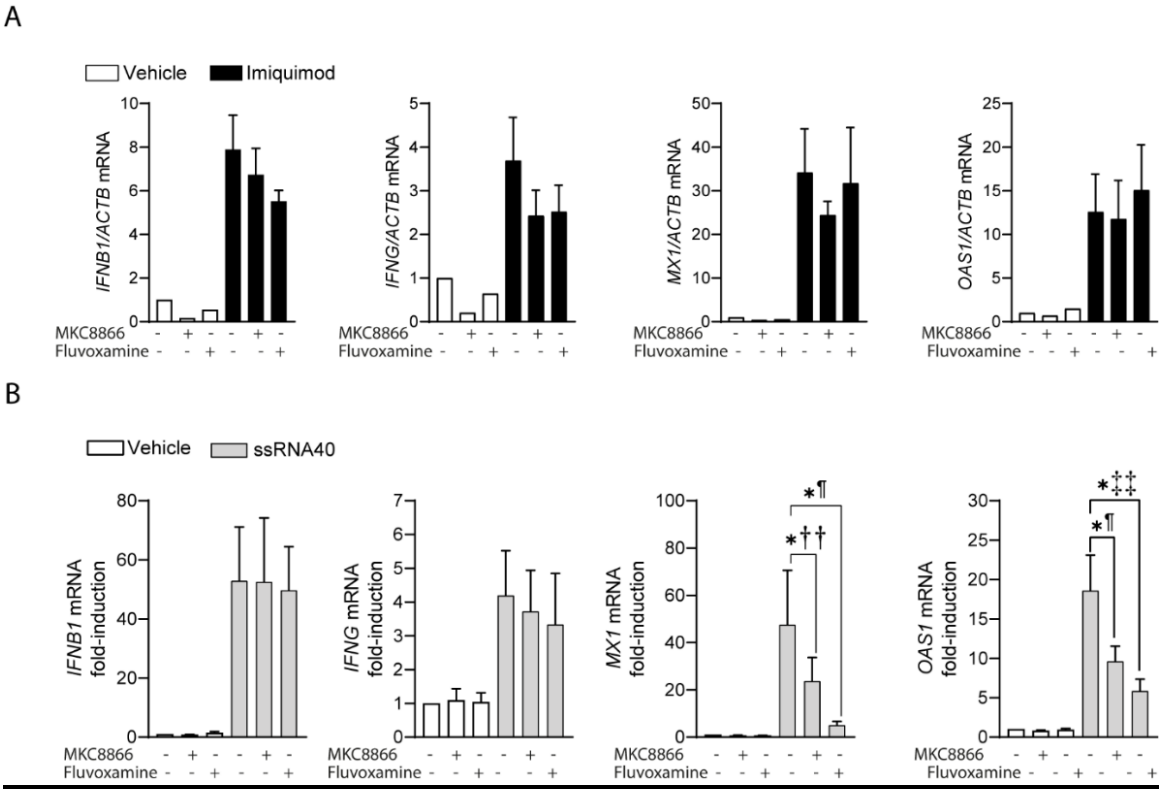

Figure 25. **IFN and ISG expression induced by imiquimod and ssRNA40.** (A-B) MDDCs were stimulated with imiquimod or ssRNA40 in the presence and absence of MKC8866 and fluvoxamine added 1 hour before stimulation. Data are presented as mean ± SEM. *p < 0.05, paired, (two-tail) Student's *t* test. ‡Kruskal-Wallis *U* test. ††Welch and Brown-Forsythe ANOVA test. ¶Paired *t* test two-ways.

Since imiquimod showed a limited capacity to induce *sXBP1*, it was posited that association with the IRE1α activator IXA4 could exert a synergistic effect. Combination of

IXA4 and imiquimod induced *sXBP1* (**Figure 26A**); however, this did not influence cytokine expression (**Figure 26B**).

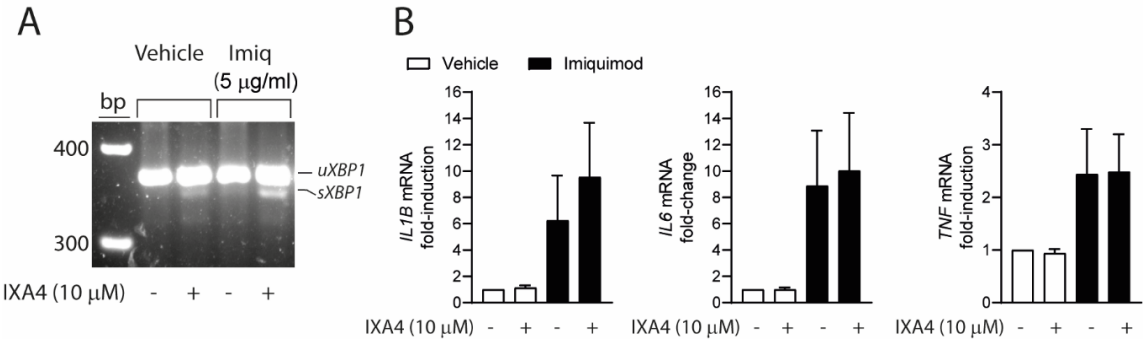

Figure 26. Effect of the IRE1α activator IXA4 on the expression of the mRNA of *IL1B*, *TNF*, and *IL6* mRNA elicited by imiquimod. (A) Effect of IX4A on *sXBP1* splicing. MDDCs were preincubated in the presence and absence of IXA4 for 30 min and then stimulated with 5 μg/ml imiquimod for 1 hour. At the end of this time, RNA was extracted and used for the assay of *XBP1*. (B) Effect of the pretreatment with IXA4 for one hour on the expression of proinflammatory cytokines induced by imiquimod. The stimulation with imiquimod was maintained for four hours before RNA extraction. Data are presented as mean ± SEM** $p < 0.01$ ratio paired *t* test, * $p < 0.05$ paired *t* test.

Conversely, IXA4 increased the expression of *IL1B* and *TNF* mRNA induced by ssRNA40 (**Figure 27A**), which agrees with the synergistic effect of sXBP1 on cytokine *trans*-activation induced by TLR2 and TLR4 [56]. In keeping with our previous report [6], sXBP1 protein was detected in nuclear extracts of MDDCs even in the absence of stimulation (**Figure 27B**). This suggests that in addition to the expression of sXBP1 protein, posttranslational modifications and/or assembly with other factors are required for transcription to start. In fact, p38 MAPK- and IKKβ-dependent phosphorylation have been found to underpin sXBP1 effect on glucose homeostasis [171, 172], and these routes are key components of TLR signaling.

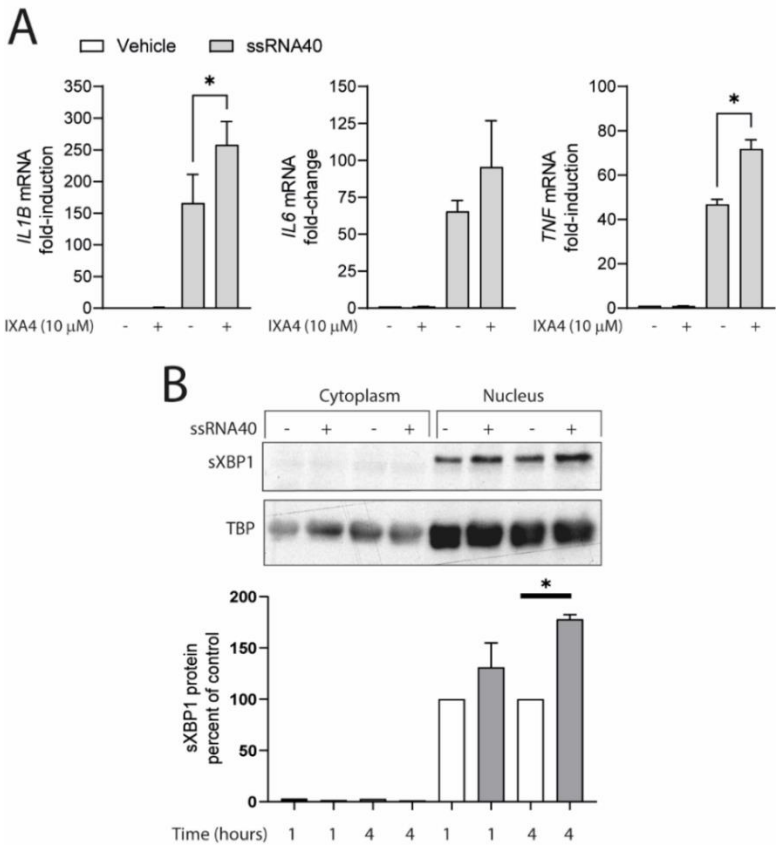

Figure 27. Effect of the IRE1α activator IXA4 on the expression of the mRNA of *IL1B*, *TNF*, and *IL6* mRNA elicited by ssRNA40. (A) MDDCs were incubated with IXA4 for 30 min and then stimulated with 2 μg/ml ssRNA40 for 4 hours. After this time, RNA was extracted and used for the RT-PCR assay of cytokine mRNA. *p < 0.05, paired (two-tail) *t* test. (B) sXBP1 protein in cytoplasm and nuclear extracts from MDDCs stimulated with ssRNA40 for 1 and 4 hours as indicated. TATA-box-binding protein (TBP) was used for normalization of the densitometric scanning.

Given that sXBP1 may play a role in the transcriptional activation of proinflammatory cytokines. ChIP assays were carried out after 1 h of stimulation with ssRNA40 to explore the binding of sXBP1 to cytokine promoters. A significant binding of sXBP1 to the promoters of *IL1B*, *IL6*, and *TNF* was observed in areas containing consensus *cis*-regulatory elements associated with position weight matrices discovered in *sXBP1* target promoters (**Figure 28A-C**). The sequences are CCACG boxes, ACGT cores, and UPRE A or UPRE B sites [173].

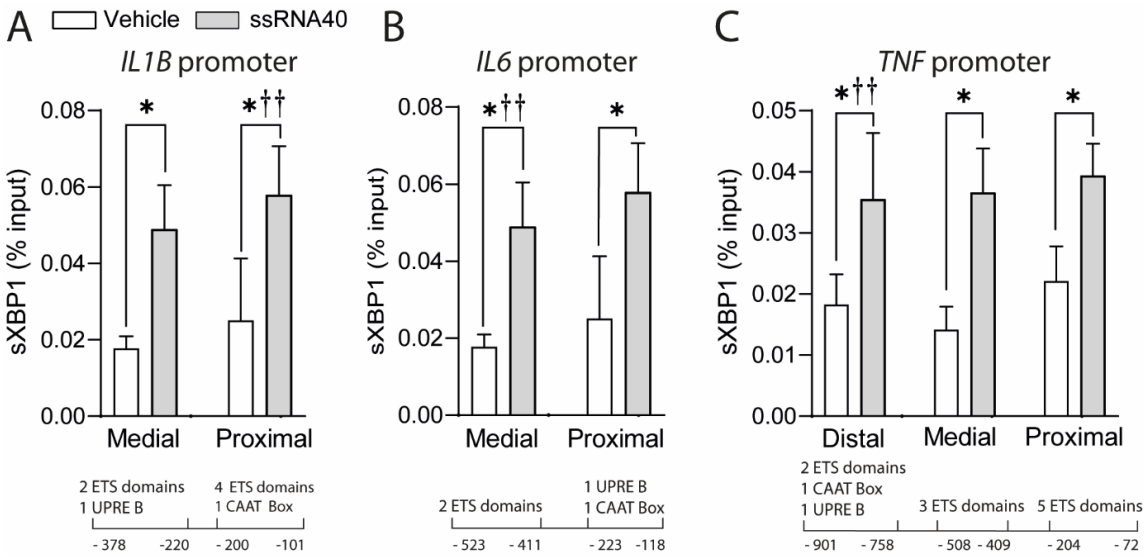

Figure 28. XBP1 binding to *IL6, TNF,* and *IL1B* promoters. (A-C) Effect of ssRNA40 on the binding of sXBP1 to the promoters of *IL1B* (left), *IL6* (middle) and *TNF* (right). The captions below the graphs indicate the distance from transcription start to the nucleotide positions where PCR primers were selected. The defined sXBP1 binding sites included in the regions spanned by the primers are indicated. Samples were obtained after one hour stimulation by 2 μg/ml ssRNA40. Data are presented as mean ± SEM. *p < 0.05. ††Ratio paired *t* test.

The inhibition of the RNAse activity of IRE1 with MKC8866 and fluvoxamine reduced the production of IL-6 and TNFα protein in MDDCs treated with ssRNA40, which confirms the involvement of sXBP1 in the *trans*-activation of these genes (**Figure 29A-B**). IL-1β was not detected in ELISA assays of MDDCs supernatants, thus suggesting that ssRNA40 does not activate the inflammasome and that an additional signal(s) is required for IL-1β secretion. Of note, the expression of pro-IL-1β was countered by MKC8866 (**Figure 29C**).

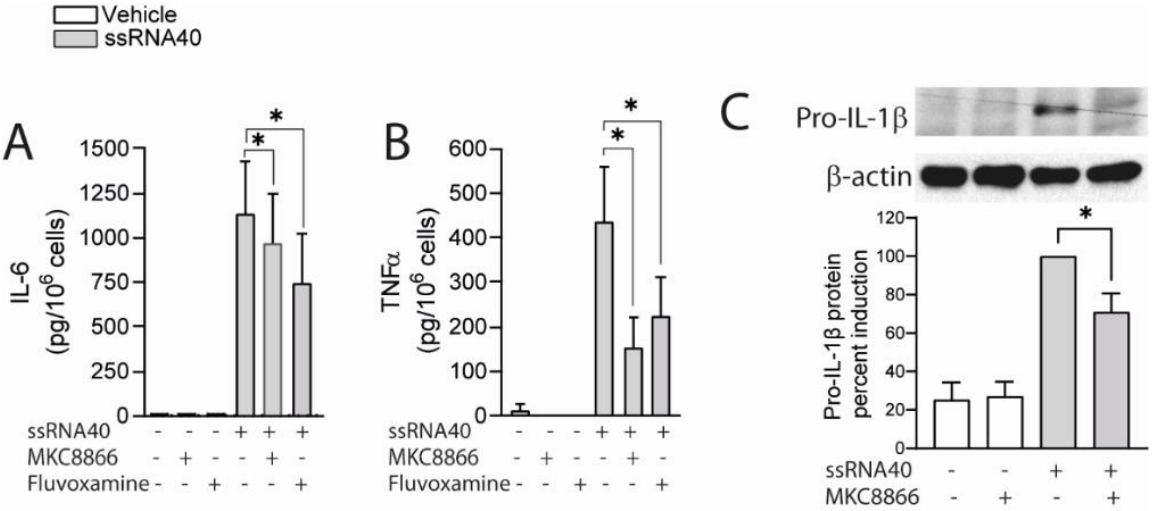

Figure 29. Effect of MKC8866 and fluvoxamine on the expression of IL-6, TNFα, and pro-IL-1β protein. (A-B) MDDCs were preincubated with MKC8866 and fluvoxamine for one hour and then stimulated overnight with ssRNA40. At the end of this period, supernatants were collected for cytokine ELISA assay. (C) Induction of the expression of pro-IL-1β by ssRNA40 and effect of MKC8866. β-actin was used for normalization. *$p < 0.05$, paired (two-tail) *t* test.

ssRNA41, a ssRNA40 derivative wherein uracil nucleotides are replaced with adenosine and does not activate TLR8-dependent signaling, did not activate cytokine expression and induced *sXBP1* to a low extent (**Figure 30A-D**). MKC8866 also inhibited the expression of *IL1B*, *IL6*, and *TNF* mRNA in ssRNA40 stimulated cells (**Figure 30B-D**).

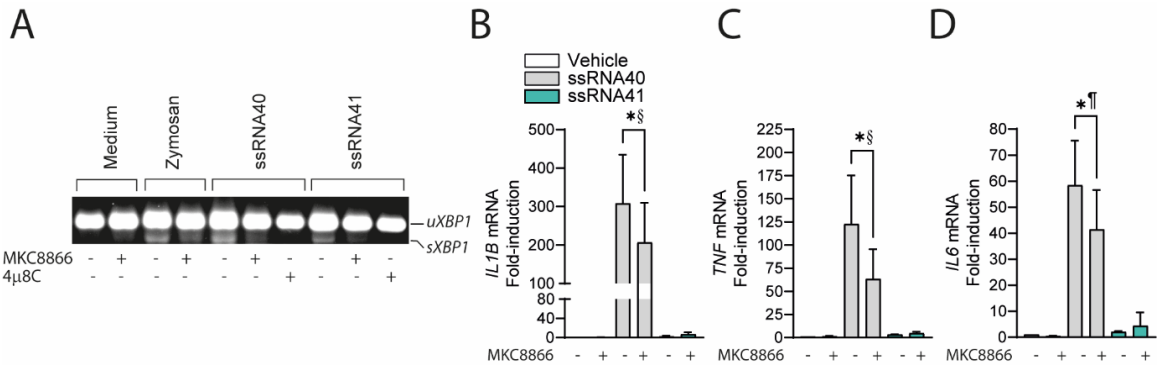

Figure 30. Comparison of ssRNA40 and ssRNA41 effects on *sXBP1* expression and TLR8-dependent signaling. (A) Effect of zymosan, ssRNA40, ssRNA41, and IRE1α endoribonuclease inhibitors on *sXBP1*. The RNA was collected after one hour of preincubation with 10 μM MKC8866 or 20 μM 4μ8C, and one hour of stimulation with 2 μg/ml of either zymosan, ssRNA40, or ssRNA41 and used for the assay of *uXBP1* and *sXBP1* mRNA. (B-D) Effect of 10 μM MKC8866 on the mRNA expression of *IL1B*, *TNF*, and *IL6* mRNA. MDDCs were maintained for one hour in the presence of MKC8866 and then stimulated with ssRNA40 or ssRNA41 for 4 hours, prior to the extraction of the RNA for cytokine assays. *p < 0.05, **p < 0.01. §Wilcoxon matched-pairs signed-rank test. ¶Paired *t* test two-ways.

The involvement of TLR8 in the effect of ssRNA40 was confirmed by the complete inhibition of the expression of *IL1B*, *TNF*, and *IL6*, as well as XBP1 splicing in the presence of the TLR8 antagonist CU-CPT9a (**Figure 31A-B**). Moreover, knocking down TLR8 mRNA with siRNA also inhibited IL1B mRNA expression (**Figure 31C**).

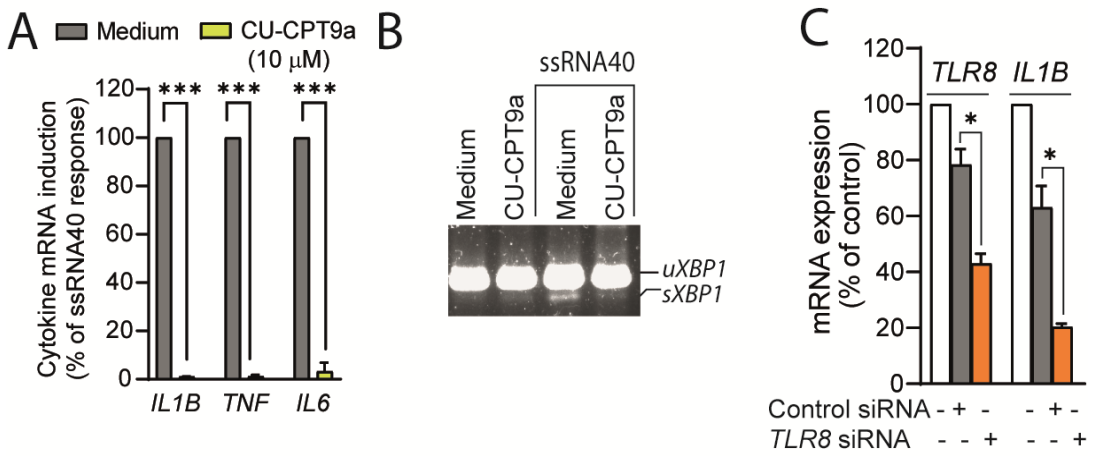

Figure 31. Pharmacological inhibition and siRNA of TLR8 in MDDCs stimulated with ssRNA40. (A-B) Effect of the TLR8 antagonist CU-CPT9a on the expression of the mRNA of cytokines and *XBP1* splicing induced by ssRNA40. ***p < 0.005, paired (two-tail) t test. (C) Effect of TLR8 knockdown with siRNA on the expression of *TLR8* and *IL1B* mRNA in response to ssRNA40. *p < 0.05, paired (two-tail) t test.

These results show that PAMPs acting on TLR8 induce a cytokine signature like that observed in BAAs and point to the central involvement of MDDCs in the innate immune response to SARS-CoV-2. The presence of *sXBP1* in nasopharyngeal swabs and BAAs, its induction by ssRNA40 in MDDCs, the effect of IRE1α RNase inhibition on the cytokine induction produced by ssRNA40, and the demonstration of sXBP1 binding to the *IL1B*, *IL6*, and *TNF* promoters suggest that TLR8-induced sXBP1 may contribute to the CS observed in severe COVID-19 disease.

PART III

***In vivo* SARS-CoV-2 infection induces UPR activation in K18-hACE2**

Ancestral SARS-CoV-2 virus cannot infect wild-type laboratory mice, which makes it necessary the use of engineered mice to perform studies. The delivery of an adenovirus expressing the human ACE2 receptor (Ad-hACE2) or the use of the K18 transgenic hACE2 (K18-hACE2) mouse provide suitable models. While Ad-hACE2 model produces a moderate ailment, lethal infection is the outcome of the K18-hACE2 disease. Indeed, Ad-hACE2 infection reported viral titres in the lungs and nasal turbinates, while K18-hACE2 disclosed spreading of the virus to other organs, such as brain, spleen, and gut [174].

Analysis of RNA extracted from homogenized whole lungs of C57BL/6 and Balb/c mice transduced *in vivo* with Ad-hACE2 prior to infection with with 1×10^4 PFU of the WA1 strain of SARS-CoV-2 (**Figure 32**), showed a similar pattern of *sXbp1* under all conditions of treatments, i.e., PBS, Ad-empty and Ad-hACE2 at 2 and 5 days post-infection (dpi) (**Figure 33**). Only infection in Ad-hACE2 transduced Balb/c mice increased *sXbp1* measured by qPCR at 5 dpi.

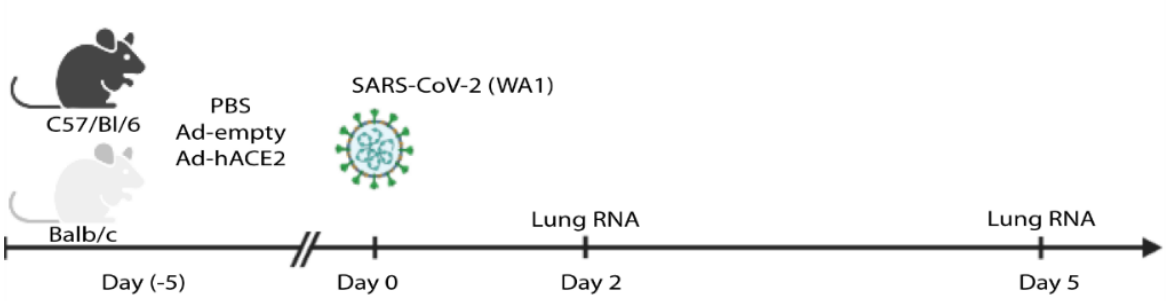

Figure 32. Experimental design used in C57/BL6 and Balb/c mice during Ad-hACE2 SARS-CoV-2 infection. C57BL/6 and Balb/c mice were transduced with 2.5×10^8 PFU of Ad-empty, Ad-hACE2, or PBS. On day 5 post-Ad administration mice were infected with 1×10^4 PFU of SARS-CoV-2 (WA1) before lungs harvesting for RNA extraction according to the indicated timeline.

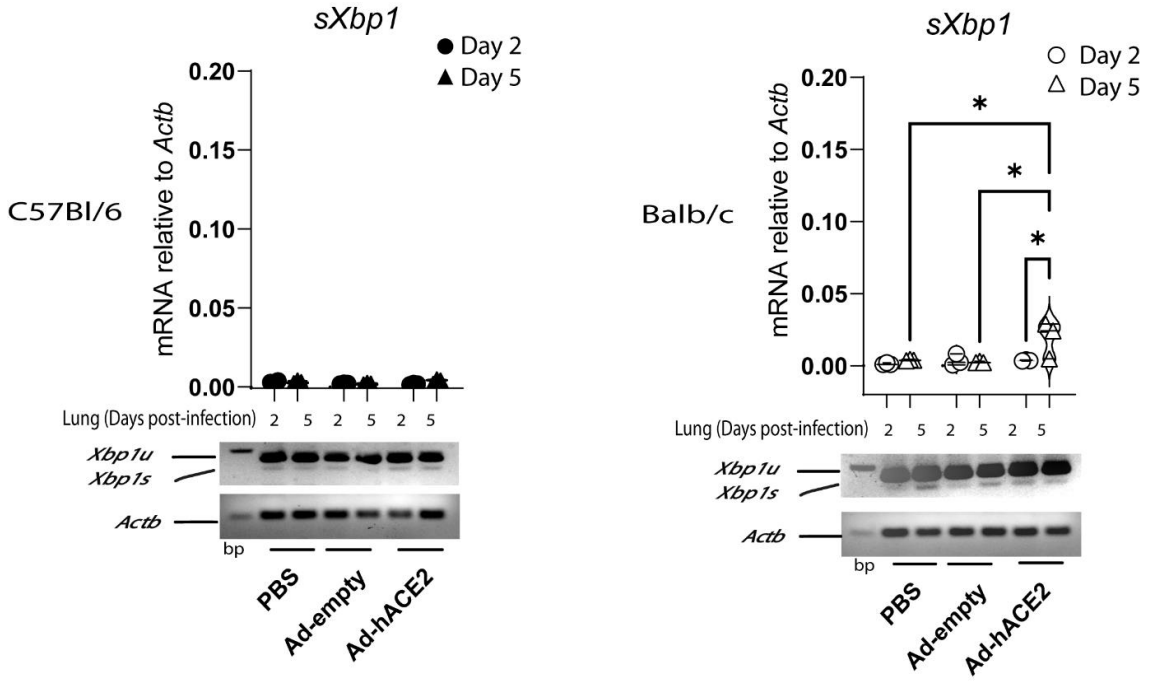

Figure 33. *Xbp1* analysis in C57/BL6 and Balb/c mice during Ad-hACE2 SARS-CoV-2 infection. Analysis by qPCR of the mRNA expression of *sXbp1* and agarose gel electrophoresis of the *XBP1* amplicons. C57BL/6 (left panel) Balb/c (right panel). Data are presented as mean ± SEM. *p < 0.05. Ordinary one-way ANOVA.

Lung expression of *Hspa5*, *Atf4*, and *Ddit3/Chop* did not show any change, thus ruling out global activation of UPR genes dependent on the Atf6 and Perk arms in C57BL/6 and Balb/c mice (**Figure 34**). These data suggest that this mice model shows a sole activation of the Ire1α-Xbp1 branch upon SARS-CoV-2 infection.

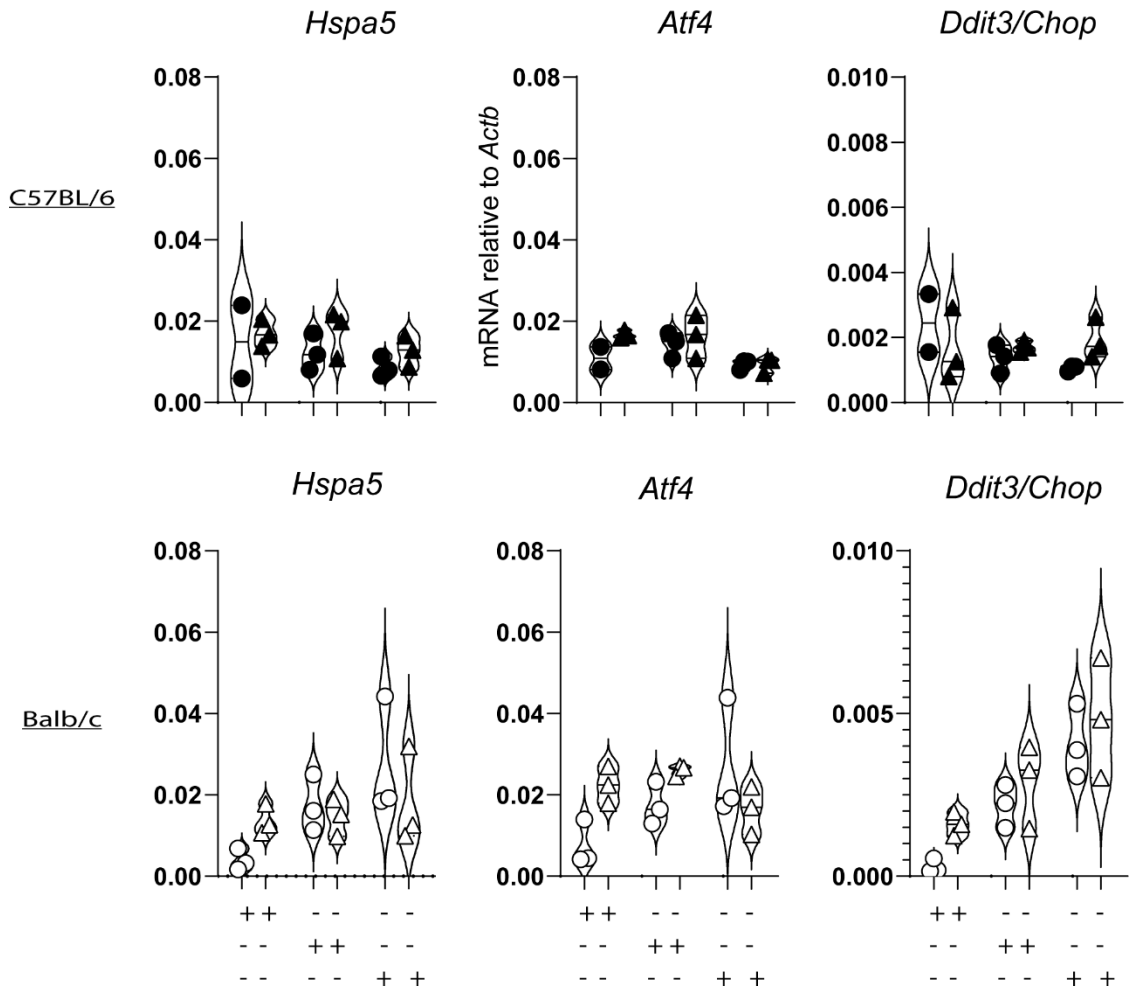

Figure 34. UPR analysis in C57/BL6 and Balb/c mice during Ad-hACE2 SARS-CoV-2 infection. Analysis by of qPCR the mRNA expression of *Hspa5*, *Atf4* and *Chop* in C57BL/6 (upper panel) and Balb/c mice (lower panel).

Ad-hACE2 mice were compared with K18-hACE2 mice infected with the WA1 strain of SARS-CoV-2 at 10^4 PFU. As shown in **Figure 35A-C**, there is a strong induction of sXbp1

at 2 dpi in comparison with animals at 5 dpi or uninfected mice at RNA and protein levels. *Hspa5* paralleled the pattern of *sXbp1* at 2 dpi, which agrees with the reported role of the chaperone Hspa5 as a host-cell receptor for SARS-CoV-2 [142, 175]. In contrast, the genes of the Perk pathway, *Atf4* and *Ddit3*/CHOP were not affected, nor CHOP protein expression (**Figure 35B-C**).

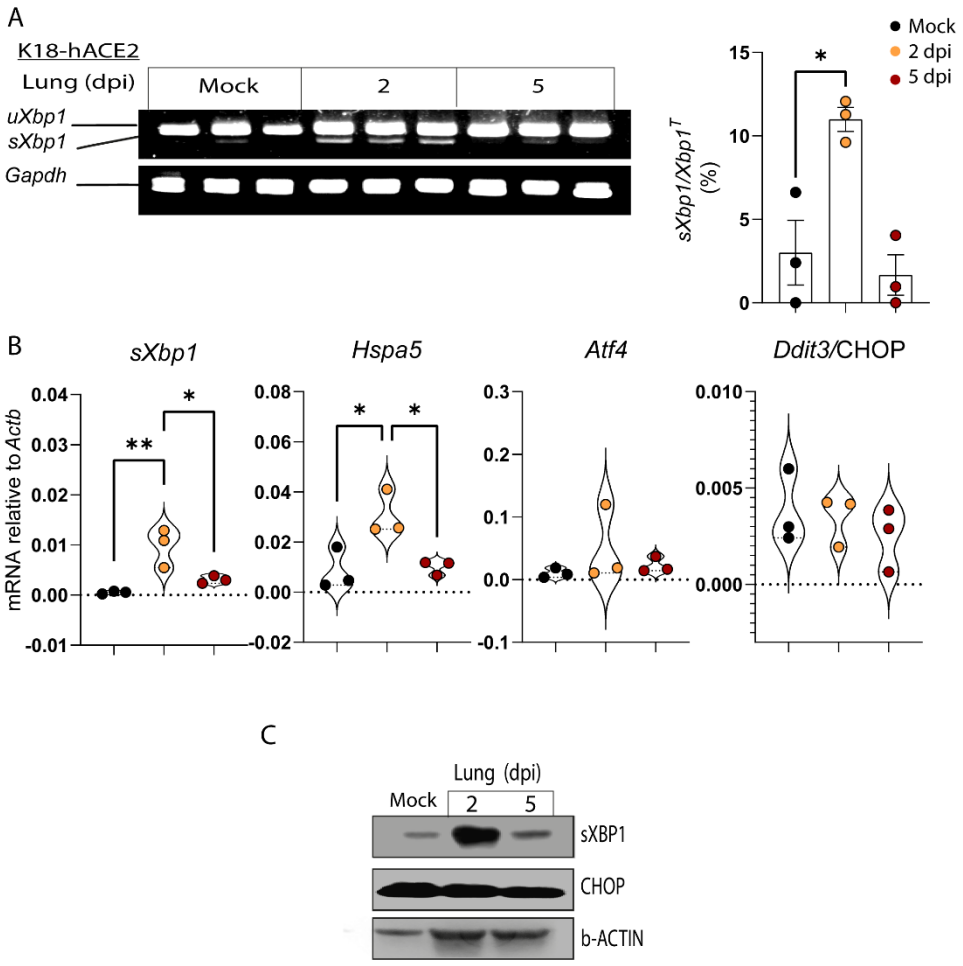

Figure 35. UPR analysis in K18-hACE2 mice during SARS-CoV-2 infection. K18-hACE2 mice were infected with 1×10^4 PFU of SARS-CoV-2 before lung harvesting for RNA and protein extraction according to the indicated timeline. (A) Analysis of *Xbp1* by PCR and resolution in agarose gel. Densitometry quantification of *sXBP1* versus total *XBP1* (*sXBP1/XBP1*^{T}) of three independent animals per condition. (B) Analysis of the mRNA of *sXbp1*, *Hspa5*, *Atf4*, and *Ddit3*/CHOP. (C) Western blot of sXBP1 and CHOP. Data are presented as mean ± SEM. *p < 0.05, **p < 0.01. Ordinary one-way ANOVA.

The mRNA extracted from mice lungs showed an increased expression of *Tnf* and *Il10* at 2 dpi, while the expression of *Il1b* showed a trend to increase that did not show statistical significance. *Ifnb*, *Il12a*, and *Il23a* mRNA decreased in mice infected at 2 and 5 dpi, while *Cxcl9* was unnafected (**Figure 36**). These data suggest a dysregulation of host immune response and antiviral defense, as deemed by the higher levels of *Tnf*, *Il1b*, and *Il10*, as well as by the lower levels of *Ifnb*, *Il12a*, and *Il23a* mRNA.

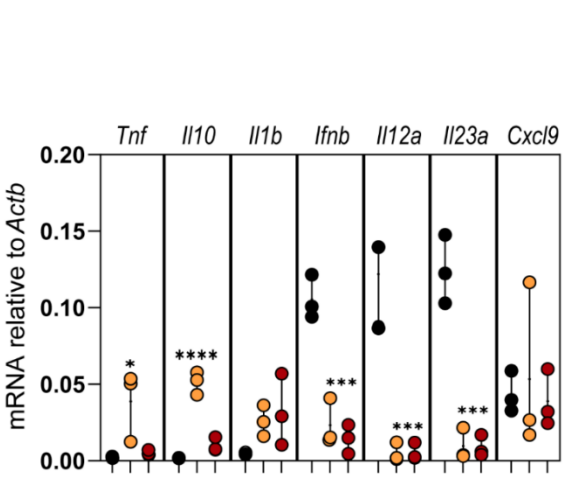

Figure 36. Cytokine signature analysis in K18-hACE2 mice during SARS-CoV-2 infection. *Tnf*, *Il10*, *Il1b*, *Ifnb*, *Il12a*, *Il23a*, and *Cxcl9* mRNA expression. Data are presented as mean ± SEM. *p < 0.05, **p < 0.01, ***p < 0.005, ****p < 0.001. Ordinary one-way ANOVA.

Viral replication of SARS-CoV-2 could affect cellular ER proteins and activate different UPR-target genes. We found an increased expression of the canonical sXbp1-target gene *Dnajb9* but not of *Sec61a1*. Gene expression analysis of the other UPR target genes such as *Herpud*, *Edem1* and *Pdia3* was not modified (**Figure 37A**). RIDD is responsible for the direct degradation of a number of mRNAs, since the IRE1α RNAse activity not only catalyzes the sequence-specific cleavage of 26 nucleotides of *XBP1* mRNA, but also a small set of mRNAs sharing the common consensus sequence CUGCAG, located in the stem loop structure [36]. RIDD dependent genes *Rpn1*, *Tapbp*, *ERp44*, *Hgsnat*, and *Bloc61a1* did not show any sign of activation in both low and high

multiplicity of infection (MOI) of SARS-CoV-2 WAI challenge at 2 and 5 dpi (**Figure 37B**).

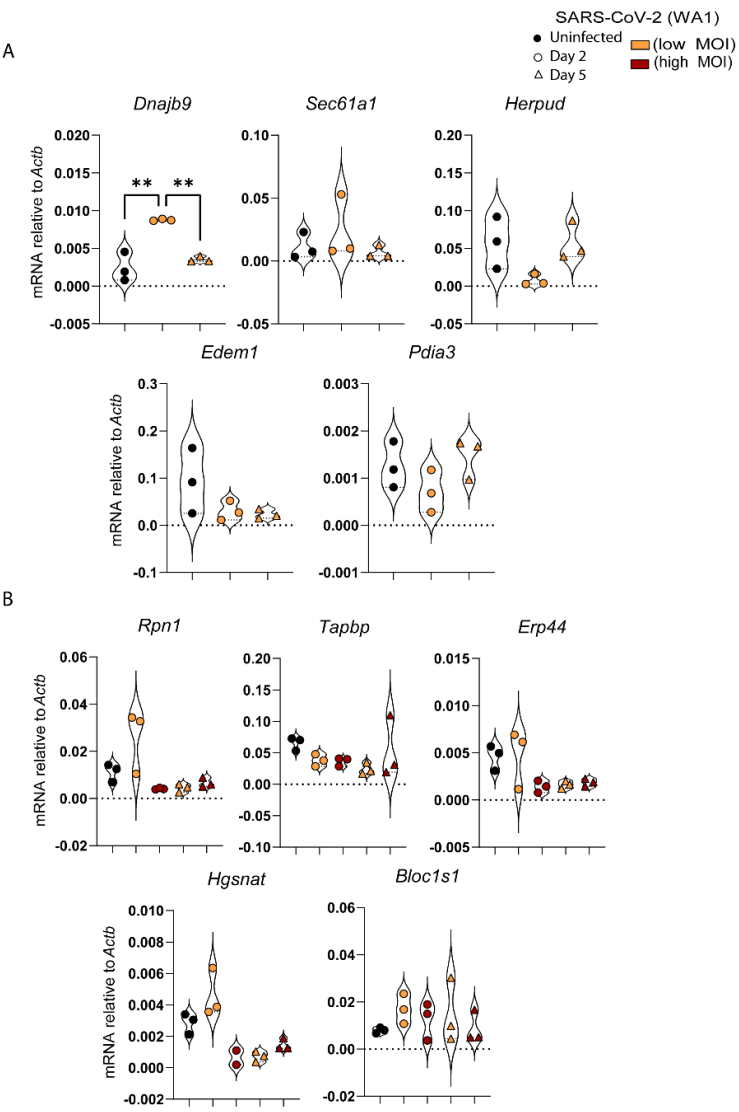

Figure 37. UPR and RIDD target genes in K18-hACE2 mice during SARS-CoV-2 infection. (A) Analysis by qPCR of the UPR-target genes expression of *Dnajb9*, *Sec61a1*, *Herpud*, *Edem1*, and *Pdia3* mRNA expression. (B) Analysis of the expression of the RIDD genes *Rpn1*, *Tapbp*, *Erp44*, *Hgsnat*, and *Bloc1s1*. Data are presented as mean ± SEM. **p < 0.01. Ordinary one-way ANOVA

In short, K18-hACE2 mice showed a strong activation of the UPR as compared to Ad-hACE2 infection, specially of the Ire1α-Xbp1 pathway, which correlates with high viral replication in the lungs. These data disclose that the Ire1α-Xbp1 branch is the preferential element of the UPR activated during the acute phase of infection.

SARS-CoV-2 infection drives activation of the Ire1α-Xbp1 arm in Syrian hamsters

Experiments in the Syrian hamster model were conducted, in view of the clinical course of the infection, which includes severe pneumonia and extrapulmonary damage around 5 dpi followed by complete resolution by day 14 [176, 177]. This poses an adequate model to study acute pneumonia, instead of the exacerbated extrapulmonary manifestations observed in the K18 mice model [178].

A systematic bioinformatic analysis to address pathways related to ER function was carried out in RNA extracted from lung samples obtained at day 6 dpi. GO enriched pathways analysis showed upregulation of chaperone mediated function and protein folding, N-linked and O-linked glycosylation during infection, including cellular response to stress and endoplasmic reticulum unfolded protein response (**Figure 38**).

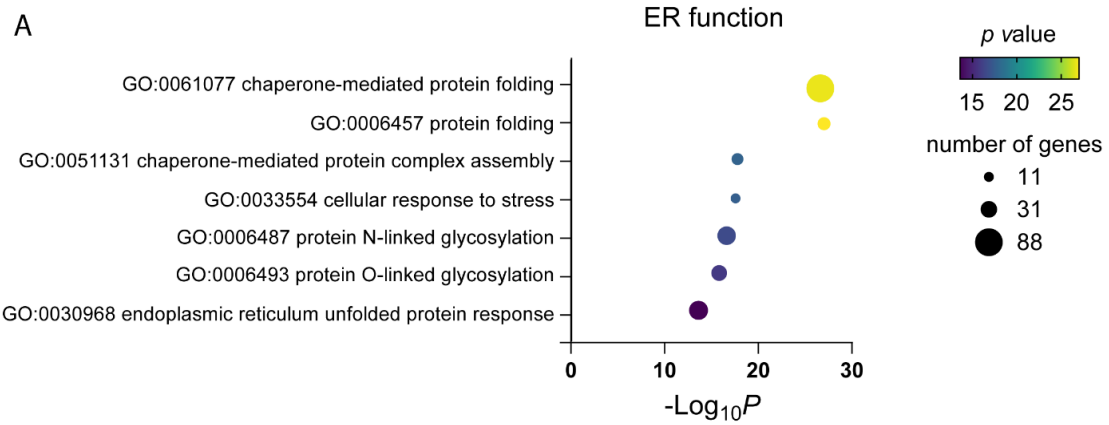

Figure 38. GO analysis of ER stress during SARS-CoV-2 infection in Syrian hamster. Syrian hamsters were infected with SARS-CoV-2 WA1 in a 50 µl suspension containing a targeted dose of 10^2 PFU, before lung harvesting for bioinformatic analysis of RNA extracted from the lungs. GO enriched pathways analysis and differential biological processes related to ER function at 6 dpi are shown. Data are represented as bubble colour with FDR<0.05, and the number of genes within the GO pathway was represented as bubble size.

We next evaluated the expression of different genes that could be involved in the activation of the UPR at 2, 4 and 6 dpi. All the UPR-target genes analysed increased over time (**Figure 39**).

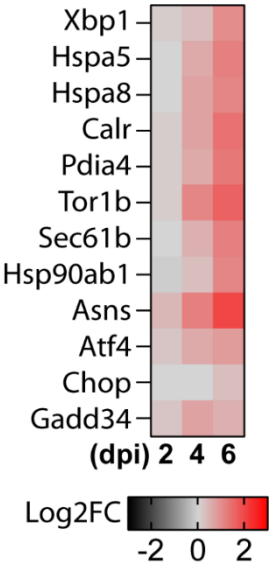

Figure 39. Heat map of ER stress genes during SARS-CoV-2 infection in Syrian hamster. Heat map of UPR target genes comparing Mock with 2, 4 and 6 dpi. Differential expression analysis was carried out by DESeq2 and data are represented as Log2FoldChange.

Upregulation of *Xbp1*, *Hspa5*, and *Hspa8* was observed, as well as various UPR-target genes, including *Calr*, *Pdia4*, *Tor1b*, *Sec61b*, *Hsp90ab1* and *Asns*. In contrast, *Atf4*, *Chop* and *Gadd34* were not significantly upregulated at 6 dpi (**Figure 40**).

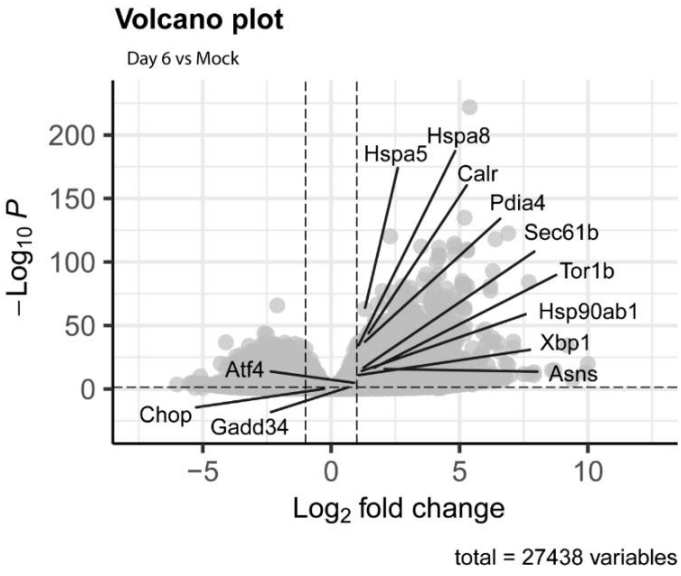

Figure 40. Volcano plot of ER stress genes during SARS-CoV-2 infection in Syrian hamster at 6 dpi. Significant genes are represented with a cut-point of 1 in Log2FoldChange and -$Log_{10}P$.

RT-qPCR analysis confirmed the bioinformatic data. In fact, the mRNA expression of *Hspa5* was upregulated at 6 dpi, while *Atf4*, *Chop*, and *Gadd34* did not reach any significant change (**Figure 41)**. This reinforces the idea that SARS-CoV-2 infection promotes activation of the Ire1α-Xbp1 arm, while it eludes the Perk/Atf4/Chop-Gadd34 branch, also observed in K18-hACE2 mice.

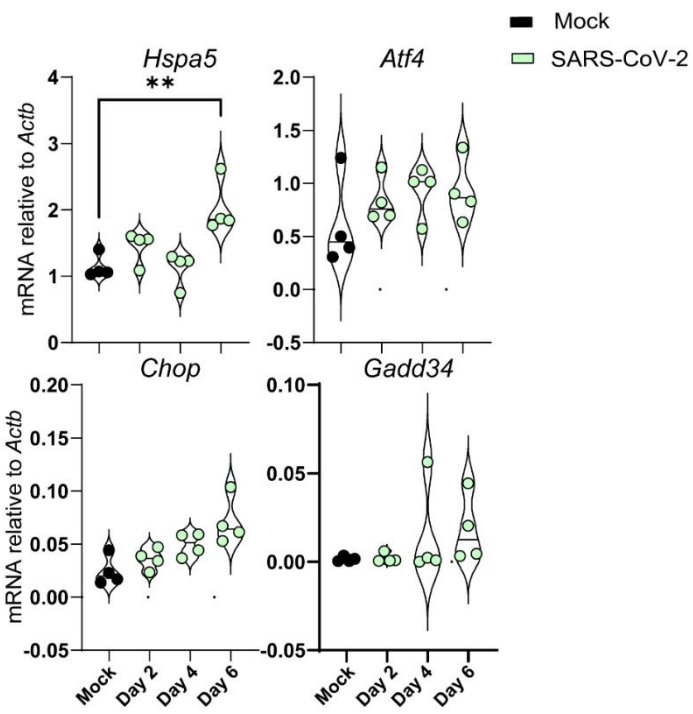

Figure 41. Analysis of genes involved in the ER stress during SARS-CoV-2 infection in Syrian hamster by RT-PCR. The mRNA expression of *Hspa5*, *Atf4*, *Chop* and *Gadd34*. Data are presented as mean ± SEM. **p < 0.01. Ordinary one-way ANOVA.

RT-PCR assays using primers flanking the *Xbp1* gene sequence to amplify the unspliced (*uXbp1*, XM_040746756.1) and the spliced version (*sXbp1*, XM_005067933.4) followed by resolution of the PCR products by agarose gel electrophoresis did not show any significant change of expression between uninfected (Mock) and infected Syrian hamsters at 2, 4 and 6 dpi (**Figure 42A**). Then, we spanned both sequences to find out a restriction enzyme PstI, that cleaves the DNA at the recognition sequence 5'-CTGCA/G-3' only present in the *uXbp1*. To confirm this fact, we digested the PCR product with PstI. Although, 24 h of incubation did not fully digest *uXbp1*, we found both fragmented

products of *uXbp1* (**Figure 42B**). The analysis suggested that *Xbp1* splicing was increased at day 2, 4 and 6 in comparison with Mock, which was confirmed using primers flanking the spliced region of *Xbp1*, where *sXBP1* expression increased at 2, 4 and 6 dpi as compared to Mock (**Figure 42C**).

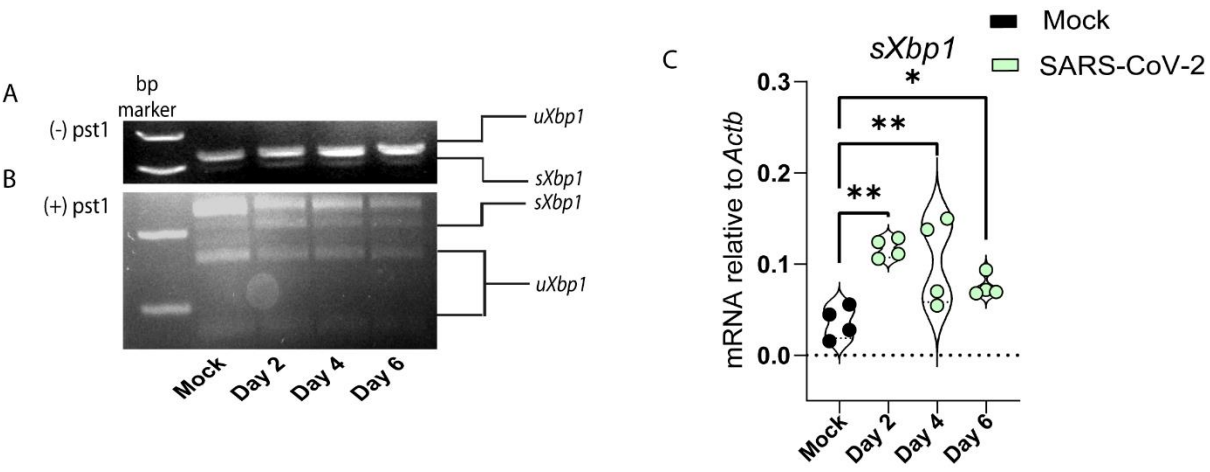

Figure 42. Analysis of the Ire1α-Xbp1 branch of the UPR during SARS-CoV-2 infection in Syrian hamster. Assay of Xbp1 restriction analysis by PstI in *uXbp1* (XM_040746756.1) and *sXbp1* (XM_005067933.4). (A) PCR product resolution in agarose gel of *uXbp1* and *sXBP1*. (B) 24 h digestion assay by Pst1 of *uXBP1*. (C) *sXBP1* gene expression in RNA extracted from harvested lungs at dpi 2, 4 and 6 analysed by qPCR. Data are presented as mean ± SEM. *p < 0.05, **p < 0.01. Ordinary one-way ANOVA.

Protein harvested from whole lungs confirmed that sXbp1 increased while CHOP was not modified at 6 dpi (**Figure 43**).

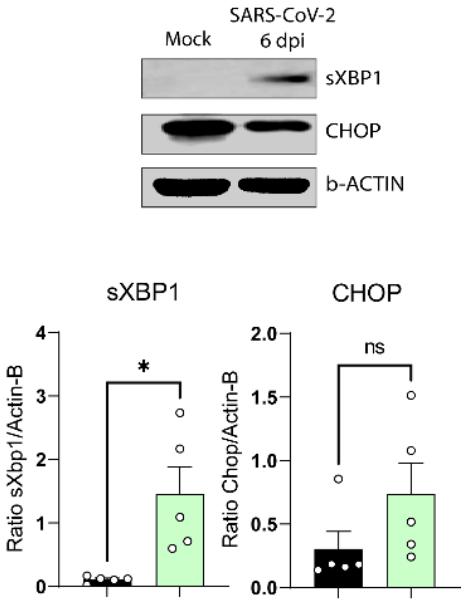

<u>Figure 43.</u> Expression of sXBP1 and CHOP during SARS-CoV-2 infection in Syrian hamster. Western blot of sXBP1 and CHOP at 6 dpi and densitometric quantification in lung samples of five animals. Data are presented as ratio of protein of the interest/β-ACTIN. *p < 0.05. Ordinary one-way ANOVA.

Taken together, these findings show that SARS-CoV-2 infected Syrian hamsters upregulate pathways related to ER function and activate the Ire1α-Xbp1 branch.

Bioinformatic analysis of Syrian hamster revealed cytokine storm during SARS-CoV-2 infection

A bioinformatic analysis focusing on GO enriched pathways related to global viral defense and inflammatory response mediated by TLRs was carried out in SARS-CoV-2 infected Syrian hamsters at 6 dpi. Upregulation in nine GO pathways related to viral defence, response to virus, viral replication and viral entry among others (**Figure 44**).

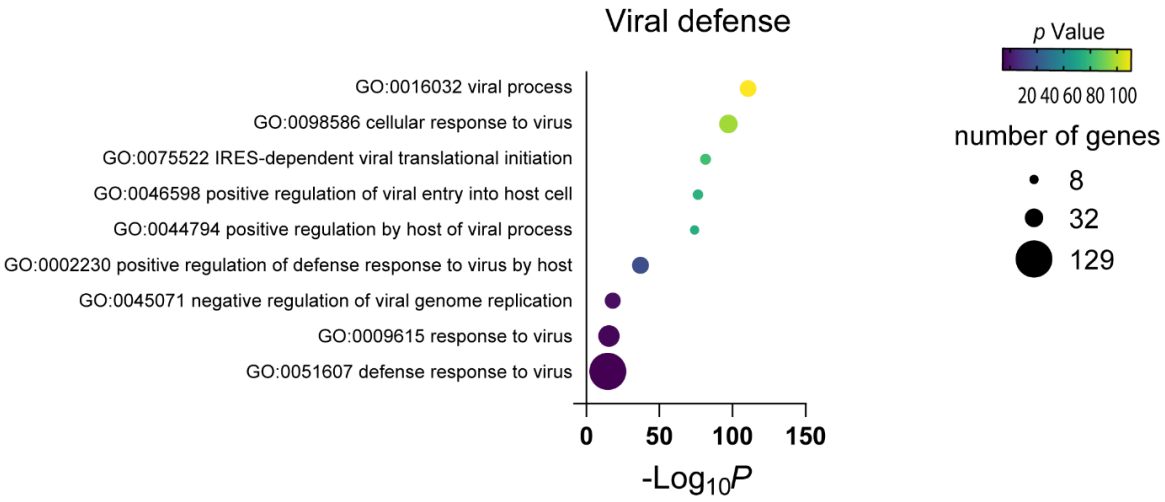

Figure 44. Syrian hamster viral defense during SARS-CoV-2 infection. GO enriched pathways analysis and differential biological processes related to viral defence at 6 dpi. Data are represented as bubble colour with FDR<0.05. The number of genes within the GO pathway is represented as bubble size**.**

Six different GO inflammatory pathways were also activated during infection, including TLR2, TLR3 and TLR7 pathways (**Figure 45**). TLR2 locates at the cell surface, which suggests its involvement in the recognition of structural proteins of SARS-CoV-2, while TLR3 and TLR7 are endosomal receptors involved in the recognition of dsRNA and ssRNA, respectively.

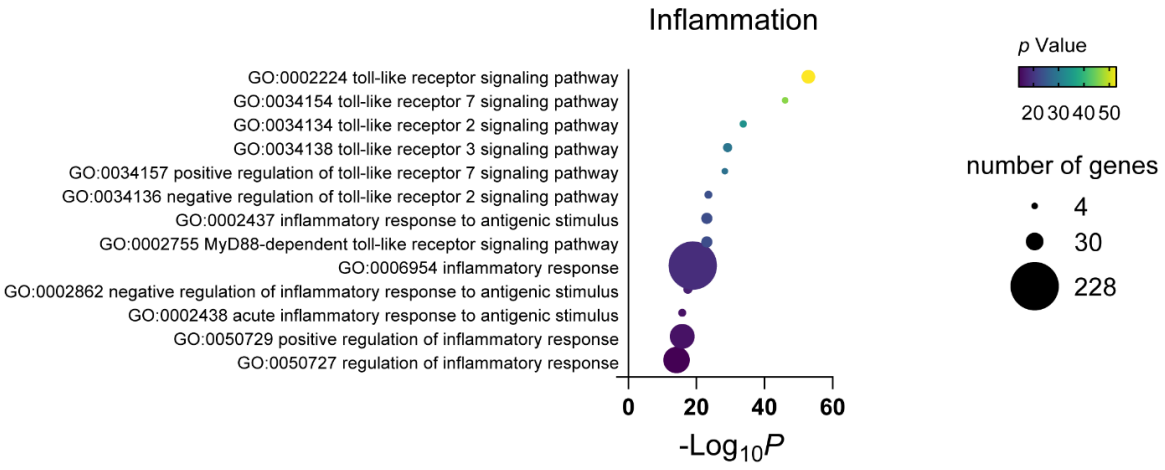

Figure 45. Syrian hamster triggers inflammatory response upon SARS-CoV-2 infection. (A-B) GO enriched pathways analysis and differential biological processes related to inflammation at 6 dpi. Data are represented as bubble colour with FDR<0.05. The number of genes within the GO pathway is represented as bubble size**.**

TLR signaling elicits canonical antiviral response involving IFN, interferon regulatory factor (IRF) and signal transducer and activator of transcription (STAT) families [179]. Differential gene expression analysis in the Syrian hamster at 2, 4 and 6 dpi showed an increase of *Irf1-9*, especially *Irf-7* (**Figure 46A**). In addition, STAT family analysis showed increased expression of *Stat1-2*, but not the other STAT family components (**Figure 46B**). Next, IFN family analysis showed increased expression of *Ifnb1*, *Ifng*, *Ifnl3*, *Isg15-20*, *Mx1* and *Oas1-2*. However, *Ifnk* and the IFN receptors *Ifnar1-2* and *Ifngr1-2* decreased during infection (**Figure 46C**). These findings suggest that IFN-mediated signaling through canonical receptors is blunted upon infection.

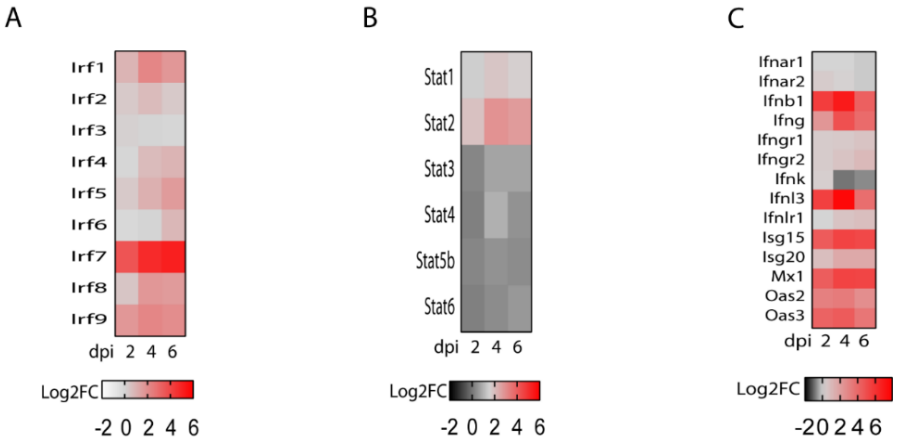

<u>Figure 46.</u> Syrian hamster triggers inflammatory response upon SARS-CoV-2 infection. (A-C) Heat map of IRF, STAT, and IFN family gene comparing Mock with 2, 4 and 6 dpi. Differential expression analysis was carried out by DESeq2, and data are represented as Log2FoldChange.

Twenty-nine different GO pathways related to signaling, regulation, and production of cytokines, including, *IL1b, IL4, IL6, IL7, IL10, IL12, IL17, TNF* related pathways and chemokines were upregulated at 6 dpi (**Figure 47**).

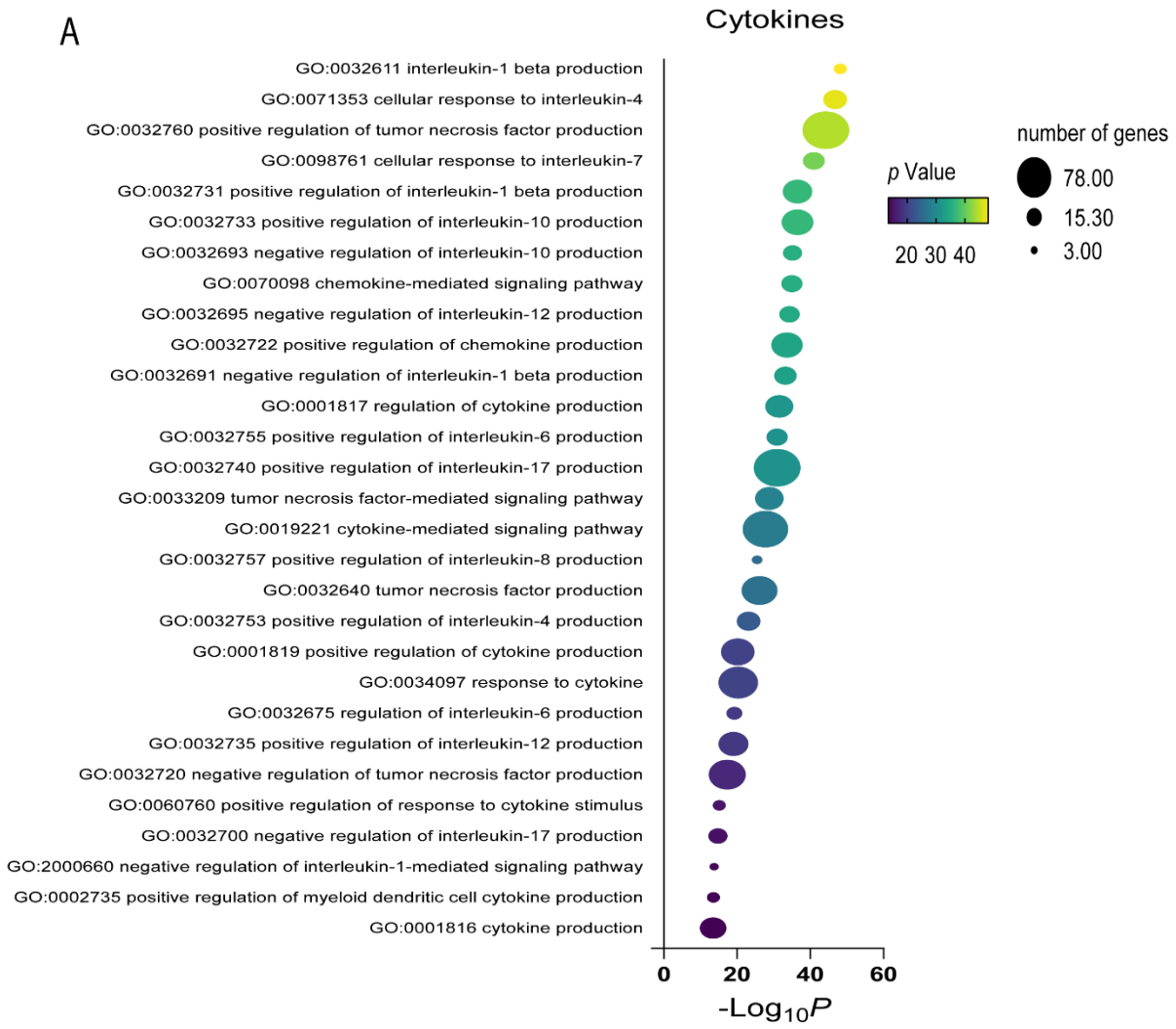

Figure 47. Syrian hamster shows an inflammatory response during SARS-CoV-2 infection that mimics cytokine storm. GO enriched pathways related to cytokine signature at 6 dpi with FDR<0.05. Data are represented as bubble colour for -Log10*P* and the number of genes within the GO pathway is represented as bubble size.

The assay of cytokine production, showed maximal expression at 6 dpi and therefore, maximal chance for cytokine storm (**Figure 48**).

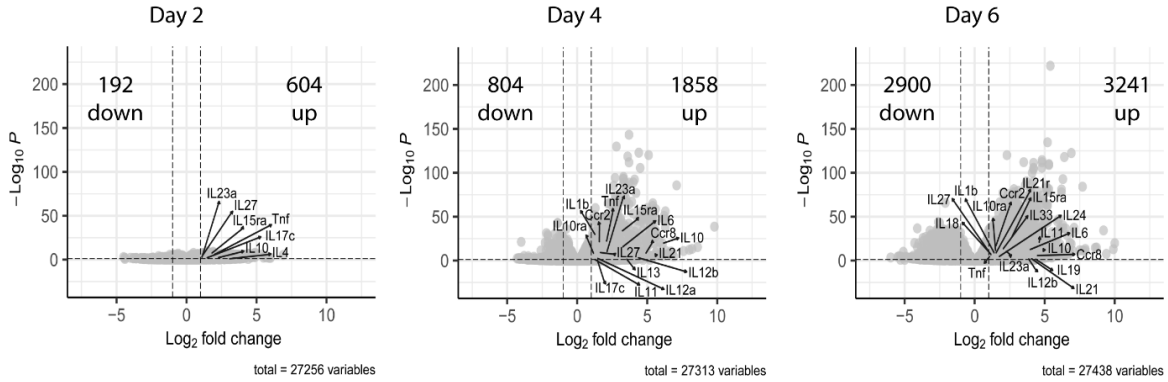

<u>Figure 48.</u> Infection of Syrian hamster drives an inflammatory response that mimics cytokine storm. Deseq2 analysis of differential expression genes between Mock and 2, 4, and 6 dpi. Volcano plot of the significant cytokines at 2, 4, and 6 dpi. Significant genes are represented with a cut-point of 1 in Log2FoldChange and -Log$_{10}$*P*.

Together, these results indicate that SARS-CoV-2 infected Syrian hamster show innate immune activation dependent on signaling routes driving viral defence and overproduction of cytokines.

Effect of fluvoxamine on viral replication and cytokine storm during MA-SARS-CoV-2 infection

Several clinical studies reported the beneficial effect of fluvoxamine in COVID-19 disease [136-138] and even proposed its use for the control of inflammation [180, 181], but only very recently its effect on the UPR has been associated with its capacity to counter CS in bacterial sepsis [133]. Based on this, we posited that fluvoxamine could target the UPR-dependent cytokine induction.

129S1 mice were infected with 10^4 PFU of MA-SARS-CoV-2 and then treated daily with 150 mg/kg of fluvoxamine for three days prior to harvesting lungs and collecting blood to analyse viral titres, immunohistopathology, and cytokine assays (**Figure 49**). This recombinant virus has several mutations, mostly at the S protein, that allows its recognition by mouse ACE2 [152].

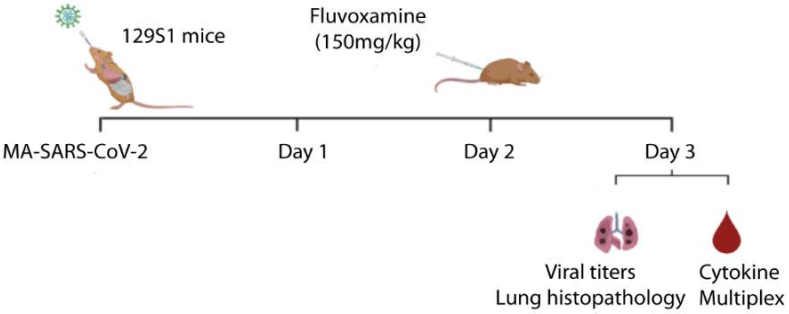

Figure 49. Representative diagram of the experimental design of fluvoxamine treatment in mice infected with MA-SARS-CoV-2. Mice 129S1 were infected with MA-SARS-CoV-2 at 10^4 MOI and treated daily with 150 mg/Kg subcutaneous of fluvoxamine, prior to lung harvesting at 3 dpi for the analysis of viral titres, protein expression, lung histopathology, and peripheral blood cytokines.

Over the course of the experiment, the weight of the animals did not show any significative change between the infected and treated group (**Figure 50A).** The analysis of lung viral

titres at 3 dpi failed to show any significant changes in mice treated with fluvoxamine. Remdesivir (100 mg/Kg) was used as a positive control of antiviral activity [101, 182] and showed a decrease of viral titres measured by TCID50 (**Figure 50B**).

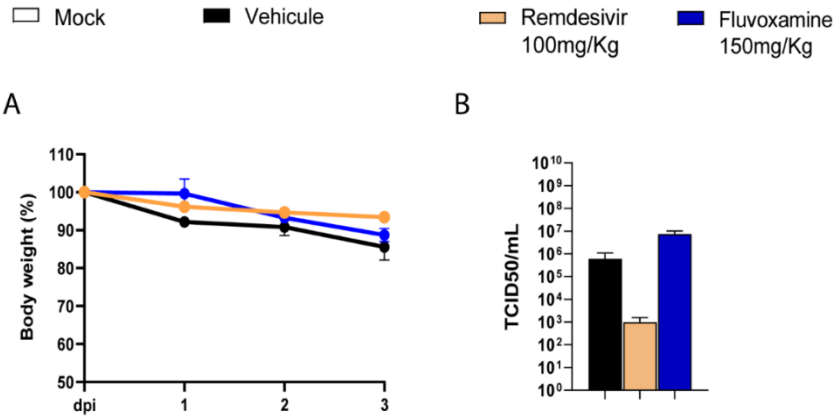

Figure 50. Body weight and viral titres analysis in 129S1 mice infected with MA-SARS-CoV-2. (B) Body weight monitoring during the experiment. (C) Viral titres measured by TCID50. Mice treated with 100 mg/Kg of remdesivir were used as an antiviral positive control.

Despite fluvoxamine did not show any effect on viral replication at early stages of mice infection, it was suggested that its effect as an agonist of SIR1 might modulate the UPR and therefore cytokine induction. Cytokine multiplex assays showed increased levels of IL-6 and TNFα that decreased upon fluvoxamine treatment. In addition, the increased levels of growth factors G-CSF and VEGF observed during infection were countered by fluvoxamine treatment. Moreover, the increased of the levels of MIP1α and CXCL1 were also counteracted by fluvoxamine treatment (**Figure 51A-C**). This data agrees with other reports showing that IL-6 [161, 183] and G-CSF [183, 184] are critical host factors increased by SARS-CoV-2 infection. In contrast, fluvoxamine did not exert any significant change in the levels of IL-10, IL-4, IFNβ and IFNγ (**Figure 51D-E**).

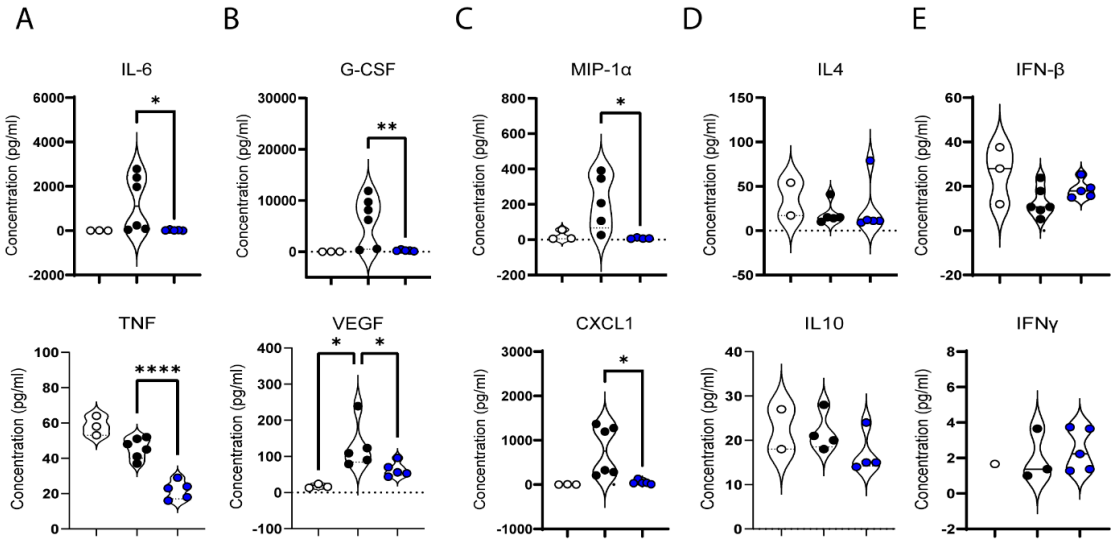

<u>Figure 51.</u> Cytokine profile in peripheral blood of 129S1 mice infected with MA-SARS-CoV-2. (A-E) Concentration of blood cytokines from 129S1 mice at 3 dpi using the MD44 Multiplex^{TM} assay comparing Mock, untreated and mice treated with fluvoxamine. Data are presented as mean ± SEM. *p < 0.05, **p < 0.01, ***p < 0.005, ****p < 0.001. Ordinary one-way ANOVA.

The effect of fluvoxamine in lung injury was addressed using digital light microscopic scans of mice lung slices. Infected and treated mice exhibited typical histopathological lesions of interstitial pneumonia as judged from haematoxylin and eosin (H&E) staining (**Figure 52A**). The semi-quantitative implementation for total pathology score increased in infected group and in treated mice. (**Figure 52B**). This was not unexpected because fluvoxamine treated animals showed high lung viral titres at 3 dpi.

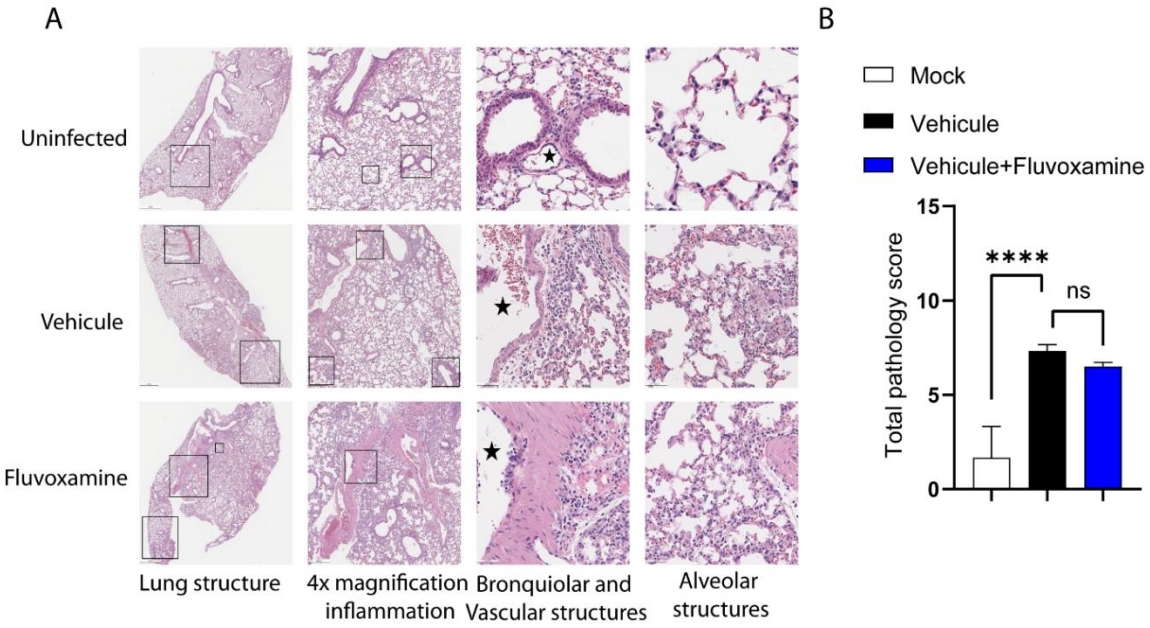

Figure 52. Histological analysis of 129S1 mice infected with MA-SARS-CoV-2. (A) H& E-stained sections of lung from 10-week-old female 129S1 mice at 3 dpi. (B) Total pathology score was examined by implementing a semi-quantitative, 5-point grading scheme that considered four different histopathological parameters. Results showed differences between uninfected, vehicle, and treated groups.

These data show that fluvoxamine counters the increased production of proinflammatory cytokines in peripheral blood during SARS-CoV-2 infection, although at early stages of infection fluvoxamine does not exert any effect on viral replication and lung damage.

The UPR arms during SARS-CoV-2 replication in human epithelial cells

Based on the *in vivo* results, experiments were designed to analyse the global UPR activation during infection with SARS-CoV-2 WA1 in ACE2-A549 cells at different MOI and timepoints. Along infection, ACE2-A549 cells increased viral RNA, which correlated with the MOI and timepoint measured (**Figure 53A**). Similar results were observed regarding the protein expression of sXBP1, CHOP and GADD34 at 4, 8, 16, and 24 hours post-infection (hpi). Increased levels of sXBP1 were observed up to 16 hpi, followed by a decrease at later times, independently of the MOI used (**Figure 53B**). These data agreed with the results reported by Nguyen et al, (2022), who found partial activation of IRE1α but not sXBP1 after 24 hpi using a higher MOI of infection. The proteins of the PERK arm CHOP and GADD34 showed the same pattern observed for sXBP1 activation, increasing early after infection, and decreasing after 24 hpi. (**Figure 53C-D**).

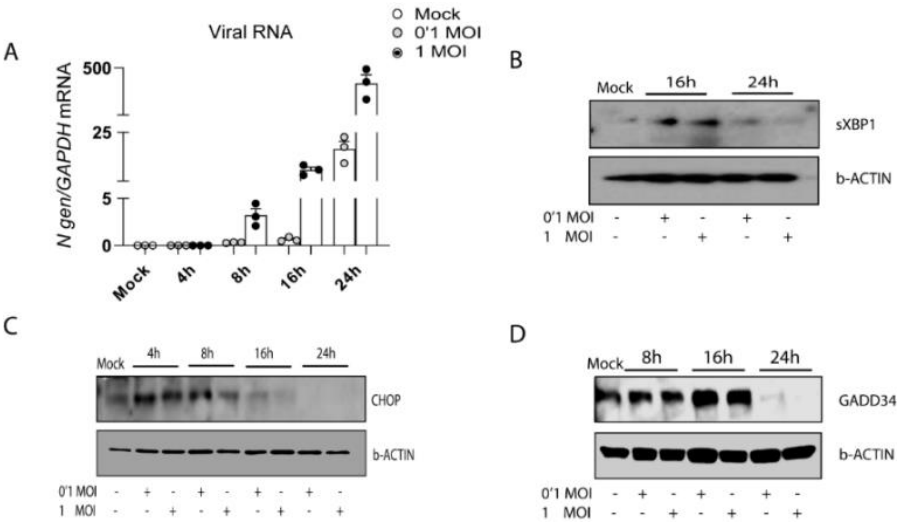

Figure 53. Time course expression of sXBP1, CHOP and GADD34 during SARS-CoV-2 infection in ACE2-A549 human epithelial cells. ACE2-A549 human epithelial cells were infected with SARS-CoV-2 according to the indicated MOI and timeline. (A) Viral load measured by qPCR. (B-D) sXBP1, CHOP and GADD34 protein expression.

To analyse the role of the UPR in viral replication, the experimental conditions to knockdown of *CHOP*, *GADD34*, and *XBP1* RNA expression were set up. 20 nM siRNA was used for transfection for 24 h, prior to stimulation with 10 µM of tunicamycin. While tunicamycin increased CHOP, GADD34, and XBP1 protein expression, the siRNA treatment reduced the expression of these proteins (**Figure 54**).

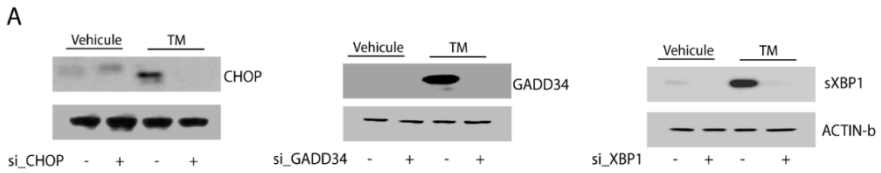

Figure 54. siRNA knockdown of CHOP, GADD34 and sXBP1. (A) 20 nM siRNA was used to knockdown of CHOP, GADD34, and XBP1 for 24 h, and then cells were stimulated with 10 µM tunicamycin for 6h, before analysis of protein expression by Western blot.

Subsequently, ACE2-A549 cells transfected with the corresponding siRNAs were infected with SARS-CoV-2 at MOI 1 for 16 h. Although, the use of siRNAs could decrease the expression of the targeted cellular proteins (**Figure 55A**), the expression of the viral S protein (**Figure 55A**), and therefore, viral titres (**Figure 55B**) did not reach any significant change.

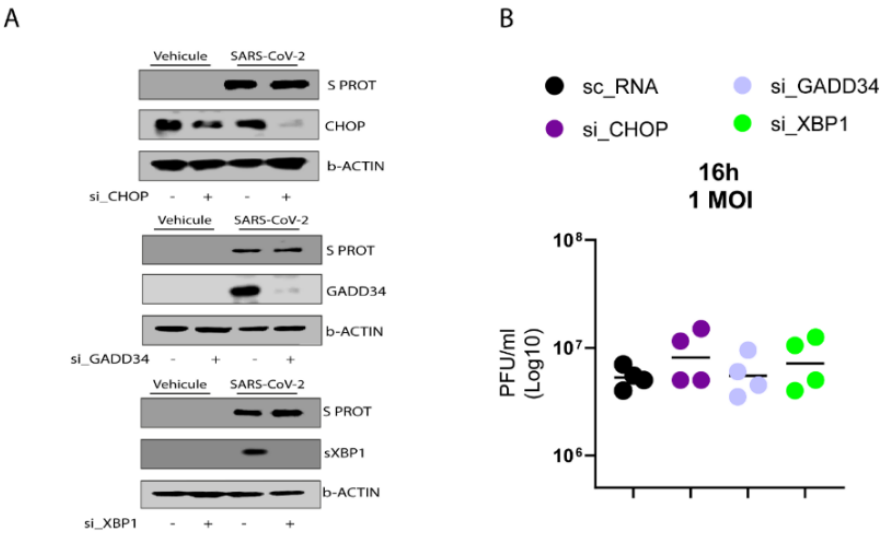

<u>Figure 55.</u> siRNA knockdown of CHOP, GADD34 and sXBP1 during SARS-CoV-2 replication. (A) siRNA knockdown of CHOP, GADD34 and XBP1 for 24h and infection with SARS-CoV-2 1MOI for 16h. (B) Plaque assay in Vero E6 with supernatant from ACE2-A549 siRNA experiment infected with SARS-CoV-2 at 1MOI for 16h.

Hence, infection of ACE2-A549 at low 0.1 and 0.2 MOI for 24 and 48 h were measured by immunostaining of N protein. Results showed that *XBP1* knockdown decreased the percent of infection in all the conditions, including *CHOP* at 0.1 and 0.2 MOI for 48 hpi and *GADD34* at 0.2 MOI for 48 hpi (**Figure 56**).

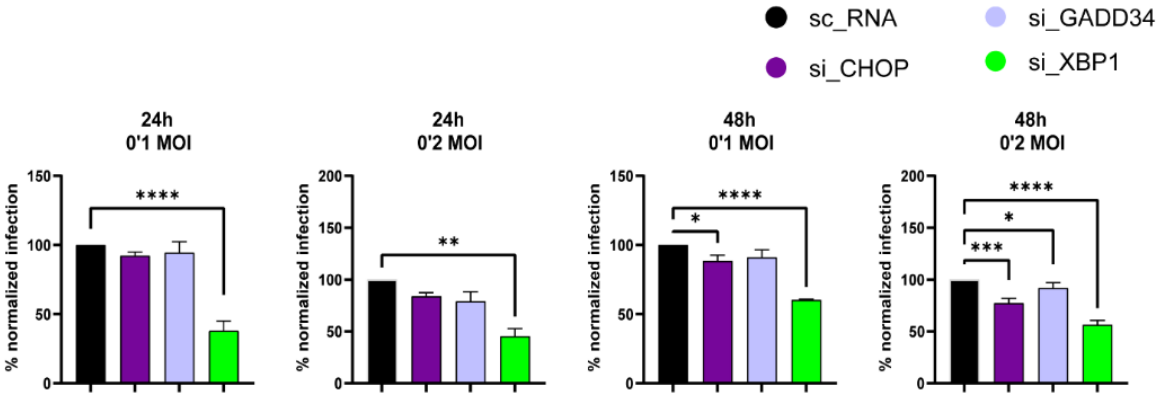

<u>Figure 56</u>. siRNA knockdown of CHOP, GADD34 and sXBP1 during SARS-CoV-2 replication. 20 nM siRNA were used to knockdown CHOP, GADD34 and XBP1 before infection with SARS-CoV-2 according to the indicated MOI and timeline before Immunostaining of NP. Percent infection was quantified as ((Infected cells/Total cells) − Background) × 100, and the DMSO control was then set to 100% infection for analysis. Data are presented as mean ± SEM. *p < 0.05, **p < 0.01, ***p < 0.005, ****p < 0.001. Ordinary two-way ANOVA.

Overall, infection of human epithelial cells with SARS-CoV-2 mimics the *in vivo* findings, although the role of sXBP1 on viral replication is context-dependent.

Analysis of the effect of different SARS-CoV-2 VOCs on the UPR and viral replication

SARS-CoV-2 VOCs have evolved in humans since the beginning of the pandemic COVID-19. This dictated the need to move on to study of different VOCs, since S protein on its own can activate the three branches of the UPR [41, 185].

HEK-293T cells were transfected for 36 h with plasmids encoding for different VOCs S proteins: WT-D614G [186], β (B1.351), γ (P.1), δ (B1.617.2), and o (BA.1 and BA.2). UPR target proteins HERPUD1 and sXBP1 were probed and tunicamycin was used as a positive control for UPR activation. Results support the notion that all the S VOCs tested increased the UPR, as judged from the levels of HERPUD1 and sXBP1 (**Figure 57A**). Moreover, *sXBP1* increased in tunicamycin treated cells, as well as during the overexpression of the different VOCs S proteins (**Figure 57B**). It should be noted that omicron S protein BA.1 and BA.2 seem to increase sXBP1 to a higher extent as compared to the other S VOCs tested.

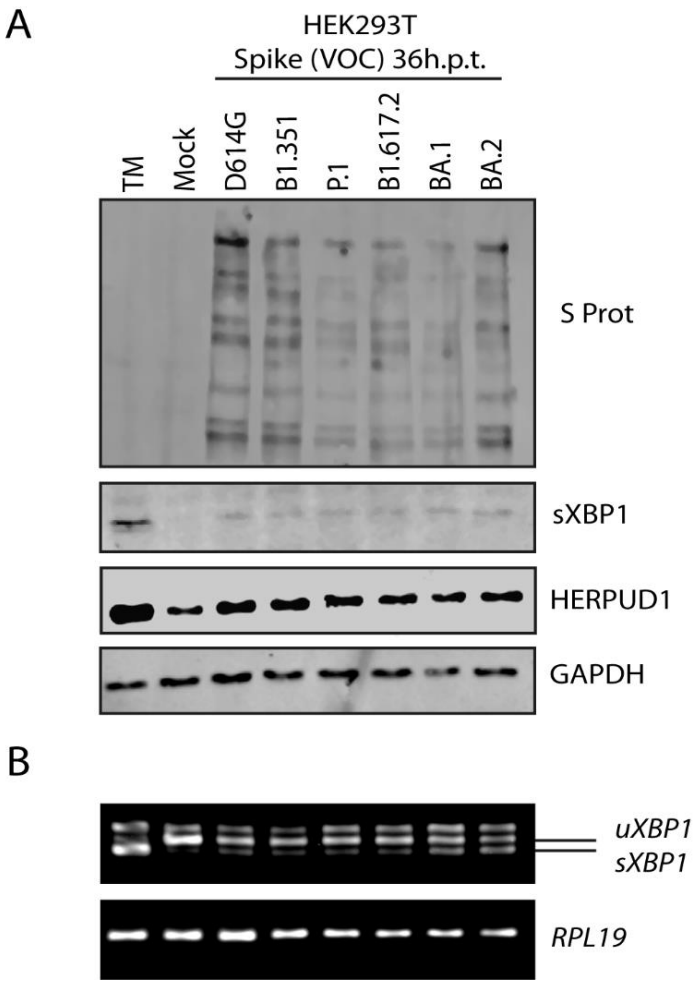

Figure 57. Mechanistic analysis of UPR activation by SARS-CoV-2 Spike protein VOCs. HEK-293T cells were transfected with plasmids encoding SARS-CoV-2 Spike VOCs and harvested at 36 hpt. (A) Western blot analysis of Spike, sXBP1, HERPUD, and GAPDH. The Immunoblot is representative of three independent biological replicates. (B) Analysis of *XBP1* by PCR and resolution in agarose gel.

Although transfection of the different VOCs of the S protein could induce the IRE1α-XBP1 branch of the UPR, it should be noted that this might not reflect what could happen during virus replication. Therefore, we decided to infect ACE2-A549/TMPRSS2 cells at 0.1 MOI for 16 h with different SARS-CoV-2 VOCs (i.e., WT-D614G, α, δ, and omicron BA.2), following the addition of the specific inhibitor of the IRE1α-XBP1 arm KIRA8, to assess virus replication.

The expression of the S protein decreased in most of the infected cells treated with KIRA8, especially in the case of WT-D614G, δ and o (**Figure 58A**). The expression of HERPUD1 protein level was not affected by KIRA8 treatment and, surprisingly, seemed to decrease in cells infected with the α and δ (**Figure 58B**). KIRA8 produced the disappearance of the

sXBP1 band observed in infected cells (**Figure 58C).** Viral RNA, measured as SARS-CoV-2 *N* gene expression, was reduced by KIRA8 (**Figure 58D**), concomitantly with the detection of lower viral titres in treated cells (**Figure 58E**), especially in the case of the δ variant. Surprisingly, viral RNA and titres in cells infected with the α variant were not reduced by KIRA8. These findings suggest that there might be a differential activation of the UPR in VOCs-infected cells, most likely due to differences in replication kinetics or protein expression.

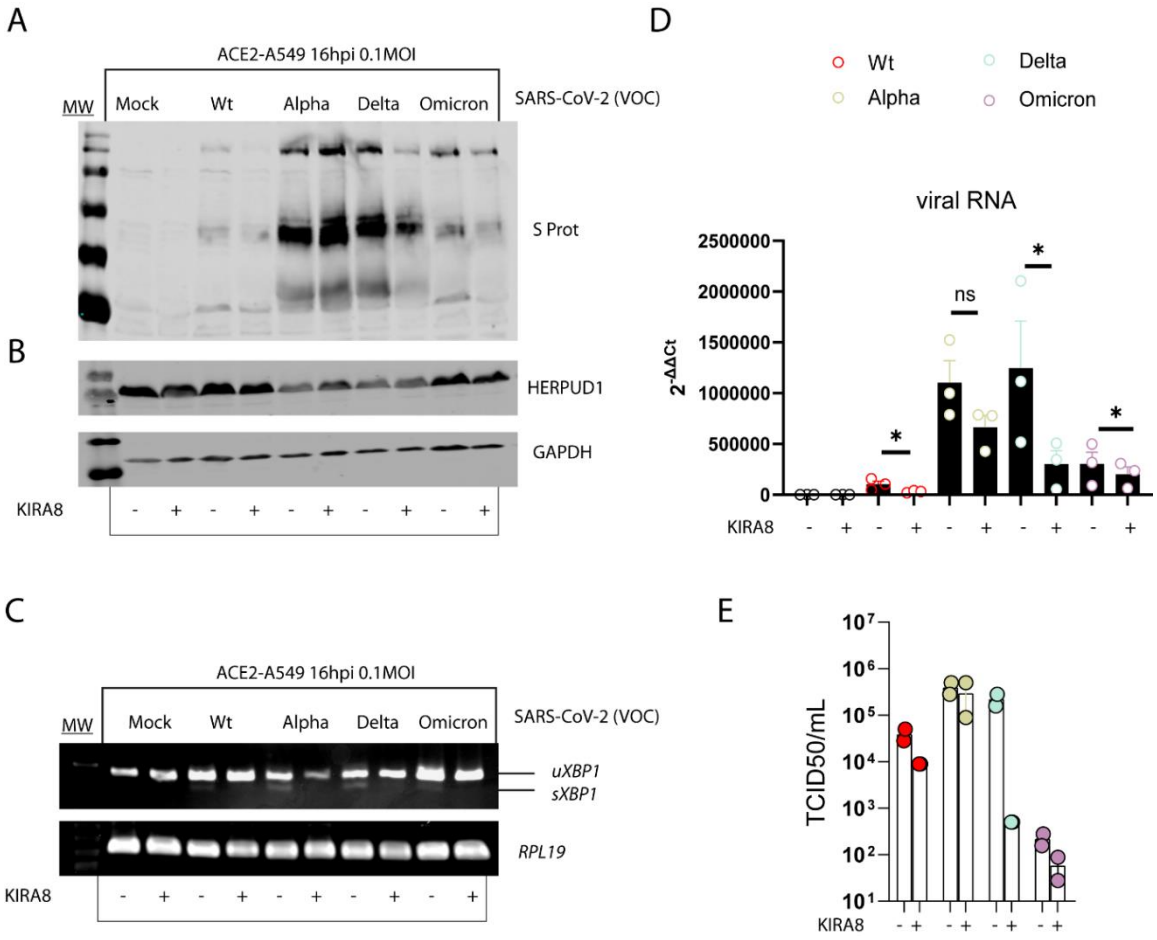

Figure 58. Specific inhibition of IRE1α-XBP1 branch of the UPR during SARS-CoV-2 replication. ACE2-A549-TMPRSS2 cells were infected with SARS-CoV-2 VOCs at 0.1 MOI. Infected cells were treated with 10 µM KIRA8 immediately after the virus absorption period and the inhibitor was maintained in the medium until cell collection 16 h later. (A-B) Representative western blot of S protein and GAPDH. (C) Analysis of *Xbp1* by PCR and resolution in agarose gel. (D) Viral RNA. (E) Viral titres measured by TCID50. Data are presented as mean ± SEM. *p < 0.05. Paired Student *t* test.

In summary, the pharmacological manipulation of the IRE1α-XBP1 branch significantly inhibits SARS-CoV-2 replication with different VOCs. This indicates that the IRE1α-XBP1 branch might be a critical cellular pathway in the replication cycle of SARS-CoV-2 infection.

VIII. Discussion

Bacterial, fungal, and viral pathogens may trigger the UPR

SARS-CoV-2 virus manipulate host signaling pathways to ensure viral replication, where different strategies were developed to take advantage of the ER stress response for optimal propagation [44, 141]. The possible activation of the UPR during SARS-CoV-2 infection prompted us to address the role of the UPR and its potential capacity to reinforce the inflammatory response as well as a host mechanism driving viral replication.

Bacterial and fungal pathogens can trigger the UPR. This is the case of TLR2 and TLR4, as main receptors involved in fungal and bacterial pattern recognition, activation of XBP1 is a mechanism necessary to sustain the production of proinflammatory cytokines in macrophages, in the absence of an archetypal ER-stress response [56, 187].

Bacterial toxins may also trigger the UPR. This has been previously reported for *Brucella abortus* [188, 189], *Streptococcus pneumoniae* [190] and *Pseudomonas aeruginosa* [191], which trigger the IRE1α-XBP1 arm of the UPR in immune and epithelial cells. In contrast, other respiratory pathogens can block the UPR. This is the case of *Legionella pneumophila*, an intracellular pathogen that replicates in an ER-associated compartment and selectively inhibits the IRE1 branch of the UPR by blocking host translation elongation. This seminal finding has allowed the characterization of a set of pathogens that block protein synthesis specifically at elongation as a common strategy used to limit the innate immune response by interfering with the UPR [192].

As regards viral infection, respiratory syncytial virus and other paramyxoviruses that replicate in cytoplasmic stress granule/inclusion bodies, drive a massive production of glycoproteins, which compete with host proteins for processing and induce an increased burden on ER/Golgi trafficking. This leads to a UPR response characterized by ATF6-

dependent *trans*-activation and IRE1α-dependent *XBP1* splicing, in the absence of a concomitant detection of PERK activation [193].

Flavivirus [194], Zika virus [195], hepatitis virus [196] and West Nile Virus [197] can also cause stress and activate the IRE1α-XBP1 arm of the UPR. Likewise, influenza A virus, a negative stranded RNA virus, also activates IRE1 with little activation of PERK and ATF6, leading to inflammation and apoptosis of primary human bronchial epithelial cells [198]. Similar responses can be assigned to coxsackievirus A16 [199], SARS-CoV-1 [200] and SARS-CoV-2 infection [201-203].

Based on these data, the principal aim of this work was to assess the activation of the UPR in SARS-CoV-2 infection. For this purpose, an approach involving several steps was implemented. Initial assays of samples of nasopharyngeal swabs and BAAs were studied to address the presence of *sXBP1*, the cytokine-signature, enzymes involved in energetic metabolism and the expression of monocytic lineage cell markers. After obtaining a profile of the transcriptional landscape, experiments were performed to address the transcriptional pattern of MDDCs stimulated with TLR7 and TLR8 agonists, as endosomal receptors involved in the recognition of ssRNA. These experiments were designed taking into account the notion that the hyperinflammatory response induced by SARS-CoV-2 depends on the presence of high levels of proinflammatory cytokines [184, 204-207]. Thereafter, experiments were performed in several experimental models of SARS-CoV-2 infection *in vivo* to confirm the findings observed in human samples. Finally, *in vitro* infections of human epithelial cells were performed to reveal the interface between the UPR and the viral life cycle, since at different steps of the replication process there are interactions with the ER to ensure the formation of the replication complex, and the efficient folding and transit of different structural proteins [35].

Innate immune mechanisms involved in SARS-CoV-2 infection

The analysis of BAAs led to the identification of myeloid-lineage differentiation footprints considered key players in innate immune response. BAAs from patients with active infection showed a low expression of markers associated with antigen presentation, survival signals during active infection. It was remarkable the low expression of HLA-DRB1 mRNA, the gene encoding the most prevalent β-subunit of HLA-DR. This agrees with the decreased expression of HLA-DR in peripheral blood monocytes of COVID-19 patients, which drives hyperinflammation and defective antigen presentation mediated by IL-6 [208].

The mechanism whereby SARS-CoV-2 activates immune cells is the subject of intensive research. Immune cells do not express ACE2 or TMPRSS2, although they may contain even more viral RNA sequences than epithelial cells [209]. Likewise, monocytes can be induced during SARS-CoV-2 infection to express proinflammatory cytokines by an indirect mechanism initiated by SARS-CoV-2 spike protein binding to platelet CD42b that entails activation of P-selectin and CD40L and drives monocyte signaling through P-selectin glycoprotein ligand-1 and CD40 [210].

This is reminiscent of the integrin-mediated adhesion, transfer of DNA-containing virions to pDCs, which drives the recognition of RNA and DNA through TLR7 and TLR9, respectively, in what is termed interferogenic synapse [211, 212]. Moreover, direct interaction of conventional dendritic cells (cDCs) with SARS-CoV-2 downregulates the expression of genes involved in antigen presentation and upregulates a proinflammatory response, thus mimicking the immune exhaustion and the hyperinflammation observed in patients [213].

The role of pDCs in SARS-CoV-2 infection has been the subject of intensive scrutiny because they are ideal candidates to protect against viral infection. Of the 23

articles that quantified pDCs in peripheral blood during COVID-19, 19 observed a significant reduction in circulating pDCs, and the prevailing notion was that pDC count declines in peripheral blood during severe disease, resulting in a phenomenon dubbed ‘‘the pDC desert’’ based on correlations between cell numbers and disease severity, as well as studies assessing the function of pDCs isolated from COVID-19 patients [214]. Although the mechanisms underlying the induction of the ‘‘pDC desert’’ are unclear, an akin condition has been reported during infection with other RNA viruses, such as HIV and hepatitis virus. Tellingly, a recent study disclosed that pDCs are the main cell type sensing SARS-CoV-2 in the blood via TLR7. This produces IFNα and drives macrophages hyperactive after contacting infected epithelial cells and in response to different stimuli, including the TLR8 agonist ORN8L [33].

Sensing of viral components by immune cells during SARS-CoV-2 infection

The analysis of the activation of the innate immune system of Syrian hamsters infected with SARS-CoV-2 showed the involvement of TLR activation. Specifically, cell surface TLR2 can recognize S protein of SARS-CoV-2 [215] and envelope (E) protein and induce the production of proinflammatory cytokines [68, 70].

A characteristic feature of SARS-CoV-2 is the capacity to shield dsRNA in DMVs to avoid TLR3 sensing [216, 217]. In fact, viral RNA capping mediated by several NSPs activities is a critical step to prevent PRR sensing during the replication cycle of SARS-CoV-2 [218]. Mechanistically, NSP13, NSP14 and NSP16 mediate the addition of a 7- methylguanyalte cap at the 5' end of viral RNA in order to elude RIG-I and MDA5 recognition, thus mimicking host RNA [219, 220].

TLR7 and TLR8 are tandem duplicated genes on the X-chromosome, the function of which shows both commonalities and specificities. TLR8 is not functional in mice and TLR7 expressed in pDCs and monocytes yields type I IFN-driven CS in severe murine influenza model [221]. Bioinformatic studies support the notion that TLR7/8 could detect nucleic acids from invading pathogens, such as SARS-CoV, SARS-CoV-2 and MERS-CoV genomes and induce acute lung injury because of hyperactivation of immune system [222]. In particular, spike peptide (aminoacid sequence 241-300) can form heterodimeric complex with human TLR8 [223]. While TLR7 is present in monocytes, macrophages, and pDCs, TLR8 expression is a hallmark of human MDDCs [162]. A pioneering study on the pathophysiology of SARS-CoV-1 outbreak showed a unique ability of SARS-CoV-1 GU-rich RNA sequences to induce proinflammatory cytokines through TLR7 in mice and TLR8 in human leukocytes [224]. This notion was extended in a recent report by comparing the effect of GU-rich RNAs from SARS-CoV-1, SARS-CoV-2, HIV-1 and ssRNA40 on

inflammasome activation and proinflammatory cytokine production. GU-rich RNA from the SARS-CoV-2 spike protein triggered the greatest inflammatory response in human macrophages via TLR8 as compared to the HIV-derived ssRNA40. Notably, SARS-CoV-2-derived ssRNA activated the inflammasome and yielded IL-1β secretion [225]. Another study compared the effect of SARS-CoV-2 ssRNA sequences in pDCs and MDDCs. While pDCs showed a robust production of IFNα, MDDCs produced five-fold as much TNFα as pDCs, thus suggesting a primary role of pDCs in the antiviral response, versus the involvement of MDDCs in inflammation [226]. This agrees with our BAAs and *in vitro* results showing TLR8 as a central element in the recognition of ssRNA virus and suggests a unique involvement of MDDCs and TLR8 in the induction of *sXBP1* and hyperinflammation. Comparison of ssRNA40 with ssRNA41 effects and the modulation of TLR8 confirms the involvement of TLR8-dependent signaling and sXBP1 in cytokine expression.

Imiquimod induced a limited set of MDDC responses, although it induced *MX1* and *OAS1* mRNA expression at levels like those produced by ssRNA40, while *IFN1B* mRNA was induced to a lower extent. The effect on proinflammatory cytokines and *sXBP1* was negligible and only reached significant values in the presence of palmitate. Of note, combination with IXA4 induced *sXBP1* but did not increase cytokine expression, which suggests sXBP1 exerts it function on cytokine expression in combination with other factors. A recent study showed that while some TLR7 variants exhibit a robust loss-of-function on type I IFNs production, other variants only have a marginal effect, thus suggesting that TLR7 shapes the anti-viral response through additional mechanisms [227]. Unfortunately, our study does not answer open questions regarding the actual role of TLR7 in SARS-CoV-2 defence and immunopathology.

Cytokine storm as a mechanism involved in SARS-CoV-2 severe pneumonia

Our findings showed a higher extent of *sXBP1* in COVID-19 disease than in patients with non-SARS-CoV-2 infection, although the mRNA levels of proinflammatory cytokines were higher in patients with other associated pneumonia. This was not fully unexpected, since viral sepsis depends on genetics and physiological conditions [80, 81] and COVID-19 patients received steroids in a regular schedule. However, stratification of patients showing active infection and *sXBP1* disclosed the association of *sXBP1* with higher levels of cytokine expression.

The association of T-cell deficiencies with systemic hyperinflammation driven by virus-host cell interaction [228] explains why in the evolution of SARS-CoV-2 pneumonia it may be distinguished an initial influenza-like syndrome with fever and unproductive cough that can be followed in some cases by severe respiratory insufficiency and multiorgan failure, which may proceed after viral proliferation has come to an end. Therefore, the delicate balance between antiviral and innate immune programs is a key determinant of clinical evolution and a proper understanding of the pathophysiological mechanism will be essential to develop effective biomarkers and therapeutics. CS has been observed in distinct clinical conditions driving an overactivated immune system, for instance, infections by cytomegalovirus [229], Epstein-Barr virus [230], group A streptococcus [231], H5N5 avian influenza virus [232], and SARS-CoV [166, 167].

In the context of COVID-19 disease, IL-6 was found significantly elevated in the serum of infected patients [233, 234] and was considered a major driver of CS [235]. The first study referred to this fact included a cohort of 20 COVID-19 patients treated with a single administration of tocilizumab, along with lopinavir, methylprednisolone, and oxygen therapy [89]. A second report described the association of tocilizumab treatment with a reduced chance of ICU admission and ventilatory support. However, a retrospective study

in 30 declining patients with severe COVID-19 pneumonia did not report significant improvement in mortality on weighted analysis [236].

Notions emerging from the analysis of human samples

The analysis of the cohort of patients with severe pneumonia showed an overall mortality lower than that observed in bacterial pneumonia. In the last case, steroid administration was occasional. The heterogeneous response among patients suggests a variety of factors dictating clinical outcome, mainly referred to the expression of the SARS-CoV-2 receptor ACE2 [237], the immune status, and the presence of comorbidities. The extent of ER stress and UPR could represent an additional factor.

The study of respiratory secretions has been a useful approach for the identification of pathogens and to give pathogenetic cues [238, 239]. This approach has been applied according to seminal studies, where bronchoscopy and lavage were used to identify immune cell types in the respiratory tract [88, 240]. Our study focussed on patients under mechanical ventilatory support whose samples were obtained during routine care by attending staff [241-243] and is in line with the use of tracheal aspirates to assess the transcriptional profiling of the lower respiratory tract in critically ill COVID-19 patients [244].

Our study has limitations because the collection of BAA samples depended on the time at which endotracheal intubation was carried out. This entails different COVID-19 disease stages before the first evidence of acute hypoxemic respiratory failure. The use of samples with a primary indication for microbiological diagnosis impeded comparison with patients without pneumonia and/or steroid treatment. The presence of covariates associated with genetics, lifestyle, microbioma and comorbidities may explain a large variation of the production of some cytokines that makes statistical comparison difficult.

Repurposing fluvoxamine in SARS-CoV-2 clinical trials

A number of small molecules with known antiviral activity against other human RNA viruses are being evaluated for efficacy in treating SARS-CoV-2 [98]. Testing the ability of available drugs as inhibitors of SARS-CoV-2 proliferation led to the clinical use of remdesivir [182]. With the purpose of testing the effect of immunomodulators in the control of COVID-19 ailment, we tested fluvoxamine as a common SSRI currently used to treat mental disorders [134]. Its beneficial effect on COVID-19 disease could be explained by its capacity to modulate the endocytic trafficking of the spike SARS-CoV-2 protein [245]. This agrees with a report on fluoxetine, another SSRI, which has been found to decrease viral titres [246], as well as cytokine expression [247].

Consistent with the experimental results, early fluvoxamine treatment in individuals with mild COVID-19 illness was associated with a reduction of signs of clinical deterioration [136]. This report gave supported to our hypothesis and suggested that the main mechanism involved in fluvoxamine effect in SARS-CoV-2 clinical evolution could be exerted through the UPR. Based on this, the present study addressed the effect of fluvoxamine in a mouse experimental model of SARS-CoV-2 infection. Results disclosed a pattern of reduction of proinflammatory cytokine induction, while viral titres were not modified. Our study supports the notion that fluvoxamine counters CS, acting as an immunomodulator rather than an antiviral drug. The low ability of fluvoxamine to decrease viral replication privileges the use of antivirals at early stages of the disease, while it may be beneficial at a late phase of severe COVID-19 pneumonia when viral replication has ended and hyperinflammation rules prognosis.

Targeting the UPR in SARS-CoV-2 infection

Our data are consistent with the notion that the Ire1α-Xbp1 arm of the UPR is the most conserved branch and its preferential recruitment as compared the other branches. In view of its activation in human samples, the analysis of different *in vivo* models and *in vitro* experiments with different VOCs were carried out. The use of different models of SARS-CoV-2 infection showed a preferential activation of the UPR in K18-hACE2 mice and Syrian hamsters as compared to Ad-ACE2 infection in C57BL/6 and Balb/c mice. Tellingly, activation of the Ire1α-Xbp1 branch correlated with overproduction of cytokines in acute infection, while *Ddit3*/CHOP mRNA and protein were not influenced by infection in both K18-hACE2 and Syrian hamster.

The association of the IRE1α-XBP1 branch with acute lung injury has been reported during infection with strains of zoonotic viruses showing poorly glycosylated proteins [248]. In addition, UPR teams up with the IFN stimulated gene human myxovirus resistance gene A (MxA) to produce cell death [249]. As regards human disease, sXBP1 activation has been found in monocytes, and together with NFKB1 and RUNX1, has been reported as a key transcription factors driving inflammation in COVID-19 disease [250]. In this connection, previous reports described that during the formation of autophagosomes, certain UPR-related proteins regulate cellular autophagy [251, 252] and help evade type I IFN response [253]. Moreover, SARS-CoV-2 coronavirus ORF-8b protein aggregates robustly induces ER stress, mitochondrial dysfunction, NLRP3 inflammasome, and caspase-independent cell death in macrophages [254]. These data underscore that the activation of the UPR following virus host-cell interaction may influence disease progression.

Several reports underscore the contribution of the UPR to viral replication in coronavirus infected cell lines [44, 45, 141, 255]. In contrast, up-regulation of IRE1α

RNase activity by cannabidiol has been found to block SARS-CoV-2 replication in a cell line derived from lung epithelial cells and in nasal turbinates of infected mice [256], while it partially activates the IRE1α-XBP1 branch in a lung epithelial cell line [257, 258]. Our findings support the implication of the IRE1α-XBP1 branch in viral replication and suggest that targeting the UPR might be effective when the IRE1α-XBP1 branch surpasses its homeostatic function to become a hyperinflammation driver.

The development of more selective drugs targeting the IRE1α-XBP1 is necessary to confirm its role in SARS-CoV-2 pneumonia. In line with this, other airway diseases such as asthma [259, 260], lung fibrosis and emphysema [261, 262] have been found to respond to pharmacological manipulation of the UPR. The scrutiny of the molecular mechanisms underlying the activation of the UPR during SARS-CoV-2 infection can support new therapeutic strategies.

IX. Concluding Remarks

The evolutionary phylogeny of the SARS-CoV-2 virus and its wide geographic spread led to the availability of a dataset from different continents numbering the genome structure of the new variants to obtain constant tracking of the ongoing COVID-19 pandemic. Although these new variants are more transmissible and less pathogenic, most of the scientific community worldwide attempted to manage the COVID-19 pandemic by rebuilding its boundaries in their field of research. The potential decreased effectiveness of vaccines and natural immune protection against these new emerging variants, prompted public health organizations to undertake initiatives to continue research in vaccines, antivirals and immunomodulators for the management of SARS-CoV-2 severe disease. Hence, our approach to understanding the immunopathological clues of SARS-CoV-2 disease has disclosed:

1. SARS-CoV-2 infection induces *sXBP1* in nasopharyngeal swab samples and in BAAs of patients under mechanical ventilation suffering from severe pneumonia.
2. The transcriptomic profile of BAAs samples from patients with severe manifestations of SARS-CoV-2 revealed lower levels of proinflammatory cytokines such as *IL6* and *IL1B* during active-COVID infection compared to non-COVID pneumonia. In contrast, the expression of the anti-inflammatory cytokine IL-10 was higher during COVID infection. Stratification of COVID-19 patients according to the presence and absence of *sXBP1,* showed increased levels of *PTGS2, TNF, IL1B,* and *IL6,* which correlated with the presence of *sXBP1*.
3. Genes encoding proteins involved in glycolysis and mitochondrial function increased during active-COVID infection as compared to both non-COVID and post-COVID infection.

4. The expression of monocyte-macrophage lineage markers related to DCs differentiation, antigen presentation, survival signals and chemokine/migration was reduced during active-COVID-19 infection in BAAs.
5. Stimulation of MDDCs with the TLR8 ligand ssRNA40 induced IRE1α-XBP1 dependent cytokine production.
6. K18-hACE2 mice model and Syrian hamster showed activation of the Ire1α-Xbp1 branch of the UPR but not of the Perk-Atf4-CHOP arm.
7. The SIR1 agonist fluvoxamine decreased cytokine levels in peripheral blood of MA-SARS-CoV-2 infected mice. However, viral titres and immunohistopathology of harvested lungs were not significantly influenced.
8. The overexpression of different VOCs of SARS-CoV-2 S protein induces the splicing of XBP1.
9. IRE1α-XBP1 modulation counteract viral replication of SARS-CoV-2 in human epithelial cells, including infection with different VOCs.

- The activation of IRE1α-XBP1 branch of the UPR in patient samples, MDDCs stimulated via TLR8, *in vivo* models of SARS-CoV-2 infection and human epithelial cells infected with different VOCs indicates that the inhibition of IRE1α RNase activity could be a therapeutic approach for severe COVID-19 disease.

X. REFERENCES

1. Stanley IA, Ribeiro SM, Giménez-Cassina A, Norberg E, Danial NN: **Changing appetites: the adaptive advantages of fuel choice**. *Trends in cell biology* 2014, **24**(2):118-127.
2. Kedia-Mehta N, Finlay DK: **Competition for nutrients and its role in controlling immune responses**. *Nat Commun* 2019, **10**(1):2123.
3. Ohradanova-Repic A, Boes M, Stockinger H: **Role of Metabolism in Regulating Immune Cell Fate Decisions**. *Frontiers in Immunology* 2020, **11**.
4. Caputa G, Castoldi A, Pearce EJ: **Metabolic adaptations of tissue-resident immune cells**. *Nature Immunology* 2019, **20**(7):793-801.
5. Mazumdar C, Driggers EM, Turka LA: **The Untapped Opportunity and Challenge of Immunometabolism: A New Paradigm for Drug Discovery**. *Cell Metabolism* 2019.
6. Márquez S, Fernández JJ, Terán-Cabanillas E, Herrero C, Alonso S, Azogil A, Montero O, Iwawaki T, Cubillos-Ruiz JR, Fernández N *et al*: **Endoplasmic reticulum stress sensor IRE1α enhances IL-23 expression by human dendritic cells**. *Frontiers in immunology* 2017, **8**:639.
7. Grootjans J, Kaser A, Kaufman RJ, Blumberg RS: **The unfolded protein response in immunity and inflammation**. *Nature Reviews Immunology* 2016, **16**(8):469-484.
8. Di Conza G, Ho P-C, Cubillos-Ruiz JR, Huang SC-C: **Control of immune cell function by the unfolded protein response**. *Nature Reviews Immunology* 2023:1-17.
9. Hu B, Huang S, Yin L: **The cytokine storm and COVID-19**. *Journal of medical virology* 2021, **93**(1):250-256.
10. Abdool Karim SS, de Oliveira T: **New SARS-CoV-2 variants—clinical, public health, and vaccine implications**. *New England Journal of Medicine* 2021, **384**(19):1866-1868.
11. Graham BS, Sullivan NJ: **Emerging viral diseases from a vaccinology perspective: preparing for the next pandemic**. *Nature immunology* 2018, **19**(1):20-28.
12. Obermeyer F, Jankowiak M, Barkas N, Schaffner SF, Pyle JD, Yurkovetskiy L, Bosso M, Park DJ, Babadi M, MacInnis BL: **Analysis of 6.4 million SARS-CoV-2 genomes identifies mutations associated with fitness**. *Science* 2022, **376**(6599):1327-1332.
13. Wang D, Zhou B, Keppel TR, Solano M, Baudys J, Goldstein J, Finn M, Fan X, Chapman AP, Bundy JL: **N-glycosylation profiles of the SARS-CoV-2 spike D614G mutant and its ancestral protein characterized by advanced mass spectrometry**. *Scientific reports* 2021, **11**(1):1-10.
14. Amoutzias GD, Nikolaidis M, Tryfonopoulou E, Chlichlia K, Markoulatos P, Oliver SG: **The remarkable evolutionary plasticity of coronaviruses by mutation and recombination: insights for the COVID-19 pandemic and the future evolutionary paths of SARS-CoV-2**. *Viruses* 2022, **14**(1):78.
15. Bouhaddou M, Reuschl A-K, Polacco BJ, Thorne LG, Ummadi MR, Ye C, Ramirez RR, Pelin A, Batra J, Jang GM: **Global landscape of the host response to SARS-CoV-2 variants reveals viral evolutionary trajectories**. *bioRxiv* 2022.
16. Raghu G, Wilson KC: **COVID-19 interstitial pneumonia: monitoring the clinical course in survivors**. *The Lancet Respiratory Medicine* 2020, **8**(9):839-842.

17. Herrera-Esposito D, de Los Campos G: **Age-specific rate of severe and critical SARS-CoV-2 infections estimated with multi-country seroprevalence studies**. *BMC infectious diseases* 2022, **22**(1):1-14.
18. Ng WH, Tipih T, Makoah NA, Vermeulen J-G, Goedhals D, Sempa JB, Burt FJ, Taylor A, Mahalingam S: **Comorbidities in SARS-CoV-2 patients: a systematic review and meta-analysis**. *MBio* 2021, **12**(1):e03647-03620.
19. Wu A, Peng Y, Huang B, Ding X, Wang X, Niu P, Meng J, Zhu Z, Zhang Z, Wang J: **Genome composition and divergence of the novel coronavirus (2019-nCoV) originating in China**. *Cell host microbe* 2020, **27**(3):325-328.
20. Zhang Q, Meng Y, Wang K, Zhang X, Chen W, Sheng J, Qiu Y, Diao H, Li L: **Inflammation and antiviral immune response associated with severe progression of COVID-19**. *Frontiers in immunology* 2021, **12**:631226.
21. Hamming I, Timens W, Bulthuis M, Lely A, Navis Gv, van Goor H, Ireland: **Tissue distribution of ACE2 protein, the functional receptor for SARS coronavirus. A first step in understanding SARS pathogenesis**. *The Journal of Pathology: A Journal of the Pathological Society of Great Britain* 2004, **203**(2):631-637.
22. Zhang Q, Xiang R, Huo S, Zhou Y, Jiang S, Wang Q, Yu F: **Molecular mechanism of interaction between SARS-CoV-2 and host cells and interventional therapy**. *Signal transduction targeted therapy* 2021, **6**(1):1-19.
23. Wang K, Chen W, Zhang Z, Deng Y, Lian J-Q, Du P, Wei D, Zhang Y, Sun X-X, Gong L: **CD147-spike protein is a novel route for SARS-CoV-2 infection to host cells**. *Signal transduction targeted therapy* 2020, **5**(1):1-10.
24. Junqueira C, Crespo Â, Ranjbar S, de Lacerda LB, Lewandrowski M, Ingber J, Parry B, Ravid S, Clark S, Schrimpf MR: **FcγR-mediated SARS-CoV-2 infection of monocytes activates inflammation**. *Nature* 2022:1-9.
25. Amraei R, Yin W, Napoleon MA, Suder EL, Berrigan J, Zhao Q, Olejnik J, Chandler KB, Xia C, Feldman J: **CD209L/L-SIGN and CD209/DC-SIGN act as receptors for SARS-CoV-2**. *ACS Central Science* 2021, **7**(7):1156-1165.
26. Hoffmann M, Kleine-Weber H, Schroeder S, Krüger N, Herrler T, Erichsen S, Schiergens TS, Herrler G, Wu N-H, Nitsche A: **SARS-CoV-2 cell entry depends on ACE2 and TMPRSS2 and is blocked by a clinically proven protease inhibitor**. *cell* 2020, **181**(2):271-280. e278.
27. Hoffmann M, Kleine-Weber H, Pöhlmann S: **A multibasic cleavage site in the spike protein of SARS-CoV-2 is essential for infection of human lung cells**. *Molecular cell* 2020, **78**(4):779-784. e775.
28. Hou YJ, Okuda K, Edwards CE, Martinez DR, Asakura T, Dinnon III KH, Kato T, Lee RE, Yount BL, Mascenik TM: **SARS-CoV-2 reverse genetics reveals a variable infection gradient in the respiratory tract**. *Cell* 2020, **182**(2):429-446. e414.
29. Ehre C: **SARS-CoV-2 infection of airway cells**. *New England Journal of Medicine* 2020, **383**(10):969-969.
30. Upadhya S, Rehman J, Malik AB, Chen S: **Mechanisms of lung injury induced by SARS-CoV-2 infection**. *Physiology* 2022, **37**(2):88-100.
31. Speranza E, Williamson BN, Feldmann F, Sturdevant GL, Pérez-Pérez L, Meade-White K, Smith BJ, Lovaglio J, Martens C, Munster VJJStm: **Single-cell RNA sequencing reveals SARS-CoV-2 infection dynamics in lungs of African green monkeys**. 2021, **13**(578):eabe8146.

32. Gao KM, Derr AG, Guo Z, Nündel K, Marshak-Rothstein A, Finberg RW, Wang JPJJi: **Human nasal wash RNA-Seq reveals distinct cell-specific innate immune responses in influenza versus SARS-CoV-2**. 2021, **6**(22).
33. Laurent P, Yang C, Rendeiro AF, Nilsson-Payant BE, Carrau L, Chandar V, Bram Y, tenOever BR, Elemento O, Ivashkiv LB: **Sensing of SARS-CoV-2 by pDCs and their subsequent production of IFN-I contribute to macrophage-induced cytokine storm during COVID-19**. *Science Immunology* 2022, **7**(75):eadd4906.
34. Grant RA, Morales-Nebreda L, Markov NS, Swaminathan S, Querrey M, Guzman ER, Abbott DA, Donnelly HK, Donayre A, Goldberg IA: **Circuits between infected macrophages and T cells in SARS-CoV-2 pneumonia**. *Nature* 2021, **590**(7847):635-641.
35. V'kovski P, Kratzel A, Steiner S, Stalder H, Thiel V: **Coronavirus biology and replication: implications for SARS-CoV-2**. *Nature Reviews Microbiology* 2021, **19**(3):155-170.
36. Hetz C, Zhang K, Kaufman RJ: **Mechanisms, regulation and functions of the unfolded protein response**. *Nature reviews Molecular cell biology* 2020, **21**(8):421-438.
37. Bettigole SE, Glimcher LH: **Endoplasmic reticulum stress in immunity**. *Annual review of immunology* 2015, **33**:107-138.
38. Chen X, Cubillos-Ruiz JR: **Endoplasmic reticulum stress signals in the tumour and its microenvironment**. *Nature Reviews Cancer* 2021, **21**(2):71-88.
39. Fung TS, Liu DX: **Coronavirus infection, ER stress, apoptosis and innate immunity**. *Frontiers in microbiology* 2014, **5**:296.
40. Snijder EJ, Limpens RW, de Wilde AH, de Jong AW, Zevenhoven-Dobbe JC, Maier HJ, Faas FF, Koster AJ, Bárcena M: **A unifying structural and functional model of the coronavirus replication organelle: Tracking down RNA synthesis**. *PLoS biology* 2020, **18**(6):e3000715.
41. Chan C-P, Siu K-L, Chin K-T, Yuen K-Y, Zheng B, Jin D-Y: **Modulation of the unfolded protein response by the severe acute respiratory syndrome coronavirus spike protein**. *Journal of virology* 2006, **80**(18):9279-9287.
42. Minakshi R, Padhan K, Rani M, Khan N, Ahmad F, Jameel S: **The SARS Coronavirus 3a protein causes endoplasmic reticulum stress and induces ligand-independent downregulation of the type 1 interferon receptor**. *PloS one* 2009, **4**(12):e8342.
43. Sung S-C, Chao C-Y, Jeng K-S, Yang J-Y, Lai MM: **The 8ab protein of SARS-CoV is a luminal ER membrane-associated protein and induces the activation of ATF6**. *Virology* 2009, **387**(2):402-413.
44. Echavarría-Consuegra L, Cook GM, Busnadiego I, Lefèvre C, Keep S, Brown K, Doyle N, Dowgier G, Franaszek K, N I: **Manipulation of the unfolded protein response: A pharmacological strategy against coronavirus infection**. *PLoS pathogens* 2021, **17**(6):e1009644.
45. DeDiego ML, Nieto-Torres JL, Jiménez-Guardeño JM, Regla-Nava JA, Alvarez E, Oliveros JC, Zhao J, Fett C, Perlman S, Enjuanes L: **Severe acute respiratory syndrome coronavirus envelope protein regulates cell stress response and apoptosis**. *PLoS pathogens* 2011, **7**(10):e1002315.
46. Zheng J, Yamada Y, Fung TS, Huang M, Chia R, Liu DX: **Identification of N-linked glycosylation sites in the spike protein and their functional impact on the replication and infectivity of coronavirus infectious bronchitis virus in cell culture**. *Virology* 2018, **513**:65-74.

47. Hetz C, Axten JM, Patterson JB: **Pharmacological targeting of the unfolded protein response for disease intervention**. *Nature chemical biology* 2019, **15**(8):764-775.
48. Marciniak SJ, Yun CY, Oyadomari S, Novoa I, Zhang Y, Jungreis R, Nagata K, Harding HP, Ron D: **CHOP induces death by promoting protein synthesis and oxidation in the stressed endoplasmic reticulum**. *Genes development* 2004, **18**(24):3066-3077.
49. Qi Z, Chen L: **Endoplasmic reticulum stress and autophagy. autophagy: biology and diseases**. In.: Springer; 2019.
50. Carreras-Sureda A, Pihán P, Hetz C: **The unfolded protein response: at the intersection between endoplasmic reticulum function and mitochondrial bioenergetics**. *Frontiers in oncology* 2017, **7**:55.
51. Gardner BM, Walter P: **Unfolded proteins are Ire1-activating ligands that directly induce the unfolded protein response**. *Science* 2011, **333**(6051):1891-1894.
52. Kimata Y, Oikawa D, Shimizu Y, Ishiwata-Kimata Y, Kohno K: **A role for BiP as an adjustor for the endoplasmic reticulum stress-sensing protein Ire1**. *The Journal of cell biology* 2004, **167**(3):445-456.
53. Yoshida H, Matsui T, Yamamoto A, Okada T, Mori K: **XBP1 mRNA is induced by ATF6 and spliced by IRE1 in response to ER stress to produce a highly active transcription factor**. *Cell* 2001, **107**(7):881-891.
54. Ghosh R, Wang L, Wang ES, Perera BGK, Igbaria A, Morita S, Prado K, Thamsen M, Caswell D, Macias H: **Allosteric inhibition of the IRE1α RNase preserves cell viability and function during endoplasmic reticulum stress**. *Cell* 2014, **158**(3):534-548.
55. Chopra S, Giovanelli P, Alvarado-Vazquez PA, Alonso S, Song M, Sandoval TA, Chae C-S, Tan C, Fonseca MM, Gutierrez S: **IRE1α–XBP1 signaling in leukocytes controls prostaglandin biosynthesis and pain**. *Science* 2019, **365**(6450).
56. Martinon F, Chen X, Lee A-H, Glimcher LH: **TLR activation of the transcription factor XBP1 regulates innate immune responses in macrophages**. *Nature immunology* 2010, **11**(5):411-418.
57. Zeng L, Liu Y-P, Sha H, Chen H, Qi L, Smith JAJTJoI: **XBP-1 couples endoplasmic reticulum stress to augmented IFN-β induction via a cis-acting enhancer in macrophages**. 2010, **185**(4):2324-2330.
58. Keestra-Gounder AM, Byndloss MX, Seyffert N, Young BM, Chávez-Arroyo A, Tsai AY, Cevallos SA, Winter MG, Pham OH, Tiffany CRJN: **NOD1 and NOD2 signalling links ER stress with inflammation**. 2016, **532**(7599):394-397.
59. Qiu Q, Zheng Z, Chang L, Zhao YS, Tan C, Dandekar A, Zhang Z, Lin Z, Gui M, Li XJTEj: **Toll-like receptor-mediated IRE1α activation as a therapeutic target for inflammatory arthritis**. 2013, **32**(18):2477-2490.
60. Sule G, Abuaita BH, Steffes PA, Fernandes AT, Estes SK, Dobry C, Pandian D, Gudjonsson JE, Kahlenberg JM, O'Riordan MXJTJoCI: **Endoplasmic reticulum stress sensor IRE1α propels neutrophil hyperactivity in lupus**. 2021, **131**(7).
61. Hansen JD, Vojtech LN, Laing KJ: **Sensing disease and danger: a survey of vertebrate PRRs and their origins**. *Developmental Comparative Immunology* 2011, **35**(9):886-897.
62. Rehwinkel J, Gack MU: **RIG-I-like receptors: their regulation and roles in RNA sensing**. *Nature Reviews Immunology* 2020, **20**(9):537-551.

63. Goubau D, Deddouche S, e Sousa CR: **Cytosolic sensing of viruses**. *Immunity* 2013, **38**(5):855-869.
64. Carty M, Guy C, Bowie AG: **Detection of viral infections by innate immunity**. *Biochemical pharmacology* 2021, **183**:114316.
65. Choudhury A, Mukherjee S: **In silico studies on the comparative characterization of the interactions of SARS-CoV-2 spike glycoprotein with ACE-2 receptor homologs and human TLRs**. *Journal of medical virology* 2020, **92**(10):2105-2113.
66. Aboudounya MM, Heads RJ: **COVID-19 and toll-like receptor 4 (TLR4): SARS-CoV-2 may bind and activate TLR4 to increase ACE2 expression, facilitating entry and causing hyperinflammation**. *Mediators of inflammation* 2021, **2021**.
67. Khan S, Shafiei MS, Longoria C, Schoggins JW, Savani RC, Zaki H: **SARS-CoV-2 spike protein induces inflammation via TLR2-dependent activation of the NF-κB pathway**. *Elife* 2021, **10**:e68563.
68. Planès R, Bert J-B, Tairi S, BenMohamed L, Bahraoui E: **SARS-CoV-2 Envelope (E) Protein Binds and Activates TLR2 Pathway: A Novel Molecular Target for COVID-19 Interventions**. *Viruses* 2022, **14**(5):999.
69. Qian Y, Lei T, Patel PS, Lee CH, Monaghan-Nichols P, Xin H-B, Qiu J, Fu M: **Direct activation of endothelial cells by SARS-CoV-2 nucleocapsid protein is blocked by Simvastatin**. *Journal of Virology* 2021, **95**(23):e01396-01321.
70. Zheng M, Karki R, Williams EP, Yang D, Fitzpatrick E, Vogel P, Jonsson CB, Kanneganti T-D: **TLR2 senses the SARS-CoV-2 envelope protein to produce inflammatory cytokines**. *Nature immunology* 2021, **22**(7):829-838.
71. Kawai T, Akira S: **Toll-like receptors and their crosstalk with other innate receptors in infection and immunity**. *Immunity* 2011, **34**(5):637-650.
72. Van Der Made CI, Simons A, Schuurs-Hoeijmakers J, Van Den Heuvel G, Mantere T, Kersten S, Van Deuren RC, Steehouwer M, Van Reijmersdal SV, Jaeger MJJ: **Presence of genetic variants among young men with severe COVID-19**. 2020, **324**(7):663-673.
73. Channappanavar R, Fehr AR, Zheng J, Wohlford-Lenane C, Abrahante JE, Mack M, Sompallae R, McCray PB, Meyerholz DK, Perlman S: **IFN-I response timing relative to virus replication determines MERS coronavirus infection outcomes**. *The Journal of clinical investigation* 2019, **129**(9):3625-3639.
74. Channappanavar R, Fehr AR, Vijay R, Mack M, Zhao J, Meyerholz DK, Perlman S: **Dysregulated type I interferon and inflammatory monocyte-macrophage responses cause lethal pneumonia in SARS-CoV-infected mice**. *Cell host microbes* 2016, **19**(2):181-193.
75. Ebermeyer T, Cognasse F, Berthelot P, Mismetti P, Garraud O, Hamzeh-Cognasse H: **Platelet innate immune receptors and TLRs: a double-edged sword**. *International Journal of Molecular Sciences* 2021, **22**(15):7894.
76. Dyavar SR, Singh R, Emani R, Pawar GP, Chaudhari VD, Podany AT, Avedissian SN, Fletcher CV, Salunke DB: **Role of toll-like receptor 7/8 pathways in regulation of interferon response and inflammatory mediators during SARS-CoV2 infection and potential therapeutic options**. *Biomedicine Pharmacotherapy* 2021, **141**:111794.
77. Singh L, Bajaj S, Gadewar M, Verma N, Ansari MN, Saeedan AS, Kaithwas G, Singh M: **Modulation of host immune response is an alternative strategy to combat SARS-CoV-2 pathogenesis**. *Frontiers in Immunology* 2021, **12**.

78. Tay MZ, Poh CM, Rénia L, MacAry PA, Ng LF: **The trinity of COVID-19: immunity, inflammation and intervention**. *Nature Reviews Immunology* 2020, **20**(6):363-374.
79. Tisoncik JR, Korth MJ, Simmons CP, Farrar J, Martin TR, Katze MG: **Into the eye of the cytokine storm**. *Microbiology Molecular Biology Reviews* 2012, **76**(1):16-32.
80. Sinha P, Matthay MA, Calfee CS: **Is a "cytokine storm" relevant to COVID-19?** *JAMA internal medicine* 2020, **180**(9):1152-1154.
81. Kox M, Waalders NJ, Kooistra EJ, Gerretsen J, Pickkers P: **Cytokine levels in critically ill patients with COVID-19 and other conditions**. *Jama* 2020, **324**(15):1565-1567.
82. Geginat J, Larghi P, Paroni M, Nizzoli G, Penatti A, Pagani M, Gagliani N, Meroni P, Abrignani S, Flavell RA: **The light and the dark sides of Interleukin-10 in immune-mediated diseases and cancer**. *Cytokine growth factor reviews* 2016, **30**:87-93.
83. Charo IF, Ransohoff RM: **The many roles of chemokines and chemokine receptors in inflammation**. *New England Journal of Medicine* 2006, **354**(6):610-621.
84. Rabaan AA, Al-Ahmed SH, Muhammad J, Khan A, Sule AA, Tirupathi R, Mutair AA, Alhumaid S, Al-Omari A, Dhawan M: **Role of inflammatory cytokines in COVID-19 patients: a review on molecular mechanisms, immune functions, immunopathology and immunomodulatory drugs to counter cytokine storm**. *Vaccines* 2021, **9**(5):436.
85. Wan S, Yi Q, Fan S, Lv J, Zhang X, Guo L, Lang C, Xiao Q, Xiao K, Yi Z: **Relationships among lymphocyte subsets, cytokines, and the pulmonary inflammation index in coronavirus (COVID-19) infected patients**. *British journal of haematology* 2020, **189**(3):428-437.
86. Gupta A, Madhavan MV, Sehgal K, Nair N, Mahajan S, Sehrawat TS, Bikdeli B, Ahluwalia N, Ausiello JC, Wan EY: **Extrapulmonary manifestations of COVID-19**. *Nature medicine* 2020, **26**(7):1017-1032.
87. Diao B, Wang C, Tan Y, Chen X, Liu Y, Ning L, Chen L, Li M, Liu Y, Wang G: **Reduction and functional exhaustion of T cells in patients with coronavirus disease 2019 (COVID-19)**. *Frontiers in immunology* 2020:827.
88. Liao L, Yang Gh: **Clinical significance of cellular immunity function and inflammatory factors assays in alveolar lavage fluid for severe COVID-19 pneumonia**. *Journal of Medical Virology* 2021, **93**(5):2979-2987.
89. Xu X, Han M, Li T, Sun W, Wang D, Fu B, Zhou Y, Zheng X, Yang Y, Li X: **Effective treatment of severe COVID-19 patients with tocilizumab**. *Proceedings of the National Academy of Sciences* 2020, **117**(20):10970-10975.
90. Jordan SC, Zakowski P, Tran HP, Smith EA, Gaultier C, Marks G, Zabner R, Lowenstein H, Oft J, Bluen B: **Compassionate use of tocilizumab for treatment of SARS-CoV-2 pneumonia**. *Clinical Infectious Diseases* 2020, **71**(12):3168-3173.
91. Galván-Román JM, Rodríguez-García SC, Roy-Vallejo E, Marcos-Jiménez A, Sánchez-Alonso S, Fernández-Díaz C, Alcaraz-Serna A, Mateu-Albero T, Rodríguez-Cortes P, Sánchez-Cerrillo I: **IL-6 serum levels predict severity and response to tocilizumab in COVID-19: An observational study**. *Journal of Allergy Clinical Immunology* 2021, **147**(1):72-80. e78.
92. Davila ML, Riviere I, Wang X, Bartido S, Park J, Curran K, Chung SS, Stefanski J, Borquez-Ojeda O, Olszewska M: **Efficacy and toxicity management of 19-28z**

CAR T cell therapy in B cell acute lymphoblastic leukemia. *Science translational medicine* 2014, **6**(224):224ra225-224ra225.
93. Wiersinga WJ, Leopold SJ, Cranendonk DR, van der Poll T: **Host innate immune responses to sepsis**. *Virulence* 2014, **5**(1):36-44.
94. De Jong HK, Van Der Poll T, Wiersinga WJ: **The systemic pro-inflammatory response in sepsis**. *Journal of innate immunity* 2010, **2**(5):422-430.
95. Casadevall A, Pirofski L-aJI, immunity: **Host-pathogen interactions: basic concepts of microbial commensalism, colonization, infection, and disease**. *Infection immunity* 2000, **68**(12):6511-6518.
96. Eljaaly K, Malibary H, Alsulami S, Albanji M, Badawi M, Al-Tawfiq JA: **Description and analysis of cytokine storm in registered COVID-19 clinical trials: a systematic review**. *Pathogens* 2021, **10**(6):692.
97. Roshanravan N, Seif F, Ostadrahimi A, Pouraghaei M, Ghaffari S: **Targeting cytokine storm to manage patients with COVID-19: a mini-review**. *Archives of medical research* 2020, **51**(7):608-612.
98. Sheahan TP, Sims AC, Graham RL, Menachery VD, Gralinski LE, Case JB, Leist SR, Pyrc K, Feng JY, Trantcheva I: **Broad-spectrum antiviral GS-5734 inhibits both epidemic and zoonotic coronaviruses**. *Science translational medicine* 2017, **9**(396).
99. Agostini ML, Andres EL, Sims AC, Graham RL, Sheahan TP, Lu X, Smith EC, Case JB, Feng JY, Jordan R: **Coronavirus susceptibility to the antiviral remdesivir (GS-5734) is mediated by the viral polymerase and the proofreading exoribonuclease**. *MBio* 2018, **9**(2):e00221-00218.
100. De Wit E, Van Doremalen N, Falzarano D, Munster VJ: **SARS and MERS: recent insights into emerging coronaviruses**. *Nature Reviews Microbiology* 2016, **14**(8):523-534.
101. Williamson BN, Feldmann F, Schwarz B, Meade-White K, Porter DP, Schulz J, Van Doremalen N, Leighton I, Yinda CK, Pérez-Pérez L: **Clinical benefit of remdesivir in rhesus macaques infected with SARS-CoV-2**. *Nature* 2020, **585**(7824):273-276.
102. Dai W, Zhang B, Jiang X-M, Su H, Li J, Zhao Y, Xie X, Jin Z, Peng J, Liu F: **Structure-based design of antiviral drug candidates targeting the SARS-CoV-2 main protease**. *Science* 2020, **368**(6497):1331-1335.
103. Yamamoto N, Matsuyama S, Hoshino T, Yamamoto N: **Nelfinavir inhibits replication of severe acute respiratory syndrome coronavirus 2 in vitro**. *BioRxiv* 2020.
104. Rosales R, McGovern BL, Rodriguez ML, Rai DK, Cardin RD, Anderson AS, Sordillo EM, van Bakel H, Simon V, García-Sastre A *et al*: **Nirmatrelvir, Molnupiravir, and Remdesivir maintain potent n vitro activity against the SARS-CoV-2 Omicron variant**. *bioRxiv* 2022:2022.2001.2017.476685.
105. Gangopadhyay KK, Mukherjee JJ, Sinha B, Ghosal S: **The role of corticosteroids in the management of critically ill patients with coronavirus disease 2019 (COVID-19): A meta-analysis**. *MedRxiv* 2020.
106. Sanders JM, Monogue ML, Jodlowski TZ, Cutrell JB: **Pharmacologic treatments for coronavirus disease 2019 (COVID-19): a review**. *Jama* 2020, **323**(18):1824-1836.
107. Wang D, Hu B, Hu C, Zhu F, Liu X, Zhang J, Wang B, Xiang H, Cheng Z, Xiong Y: **Clinical characteristics of 138 hospitalized patients with 2019 novel coronavirus–infected pneumonia in Wuhan, China**. *Jama* 2020, **323**(11):1061-1069.

108. Zha L, Li S, Pan L, Tefsen B, Li Y, French N, Chen L, Yang G, Villanueva EV: **Corticosteroid treatment of patients with coronavirus disease 2019 (COVID-19)**. *Medical Journal of Australia* 2020, **212**(9):416-420.
109. Shang L, Zhao J, Hu Y, Du R, Cao B: **On the use of corticosteroids for 2019-nCoV pneumonia**. *The Lancet* 2020, **395**(10225):683-684.
110. Cao Y, Li L, Feng Z, Wan S, Huang P, Sun X, Wen F, Huang X, Ning G, Wang W: **Comparative genetic analysis of the novel coronavirus (2019-nCoV/SARS-CoV-2) receptor ACE2 in different populations. Cell Discov. 2020; 6: 11**. 2020.
111. Ho M-S, Chen W-J, Chen H-Y, Lin S-F, Wang M-C, Di J, Lu Y-T, Liu C-L, Chang S-C, Chao C-L: **Neutralizing antibody response and SARS severity**. *Emerging infectious diseases* 2005, **11**(11):1730.
112. Ter Meulen J, Bakker AB, Van Den Brink EN, Weverling GJ, Martina BE, Haagmans BL, Kuiken T, De Kruif J, Preiser W, Spaan W: **Human monoclonal antibody as prophylaxis for SARS coronavirus infection in ferrets**. *The Lancet* 2004, **363**(9427):2139-2141.
113. Park T, Lee S-Y, Kim S, Kim MJ, Kim HG, Jun S, Kim SI, Kim BT, Park EC, Park D: **Spike protein binding prediction with neutralizing antibodies of SARS-CoV-2**. *BioRxiv* 2020.
114. Sui J, Li W, Murakami A, Tamin A, Matthews LJ, Wong SK, Moore MJ, Tallarico ASC, Olurinde M, Choe H: **Potent neutralization of severe acute respiratory syndrome (SARS) coronavirus by a human mAb to S1 protein that blocks receptor association**. *Proceedings of the National Academy of Sciences* 2004, **101**(8):2536-2541.
115. Zhu Z, Chakraborti S, He Y, Roberts A, Sheahan T, Xiao X, Hensley LE, Prabakaran P, Rockx B, Sidorov IA: **Potent cross-reactive neutralization of SARS coronavirus isolates by human monoclonal antibodies**. *Proceedings of the National Academy of Sciences* 2007, **104**(29):12123-12128.
116. Walls AC, Park Y-J, Tortorici MA, Wall A, McGuire AT, Veesler D: **Structure, function, and antigenicity of the SARS-CoV-2 spike glycoprotein**. *Cell* 2020, **181**(2):281-292. e286.
117. Wölfel R, Corman VM, Guggemos W, Seilmaier M, Zange S, Müller MA, Niemeyer D, Jones TC, Vollmar P, Rothe C: **Virological assessment of hospitalized patients with COVID-2019**. *Nature* 2020, **581**(7809):465-469.
118. Ahn JY, Sohn Y, Lee SH, Cho Y, Hyun JH, Baek YJ, Jeong SJ, Kim JH, Ku NS, Yeom J-S: **Use of convalescent plasma therapy in two COVID-19 patients with acute respiratory distress syndrome in Korea**. *Journal of Korean medical science* 2020, **35**(14).
119. Duan K, Liu B, Li C, Zhang H, Yu T, Qu J, Zhou M, Chen L, Meng S, Hu Y: **Effectiveness of convalescent plasma therapy in severe COVID-19 patients**. *Proceedings of the National Academy of Sciences* 2020, **117**(17):9490-9496.
120. Pei S, Yuan X, Zhang Z, Yao R, Xie Y, Shen M, Li B, Chen X, Yin M: **Convalescent plasma to treat COVID-19: Chinese strategy and experiences**. *medRxiv* 2020.
121. Shen C, Wang Z, Zhao F, Yang Y, Li J, Yuan J, Wang F, Li D, Yang M, Xing L: **Treatment of 5 critically ill patients with COVID-19 with convalescent plasma**. *Jama* 2020, **323**(16):1582-1589.
122. Zhang B, Liu S, Tan T, Huang W, Dong Y, Chen L, Chen Q, Zhang L, Zhong Q, Zhang X: **Treatment with convalescent plasma for critically ill patients with**

severe acute respiratory syndrome coronavirus 2 infection. *Chest* 2020, **158**(1):e9-e13.
123. Focosi D, Franchini M, Joyner MJ, Casadevall A: **Comparative analysis of antibody responses from COVID-19 convalescents receiving various vaccines reveals consistent high neutralizing activity for SARS-CoV-2 variant of concern omicron.** *MedRxiv* 2021.
124. Abu-Raddad LJ, Chemaitelly H, Butt AA: **Effectiveness of the BNT162b2 Covid-19 Vaccine against the B. 1.1. 7 and B. 1.351 Variants**. *New England Journal of Medicine* 2021, **385**(2):187-189.
125. Wang P, Nair MS, Liu L, Iketani S, Luo Y, Guo Y, Wang M, Yu J, Zhang B, Kwong PD: **Antibody resistance of SARS-CoV-2 variants B. 1.351 and B. 1.1. 7**. *Nature* 2021, **593**(7857):130-135.
126. Kekuda R, Prasad PD, Fei Y-J, Leibach FH, Ganapathy V: **Cloning and functional expression of the human type 1 sigma receptor (hSigmaR1)**. *Biochemical biophysical research communications* 1996, **229**(2):553-558.
127. Mei J, Pasternak GW: **Molecular cloning and pharmacological characterization of the rat sigma1 receptor**. *Biochemical pharmacology* 2001, **62**(3):349-355.
128. Vela JM: **Repurposing sigma-1 receptor ligands for COVID-19 therapy?** *Frontiers in pharmacology* 2020:1716.
129. Abate C, Niso M, Abatematteo FS, Contino M, Colabufo NA, Berardi F: **PB28, the sigma-1 and sigma-2 receptors modulator with potent anti–SARS-CoV-2 activity: a review about its pharmacological properties and structure affinity relationships**. *Frontiers in pharmacology* 2020:1833.
130. Hashimoto K: **Repurposing of CNS drugs to treat COVID-19 infection: targeting the sigma-1 receptor**. *European archives of psychiatry clinical neuroscience* 2021, **271**(2):249-258.
131. Alam S, Abdullah CS, Aishwarya R, Orr AW, Traylor J, Miriyala S, Panchatcharam M, Pattillo CB, Bhuiyan M: **Sigmar1 regulates endoplasmic reticulum stress-induced C/EBP-homologous protein expression in cardiomyocytes**. *Bioscience reports* 2017, **37**(4).
132. Gordon DE, Hiatt J, Bouhaddou M, Rezelj VV, Ulferts S, Braberg H, Jureka AS, Obernier K, Guo JZ, Batra J: **Comparative host-coronavirus protein interaction networks reveal pan-viral disease mechanisms**. *Science* 2020, **370**(6521):eabe9403.
133. Rosen DA, Seki SM, Fernández-Castañeda A, Beiter RM, Eccles JD, Woodfolk JA, Gaultier A: **Modulation of the sigma-1 receptor–IRE1 pathway is beneficial in preclinical models of inflammation and sepsis**. *Science translational medicine* 2019, **11**(478).
134. Omori IM, Watanabe N, Nakagawa A, Cipriani A, Barbui C, McGuire H, Churchill R, Furukawa TA: **Fluvoxamine versus other anti-depressive agents for depression**. *Cochrane Database of Systematic Reviews* 2010(3).
135. Omi T, Tanimukai H, Kanayama D, Sakagami Y, Tagami S, Okochi M, Morihara T, Sato M, Yanagida K, Kitasyoji A: **Fluvoxamine alleviates ER stress via induction of Sigma-1 receptor**. *Cell death disease* 2014, **5**(7):e1332-e1332.
136. Lenze EJ, Mattar C, Zorumski CF, Stevens A, Schweiger J, Nicol GE, Miller JP, Yang L, Yingling M, Avidan MS: **Fluvoxamine vs placebo and clinical deterioration in outpatients with symptomatic COVID-19: a randomized clinical trial**. *Jama* 2020, **324**(22):2292-2300.

137. Seftel D, Boulware DR: **Prospective cohort of fluvoxamine for early treatment of coronavirus disease 19**. In: *Open Forum Infectious Diseases: 2021*. Oxford University Press US: ofab050.
138. Sax P: **Could this be our first effective, inexpensive, widely available outpatient treatment for COVID-19? NEJM J Watch**. In.; 2021.
139. Reis G, dos Santos Moreira-Silva EA, Silva DCM, Thabane L, Milagres AC, Ferreira TS, Dos Santos CVQ, de Souza Campos VH, Nogueira AMR, de Almeida APFG: **Effect of early treatment with fluvoxamine on risk of emergency care and hospitalisation among patients with COVID-19: the TOGETHER randomised, platform clinical trial**. *J The Lancet Global Health* 2022, **10**(1):e42-e51.
140. Rodríguez M, Márquez S, Montero O, Alonso S, Frade JG, Crespo MS, Fernández N: **Pharmacological inhibition of eicosanoids and platelet-activating factor signaling impairs zymosan-induced release of IL-23 by dendritic cells**. *Biochemical pharmacology* 2016, **102**:78-96.
141. Shaban MS, Müller C, Mayr-Buro C, Weiser H, Meier-Soelch J, Albert BV, Weber A, Linne U, Hain T, Babayev I: **Multi-level inhibition of coronavirus replication by chemical ER stress**. *Nature communications* 2021, **12**(1):1-20.
142. Shin W-J, Ha DP, Machida K, Lee AS: **The stress-inducible ER chaperone GRP78/BiP is upregulated during SARS-CoV-2 infection and acts as a pro-viral protein**. *Nature Communications* 2022, **13**(1):1-6.
143. White KM, Rosales R, Yildiz S, Kehrer T, Miorin L, Moreno E, Jangra S, Uccellini MB, Rathnasinghe R, Coughlan L: **Plitidepsin has potent preclinical efficacy against SARS-CoV-2 by targeting the host protein eEF1A**. *Science* 2021, **371**(6532):926-931.
144. Varona JF, Landete P, Lopez-Martin JA, Estrada V, Paredes R, Guisado-Vasco P, de Orueta LF, Torralba M, Fortun J, Vates R: **Preclinical and randomized phase I studies of plitidepsin in adults hospitalized with COVID-19**. *Life Science Alliance* 2022, **5**(4).
145. Organization WH: **Clinical management of severe acute respiratory infection (SARI) when COVID-19 disease is suspected: interim guidance, 13 March 2020**. In.: World Health Organization; 2020.
146. Fan E, Del Sorbo L, Goligher EC, Hodgson CL, Munshi L, Walkey AJ, Adhikari NK, Amato MB, Branson R, Brower RGJAjor *et al*: **An official American Thoracic Society/European Society of Intensive Care Medicine/Society of Critical Care Medicine clinical practice guideline: mechanical ventilation in adult patients with acute respiratory distress syndrome**. 2017, **195**(9):1253-1263.
147. Daniloski Z, Jordan TX, Wessels H-H, Hoagland DA, Kasela S, Legut M, Maniatis S, Mimitou EP, Lu L, Geller E: **Identification of required host factors for SARS-CoV-2 infection in human cells**. *Cell* 2021, **184**(1):92-105. e116.
148. Rihn SJ, Merits A, Bakshi S, Turnbull ML, Wickenhagen A, Alexander AJ, Baillie C, Brennan B, Brown F, Brunker K: **A plasmid DNA-launched SARS-CoV-2 reverse genetics system and coronavirus toolkit for COVID-19 research**. *PLoS biology* 2021, **19**(2):e3001091.
149. Reuschl A-K, Thorne LG, Zuliani-Alvarez L, Bouhaddou M, Obernier K, Hiatt J, Soucheray M, Turner J, Fabius JM, Nguyen GT: **Host-directed therapies against early-lineage SARS-CoV-2 retain efficacy against B. 1.1. 7 variant**. *BioRxiv* 2021.

150. Dejnirattisai W, Huo J, Zhou D, Zahradník J, Supasa P, Liu C, Duyvesteyn HM, Ginn HM, Mentzer AJ, Tuekprakhon A: **SARS-CoV-2 Omicron-B. 1.1. 529 leads to widespread escape from neutralizing antibody responses**. *Cell* 2022, **185**(3):467-484. e415.
151. Nutalai R, Zhou D, Tuekprakhon A, Ginn HM, Supasa P, Liu C, Huo J, Mentzer AJ, Duyvesteyn HM, Dijokaite-Guraliuc A: **Potent cross-reactive antibodies following Omicron breakthrough in vaccinees**. *Cell* 2022.
152. Rathnasinghe R, Jangra S, Ye C, Cupic A, Singh G, Martínez-Romero C, Mulder LC, Kehrer T, Yildiz S, Choi A: **Characterization of SARS-CoV-2 Spike mutations important for infection of mice and escape from human immune sera**. *Nature Communications* 2022, **13**(1):1-14.
153. Wu D, Smyth GK: **Camera: a competitive gene set test accounting for inter-gene correlation**. *Nucleic acids research* 2012, **40**(17):e133-e133.
154. Darnell ME, Subbarao K, Feinstone SM, Taylor DR: **Inactivation of the coronavirus that induces severe acute respiratory syndrome, SARS-CoV**. *Journal of virological methods* 2004, **121**(1):85-91.
155. van Essen MF, Schlagwein N, van Gijlswijk-Janssen DJ, Anholts JD, Eikmans M, Ruben JM, van Kooten C: **Culture medium used during small interfering RNA (siRNA) transfection determines the maturation status of dendritic cells**. *Journal of immunological methods* 2020, **479**:112748.
156. Amanat F, White KM, Miorin L, Strohmeier S, McMahon M, Meade P, Liu WC, Albrecht RA, Simon V, Martinez-Sobrido L: **An in vitro microneutralization assay for SARS-CoV-2 serology and drug screening**. *Current protocols in microbiology* 2020, **58**(1):e108.
157. Rodríguez M, Domingo E, Alonso S, Frade JG, Eiros J, Crespo MS, Fernández N: **The unfolded protein response and the phosphorylations of activating transcription factor 2 in the trans-activation of il23a promoter produced by β-glucans**. *Journal of Biological Chemistry* 2014, **289**(33):22942-22957.
158. Krähling V, Stein DA, Spiegel M, Weber F, Mühlberger E: **Severe acute respiratory syndrome coronavirus triggers apoptosis via protein kinase R but is resistant to its antiviral activity**. *Journal of virology* 2009, **83**(5):2298-2309.
159. Li Y, Renner DM, Comar CE, Whelan JN, Reyes HM, Cardenas-Diaz FL, Truitt R, Tan LH, Dong B, Alysandratos KD: **SARS-CoV-2 induces double-stranded RNA-mediated innate immune responses in respiratory epithelial-derived cells and cardiomyocytes**. *Proceedings of the National Academy of Sciences* 2021, **118**(16):e2022643118.
160. Andolfo I, Russo R, Lasorsa VA, Cantalupo S, Rosato BE, Bonfiglio F, Frisso G, Abete P, Cassese GM, Servillo G: **Common variants at 21q22. 3 locus influence MX1 and TMPRSS2 gene expression and susceptibility to severe COVID-19**. *Iscience* 2021, **24**(4):102322.
161. Hadjadj J, Yatim N, Barnabei L, Corneau A, Boussier J, Smith N, Péré H, Charbit B, Bondet V, Chenevier-Gobeaux C: **Impaired type I interferon activity and inflammatory responses in severe COVID-19 patients**. *Science* 2020, **369**(6504):718-724.
162. Song R, Gao Y, Dozmorov I, Malladi V, Saha I, McDaniel MM, Parameswaran S, Liang C, Arana C, Zhang B: **IRF1 governs the differential interferon-stimulated gene responses in human monocytes and macrophages by regulating chromatin accessibility**. *Cell reports* 2021, **34**(12):108891.
163. O'Carroll SM, O'Neill LA: **Targeting immunometabolism to treat COVID-19**. *Immunotherapy Advances* 2021, **1**(1):ltab013.

164. Vargas P, Barbier L, Sáez PJ, Piel M: **Mechanisms for fast cell migration in complex environments**. *Current Opinion in Cell Biology* 2017, **48**:72-78.
165. Mogilenko DA, Haas JT, L'homme L, Fleury S, Quemener S, Levavasseur M, Becquart C, Wartelle J, Bogomolova A, Pineau L: **Metabolic and innate immune cues merge into a specific inflammatory response via the UPR**. *Cell* 2019, **177**(5):1201-1216. e1219.
166. Karki R, Sharma BR, Tuladhar S, Williams EP, Zalduondo L, Samir P, Zheng M, Sundaram B, Banoth B, Malireddi RS: **Synergism of TNF-α and IFN-γ triggers inflammatory cell death, tissue damage, and mortality in SARS-CoV-2 infection and cytokine shock syndromes**. *Cell* 2021, **184**(1):149-168. e117.
167. Huang KJ, Su IJ, Theron M, Wu YC, Lai SK, Liu CC, Lei HY: **An interferon-γ-related cytokine storm in SARS patients**. *Journal of medical virology* 2005, **75**(2):185-194.
168. Broggi A, Ghosh S, Sposito B, Spreafico R, Balzarini F, Lo Cascio A, Clementi N, De Santis M, Mancini N, Granucci FJS: **Type III interferons disrupt the lung epithelial barrier upon viral recognition**. *Science* 2020, **369**(6504):706-712.
169. Gao DK, Salomonis N, Henderlight M, Woods C, Thakkar K, Grom AA, Thornton S, Jordan MB, Wikenheiser-Brokamp KA, Schulert GS: **IFN-γ is essential for alveolar macrophage–driven pulmonary inflammation in macrophage activation syndrome**. *JCI insight* 2021, **6**(17).
170. Verma AK, Bauer C, Palani S, Metzger DW, Sun KJTJoI: **IFN-γ Drives TNF-α Hyperproduction and Lethal Lung Inflammation during Antibiotic Treatment of Postinfluenza Staphylococcus aureus Pneumonia**. *The Journal of Immunology* 2021, **207**(5):1371-1376.
171. Lee J, Sun C, Zhou Y, Lee J, Gokalp D, Herrema H, Park SW, Davis RJ, Ozcan U: **p38 MAPK–mediated regulation of Xbp1s is crucial for glucose homeostasis**. *Nature medicine* 2011, **17**(10):1251-1260.
172. Liu J, Ibi D, Taniguchi K, Lee J, Herrema H, Akosman B, Mucka P, Hernandez MAS, Uyar MF, Park SW: **Inflammation improves glucose homeostasis through IKKβ-XBP1s interaction**. *Cell* 2016, **167**(4):1052-1066. e1018.
173. Acosta-Alvear D, Zhou Y, Blais A, Tsikitis M, Lents NH, Arias C, Lennon CJ, Kluger Y, Dynlacht BD: **XBP1 controls diverse cell type-and condition-specific transcriptional regulatory networks**. *Molecular cell* 2007, **27**(1):53-66.
174. Rathnasinghe R, Strohmeier S, Amanat F, Gillespie VL, Krammer F, García-Sastre A, Coughlan L, Schotsaert M, Uccellini MB: **Comparison of transgenic and adenovirus hACE2 mouse models for SARS-CoV-2 infection**. *Emerging microbes infections* 2020, **9**(1):2433-2445.
175. Ibrahim IM, Abdelmalek DH, Elshahat ME, Elfiky AA: **COVID-19 spike-host cell receptor GRP78 binding site prediction**. *Journal of Infection* 2020, **80**(5):554-562.
176. Chan JF-W, Zhang AJ, Yuan S, Poon VK-M, Chan CC-S, Lee AC-Y, Chan W-M, Fan Z, Tsoi H-W, Wen L: **Simulation of the clinical and pathological manifestations of coronavirus disease 2019 (COVID-19) in a golden Syrian hamster model: implications for disease pathogenesis and transmissibility**. *Clinical infectious diseases* 2020, **71**(9):2428-2446.
177. Imai M, Iwatsuki-Horimoto K, Hatta M, Loeber S, Halfmann PJ, Nakajima N, Watanabe T, Ujie M, Takahashi K, Ito M: **Syrian hamsters as a small animal model for SARS-CoV-2 infection and countermeasure development**. *Proceedings of the National Academy of Sciences* 2020, **117**(28):16587-16595.

178. Clark JJ, Penrice-Randal R, Sharma P, Kipar A, Dong X, Pennington SH, Marriott AE, Colombo S, Davidson A, Williamson MK: **Sequential infection with influenza A virus followed by severe acute respiratory syndrome coronavirus 2 (SARS-CoV-2) leads to more severe disease and encephalitis in a mouse model of COVID-19**. *bioRxiv* 2021:2020.2010. 2013.334532.
179. Mogensen TH: **IRF and STAT transcription factors-from basic biology to roles in infection, protective immunity, and primary immunodeficiencies**. *Frontiers in immunology* 2019, **9**:3047.
180. Szabo A, Kovacs A, Frecska E, Rajnavolgyi E: **Psychedelic N, N-dimethyltryptamine and 5-methoxy-N, N-dimethyltryptamine modulate innate and adaptive inflammatory responses through the sigma-1 receptor of human monocyte-derived dendritic cells**. *PloS one* 2014, **9**(8):e106533.
181. Ghareghani M, Zibara K, Sadeghi H, Dokoohaki S, Sadeghi H, Aryanpour R, Ghanbari A: **Fluvoxamine stimulates oligodendrogenesis of cultured neural stem cells and attenuates inflammation and demyelination in an animal model of multiple sclerosis**. *Scientific reports* 2017, **7**(1):1-17.
182. Wang M, Cao R, Zhang L, Yang X, Liu J, Xu M, Shi Z, Hu Z, Zhong W, Xiao G: **Remdesivir and chloroquine effectively inhibit the recently emerged novel coronavirus (2019-nCoV) in vitro**. *Cell research* 2020, **30**(3):269-271.
183. Huang C, Wang Y, Li X, Ren L, Zhao J, Hu Y, Zhang L, Fan G, Xu J, Gu X: **Clinical features of patients infected with 2019 novel coronavirus in Wuhan, China**. *The lancet* 2020, **395**(10223):497-506.
184. Yang Y, Shen C, Li J, Yuan J, Wei J, Huang F, Wang F, Li G, Li Y, Xing L: **Plasma IP-10 and MCP-3 levels are highly associated with disease severity and predict the progression of COVID-19**. *Journal of Allergy Clinical Immunology* 2020, **146**(1):119-127. e114.
185. Versteeg GA, Van De Nes PS, Bredenbeek PJ, Spaan WJ: **The coronavirus spike protein induces endoplasmic reticulum stress and upregulation of intracellular chemokine mRNA concentrations**. *Journal of virology* 2007, **81**(20):10981-10990.
186. Plante JA, Liu Y, Liu J, Xia H, Johnson BA, Lokugamage KG, Zhang X, Muruato AE, Zou J, Fontes-Garfias CR: **Spike mutation D614G alters SARS-CoV-2 fitness**. *Nature* 2021, **592**(7852):116-121.
187. Celli J, Tsolis RM: **Bacteria, the endoplasmic reticulum and the unfolded protein response: friends or foes?** *Nature Reviews Microbiology* 2015, **13**(2):71-82.
188. Taguchi Y, Imaoka K, Kataoka M, Uda A, Nakatsu D, Horii-Okazaki S, Kunishige R, Kano F, Murata M: **Yip1A, a novel host factor for the activation of the IRE1 pathway of the unfolded protein response during Brucella infection**. *PLoS pathogens* 2015, **11**(3):e1004747.
189. Zhou D, Zhi F-J, Qi M-Z, Bai F-R, Zhang G, Li J-M, Liu H, Chen H-T, Lin P-F, Tang K-Q: **Brucella induces unfolded protein response and inflammatory response via GntR in alveolar macrophages**. *Oncotarget* 2018, **9**(4):5184.
190. Loose M, Hudel M, Zimmer K-P, Garcia E, Hammerschmidt S, Lucas R, Chakraborty T, Pillich H: **Pneumococcal hydrogen peroxide–induced stress signaling regulates inflammatory genes**. *The Journal of infectious diseases* 2015, **211**(2):306-316.
191. van ‘t Wout EF, van Schadewijk A, van Boxtel R, Dalton LE, Clarke HJ, Tommassen J, Marciniak SJ, Hiemstra PS: **Virulence factors of Pseudomonas**

aeruginosa induce both the unfolded protein and integrated stress responses in airway epithelial cells. *PLoS pathogens* 2015, **11**(6):e1004946.
192. Hempstead AD, Isberg RR: **Inhibition of host cell translation elongation by Legionella pneumophila blocks the host cell unfolded protein response**. *Proceedings of the National Academy of Sciences* 2015, **112**(49):E6790-E6797.
193. Cervantes-Ortiz SL, Zamorano Cuervo N, Grandvaux N: **Respiratory syncytial virus and cellular stress responses: impact on replication and physiopathology**. *Viruses* 2016, **8**(5):124.
194. Yu C-Y, Hsu Y-W, Liao C-L, Lin Y-L: **Flavivirus infection activates the XBP1 pathway of the unfolded protein response to cope with endoplasmic reticulum stress**. *Journal of virology* 2006, **80**(23):11868-11880.
195. Tan Z, Zhang W, Sun J, Fu Z, Ke X, Zheng C, Zhang Y, Li P, Liu Y, Hu Q: **ZIKV infection activates the IRE1-XBP1 and ATF6 pathways of unfolded protein response in neural cells**. *Journal of neuroinflammation* 2018, **15**(1):1-16.
196. Bechill J, Chen Z, Brewer JW, Baker SC: **Mouse hepatitis virus infection activates the Ire1/XBP1 pathway of the unfolded protein response**. In: *The Nidoviruses*. Springer; 2006: 139-144.
197. Medigeshi GR, Lancaster AM, Hirsch AJ, Briese T, Lipkin WI, DeFilippis V, Früh K, Mason PW, Nikolich-Zugich J, Nelson JA: **West Nile virus infection activates the unfolded protein response, leading to CHOP induction and apoptosis**. *Journal of virology* 2007, **81**(20):10849-10860.
198. Hassan IH, Zhang MS, Powers LS, Shao JQ, Baltrusaitis J, Rutkowski DT, Legge K, Monick MM: **Influenza A viral replication is blocked by inhibition of the inositol-requiring enzyme 1 (IRE1) stress pathway**. *Journal of Biological Chemistry* 2012, **287**(7):4679-4689.
199. Zhu G, Zheng Y, Zhang L, Shi Y, Li W, Liu Z, Peng B, Yin J, Liu W, He X: **Coxsackievirus A16 infection triggers apoptosis in RD cells by inducing ER stress**. *Biochemical biophysical research communications* 2013, **441**(4):856-861.
200. Liao Y, Fung TS, Huang M, Fang SG, Zhong Y, Liu DX: **Upregulation of CHOP/GADD153 during coronavirus infectious bronchitis virus infection modulates apoptosis by restricting activation of the extracellular signal-regulated kinase pathway**. *Journal of virology* 2013, **87**(14):8124-8134.
201. Köseler A, Sabirli R, Gören T, Türkçüer I, Kurt Ö: **Endoplasmic reticulum stress markers in SARS-COV-2 infection and pneumonia: case-control study**. *in vivo* 2020, **34**(3 suppl):1645-1650.
202. Palmeira A, Sousa E, Köseler A, Sabirli R, Gören T, Türkçüer İ, Kurt Ö, Pinto MM, Vasconcelos MH: **Preliminary virtual screening studies to identify GRP78 inhibitors which may interfere with SARS-CoV-2 infection**. *Pharmaceuticals* 2020, **13**(6):132.
203. Sabirli R, Koseler A, Goren T, Turkcuer I, Kurt O: **High GRP78 levels in Covid-19 infection: A case-control study**. *Life Sciences* 2021, **265**:118781.
204. Herold T, Jurinovic V, Arnreich C, Lipworth BJ, Hellmuth JC, von Bergwelt-Baildon M, Klein M, Weinberger T: **Elevated levels of IL-6 and CRP predict the need for mechanical ventilation in COVID-19**. *Journal of Allergy Clinical Immunology* 2020, **146**(1):128-136. e124.
205. Mehta P, McAuley DF, Brown M, Sanchez E, Tattersall RS, Manson JJ: **COVID-19: consider cytokine storm syndromes and immunosuppression**. *The lancet* 2020, **395**(10229):1033-1034.

206. Wu C, Chen X, Cai Y, Zhou X, Xu S, Huang H, Zhang L, Zhou X, Du C, Zhang Y: **Risk factors associated with acute respiratory distress syndrome and death in patients with coronavirus disease 2019 pneumonia in Wuhan, China**. *JAMA internal medicine* 2020, **180**(7):934-943.
207. Zhang X, Tan Y, Ling Y, Lu G, Liu F, Yi Z, Jia X, Wu M, Shi B, Xu S: **Viral and host factors related to the clinical outcome of COVID-19**. *Nature* 2020, **583**(7816):437-440.
208. Giamarellos-Bourboulis EJ, Netea MG, Rovina N, Akinosoglou K, Antoniadou A, Antonakos N, Damoraki G, Gkavogianni T, Adami M-E, Katsaounou P: **Complex immune dysregulation in COVID-19 patients with severe respiratory failure**. *Cell host microbes* 2020, **27**(6):992-1000. e1003.
209. Ren X, Wen W, Fan X, Hou W, Su B, Cai P, Li J, Liu Y, Tang F, Zhang F: **COVID-19 immune features revealed by a large-scale single-cell transcriptome atlas**. *Cell* 2021, **184**(7):1895-1913. e1819.
210. Li T, Yang Y, Li Y, Wang Z, Ma F, Luo R, Xu X, Zhou G, Wang J, Niu J: **Platelets mediate inflammatory monocyte activation by SARS-CoV-2 spike protein**. *The Journal of clinical investigation* 2022, **132**(4).
211. Assil S, Coléon S, Dong C, Décembre E, Sherry L, Allatif O, Webster B, Dreux M: **Plasmacytoid dendritic cells and infected cells form an interferogenic synapse required for antiviral responses**. *Cell host microbe* 2019, **25**(5):730-745. e736.
212. Yun TJ, Igarashi S, Zhao H, Perez OA, Pereira MR, Zorn E, Shen Y, Goodrum F, Rahman A, Sims PA: **Human plasmacytoid dendritic cells mount a distinct antiviral response to virus-infected cells**. *Science immunology* 2021, **6**(58):eabc7302.
213. Marongiu L, Protti G, Facchini FA, Valache M, Mingozzi F, Ranzani V, Putignano AR, Salviati L, Bevilacqua V, Curti S: **Maturation signatures of conventional dendritic cell subtypes in COVID-19 suggest direct viral sensing**. *European Journal of Immunology* 2022, **52**(1):109-122.
214. Van der Sluis RM, Holm CK, Jakobsen MR: **Plasmacytoid dendritic cells during COVID-19: Ally or adversary?** *Cell Reports* 2022:111148.
215. Choudhury A, Das NC, Patra R, Mukherjee S: **In silico analyses on the comparative sensing of SARS-CoV-2 mRNA by the intracellular TLRs of humans**. *Journal of Medical Virology* 2021, **93**(4):2476-2486.
216. Klein S, Cortese M, Winter SL, Wachsmuth-Melm M, Neufeldt CJ, Cerikan B, Stanifer ML, Boulant S, Bartenschlager R, Chlanda P: **SARS-CoV-2 structure and replication characterized by in situ cryo-electron tomography**. *Nature communications* 2020, **11**(1):1-10.
217. Hagemeijer MC, Monastyrska I, Griffith J, van der Sluijs P, Voortman J, en Henegouwen PMvB, Vonk AM, Rottier PJ, Reggiori F, De Haan CA: **Membrane rearrangements mediated by coronavirus nonstructural proteins 3 and 4**. *Virology* 2014, **458**:125-135.
218. Romano M, Ruggiero A, Squeglia F, Maga G, Berisio R: **A structural view of SARS-CoV-2 RNA replication machinery: RNA synthesis, proofreading and final capping**. *Cells* 2020, **9**(5):1267.
219. Rosas-Lemus M, Minasov G, Shuvalova L, Inniss NL, Kiryukhina O, Brunzelle J, Satchell KJ: **High-resolution structures of the SARS-CoV-2 2′-O-methyltransferase reveal strategies for structure-based inhibitor design**. *Science signaling* 2020, **13**(651):eabe1202.

220. Viswanathan T, Arya S, Chan S-H, Qi S, Dai N, Misra A, Park J-G, Oladunni F, Kovalskyy D, Hromas RA: **Structural basis of RNA cap modification by SARS-CoV-2**. *Nature communications* 2020, **11**(1):1-7.
221. Rappe JC, Finsterbusch K, Crotta S, Mack M, Priestnall SL, Wack A: **A TLR7 antagonist restricts interferon-dependent and-independent immunopathology in a mouse model of severe influenza**. *Journal of Experimental Medicine* 2021, **218**(11):e20201631.
222. Moreno-Eutimio MA, López-Macías C, Pastelin-Palacios R: **Bioinformatic analysis and identification of single-stranded RNA sequences recognized by TLR7/8 in the SARS-CoV-2, SARS-CoV, and MERS-CoV genomes**. *Microbes infection* 2020, **22**(4-5):226-229.
223. Dasgupta S, Bandyopadhyay M: **Molecular docking of SARS-COV-2 Spike epitope sequences identifies heterodimeric peptide-protein complex formation with human Zo-1, TLR8 and brain specific glial proteins**. *Medical hypotheses* 2021, **157**:110706.
224. Li Y, Chen M, Cao H, Zhu Y, Zheng J, Zhou H, infection: **Extraordinary GU-rich single-strand RNA identified from SARS coronavirus contributes an excessive innate immune response**. *Microbes* 2013, **15**(2):88-95.
225. Campbell GR, To RK, Hanna J, Spector SA: **SARS-CoV-2, SARS-CoV-1, and HIV-1 derived ssRNA sequences activate the NLRP3 inflammasome in human macrophages through a non-classical pathway**. *Iscience* 2021, **24**(4):102295.
226. Salvi V, Nguyen HO, Sozio F, Schioppa T, Gaudenzi C, Laffranchi M, Scapini P, Passari M, Barbazza I, Tiberio L: **SARS-CoV-2–associated ssRNAs activate inflammation and immunity via TLR7/8**. *JCI insight* 2021, **6**(18).
227. Fallerini C, Daga S, Mantovani S, Benetti E, Picchiotti N, Francisci D, Paciosi F, Schiaroli E, Baldassarri M, Fava F: **Association of Toll-like receptor 7 variants with life-threatening COVID-19 disease in males: findings from a nested case-control study**. *elife* 2021, **10**:e67569.
228. Riva G, Nasillo V, Tagliafico E, Trenti T, Comoli P, Luppi M: **COVID-19: more than a cytokine storm**. *Critical care* 2020, **24**(1):1-3.
229. Barry S, Johnson M, Janossy G: **Cytopathology or immunopathology? The puzzle of cytomegalovirus pneumonitis revisited**. *Bone marrow transplantation* 2000, **26**(6):591-597.
230. Imashuku S: **Clinical features and treatment strategies of Epstein–Barr virus-associated hemophagocytic lymphohistiocytosis**. *Critical reviews in oncology/hematology* 2002, **44**(3):259-272.
231. Bisno A, Brito M, Collins C: **Molecular basis of group A streptococcal virulence**. *The Lancet infectious diseases* 2003, **3**(4):191-200.
232. Yuen K, Wong S: **Human infection by avian influenza A H5N1**. *Hong Kong Medical Journal* 2005.
233. Magro G: **SARS-CoV-2 and COVID-19: Is interleukin-6 (IL-6) the 'culprit lesion'of ARDS onset? What is there besides Tocilizumab? SGP130Fc**. *Cytokine: X* 2020, **2**(2):100029.
234. Su H, Lei C-T, Zhang C: **Interleukin-6 signaling pathway and its role in kidney disease: an update**. *Frontiers in immunology* 2017, **8**:405.
235. Moore JB, June CH: **Cytokine release syndrome in severe COVID-19**. *Science* 2020, **368**(6490):473-474.
236. Roumier M, Paule R, Groh M, Vallée A, Ackermann F, Group FC-S: **Interleukin-6 blockade for severe COVID-19**. *medrxiv* 2020.

237. Hirano T, Murakami M: **COVID-19: a new virus, but a familiar receptor and cytokine release syndrome**. *Immunity* 2020, **52**(5):731-733.
238. Baselski VS, Wunderink RG: **Bronchoscopic diagnosis of pneumonia**. *Clinical microbiology reviews* 1994, **7**(4):533-558.
239. Shin YM, Oh Y-M, Kim MN, Shim TS, Lim C-M, Do Lee S, Koh Y, Kim WS, Kim DS, Hong S-B: **Usefulness of quantitative endotracheal aspirate cultures in intensive care unit patients with suspected pneumonia**. *Journal of Korean medical science* 2011, **26**(7):865-869.
240. Zhou Z, Ren L, Zhang L, Zhong J, Xiao Y, Jia Z, Guo L, Yang J, Wang C, Jiang S: **Heightened innate immune responses in the respiratory tract of COVID-19 patients**. *Cell host microbe* 2020, **27**(6):883-890. e882.
241. Szabo PA, Dogra P, Gray JI, Wells SB, Connors TJ, Weisberg SP, Krupska I, Matsumoto R, Poon MM, Idzikowski E: **Longitudinal profiling of respiratory and systemic immune responses reveals myeloid cell-driven lung inflammation in severe COVID-19**. *Immunity* 2021, **54**(4):797-814. e796.
242. Connors TJ, Ravindranath TM, Bickham KL, Gordon CL, Zhang F, Levin B, Baird JS, Farber DL: **Airway CD8+ T cells are associated with lung injury during infant viral respiratory tract infection**. *American journal of respiratory cell molecular biology* 2016, **54**(6):822-830.
243. Connors TJ, Baird JS, Yopes MC, Zens KD, Pethe K, Ravindranath TM, Ho S-h, Farber DL: **Developmental regulation of effector and resident memory T cell generation during pediatric viral respiratory tract infection**. *The Journal of Immunology* 2018, **201**(2):432-439.
244. Sarma A, Christenson SA, Byrne A, Mick E, Pisco AO, DeVoe C, Deiss T, Ghale R, Zha BS, Tsitsiklis A: **Tracheal aspirate RNA sequencing identifies distinct immunological features of COVID-19 ARDS**. *Nature communications* 2021, **12**(1):1-10.
245. Glebov OO: **Low-Dose Fluvoxamine Modulates Endocytic Trafficking of SARS-CoV-2 Spike Protein: A Potential Mechanism for Anti-COVID-19 Protection by Antidepressants**. *frontiers in pharmacology* 2021, **12**.
246. Zimniak M, Kirschner L, Hilpert H, Geiger N, Danov O, Oberwinkler H, Steinke M, Sewald K, Seibel J, Bodem J: **The serotonin reuptake inhibitor Fluoxetine inhibits SARS-CoV-2 in human lung tissue**. *Scientific reports* 2021, **11**(1):1-5.
247. Takenaka Y, Tanaka R, Kitabatake K, Kuramochi K, Aoki S, Tsukimoto M: **Profiling differential effects of five selective serotonin reuptake inhibitors on TLRs-dependent and-independent IL-6 production in immune cells identifies fluoxetine as preferred anti-inflammatory drug candidate**. *Frontiers in Pharmacology* 2022:2258.
248. Hrincius ER, Liedmann S, Finkelstein D, Vogel P, Gansebom S, Samarasinghe AE, You D, Cormier SA, McCullers JA: **Acute lung injury results from innate sensing of viruses by an ER stress pathway**. *Cell reports* 2015, **11**(10):1591-1603.
249. Numajiri Haruki A, Naito T, Nishie T, Saito S, Nagata K, Research C: **Interferon-inducible antiviral protein MxA enhances cell death triggered by endoplasmic reticulum stress**. *Journal of Interferon* 2011, **31**(11):847-856.
250. Liu N, Jiang C, Cai P, Shen Z, Sun W, Xu H, Fang M, Yao X, Zhu L, Gao X: **Single-cell analysis of COVID-19, sepsis, and HIV infection reveals hyperinflammatory and immunosuppressive signatures in monocytes**. *Cell reports* 2021, **37**(1):109793.

251. Fung TS, Liu DX: **The ER stress sensor IRE1 and MAP kinase ERK modulate autophagy induction in cells infected with coronavirus infectious bronchitis virus**. *Virology* 2019, **533**:34-44.
252. Zou D, Xu J, Duan X, Xu X, Li P, Cheng L, Zheng L, Li X, Zhang Y, Wang X: **Porcine epidemic diarrhea virus ORF3 protein causes endoplasmic reticulum stress to facilitate autophagy**. *Veterinary microbiology* 2019, **235**:209-219.
253. Ma Y, Wang C, Xue M, Fu F, Zhang X, Li L, Yin L, Xu W, Feng L, Liu P: **The coronavirus transmissible gastroenteritis virus evades the type I interferon response through IRE1α-mediated manipulation of the microRNA miR-30a-5p/SOCS1/3 axis**. *Journal of virology* 2018, **92**(22):e00728-00718.
254. Shi C-S, Nabar NR, Huang N-N, Kehrl JH: **SARS-Coronavirus Open Reading Frame-8b triggers intracellular stress pathways and activates NLRP3 inflammasomes**. *Cell death discovery* 2019, **5**(1):1-12.
255. Rosa-Fernandes L, Lazari LC, da Silva JM, de Morais Gomes V, Machado RRG, dos Santos AF, Araujo DB, Coutinho JVP, Arini GS, Angeli CB: **SARS-CoV-2 activates ER stress and Unfolded protein response**. *bioRxiv* 2021.
256. Nguyen LC, Yang D, Nicolaescu V, Best TJ, Gula H, Saxena D, Gabbard JD, Chen S-N, Ohtsuki T, Friesen JB: **Cannabidiol inhibits SARS-CoV-2 replication through induction of the host ER stress and innate immune responses**. *Science advances* 2022:eabi6110.
257. Kamel W, Noerenberg M, Cerikan B, Chen H, Järvelin AI, Kammoun M, Lee JY, Shuai N, Garcia-Moreno M, Andrejeva A: **Global analysis of protein-RNA interactions in SARS-CoV-2-infected cells reveals key regulators of infection**. *Molecular cell* 2021, **81**(13):2851-2867. e2857.
258. Nguyen LC, Renner DM, Silva D, Yang D, Parenti NA, Medina KM, Nicolaescu V, Gula H, Drayman N, Valdespino A: **SARS-CoV-2 Diverges from Other Betacoronaviruses in Only Partially Activating the IRE1a/XBP1 Endoplasmic Reticulum Stress Pathway in Human Lung-Derived Cells**. *mBio* 2022.
259. Kim SR, Im Kim D, Kang MR, Lee KS, Park SY, Jeong JS, Lee YC: **Endoplasmic reticulum stress influences bronchial asthma pathogenesis by modulating nuclear factor κB activation**. *Journal of allergy clinical immunology* 2013, **132**(6):1397-1408. e1311.
260. Makhija L, Krishnan V, Rehman R, Chakraborty S, Maity S, Mabalirajan U, Chakraborty K, Ghosh B, Agrawal A: **Chemical chaperones mitigate experimental asthma by attenuating endoplasmic reticulum stress**. *American journal of respiratory cell molecular biology* 2014, **50**(5):923-931.
261. Tanaka Y, Ishitsuka Y, Hayasaka M, Yamada Y, Miyata K, Endo M, Kondo Y, Moriuchi H, Irikura M, Tanaka K-i: **The exacerbating roles of CCAAT/enhancer-binding protein homologous protein (CHOP) in the development of bleomycin-induced pulmonary fibrosis and the preventive effects of tauroursodeoxycholic acid (TUDCA) against pulmonary fibrosis in mice**. *Pharmacological research* 2015, **99**:52-62.
262. Aggarwal S, Ahmad I, Lam A, Carlisle MA, Li C, Wells JM, Raju SV, Athar M, Rowe SM, Dransfield MT: **Heme scavenging reduces pulmonary endoplasmic reticulum stress, fibrosis, and emphysema**. *JCI insight* 2018, **3**(21).

XI. Scientific report

Preprints, Original, Peer Reviewed Articles

1. **Fernandez JJ**, Mancebo C, Garcinuno S, March G, Alvarez Y, Alonso S, et al. IRE1α-XBP1 Activation Elicited by Viral Singled Stranded RNA via TLR8 May Modulate Lung Cytokine Induction in SARS-CoV-2 Pneumonia. 2022:2022.01.26.22269752. *bioRvix*.
2. Deepika Awasthi, Sahil Chopra, Byuri A. Cho, Alexander Emmanuelli, Tito A. Sandoval, Sung-Min Hwang, Chang-Suk Chae, Camilla Salvagno, Chen Tan, Liliana Vasquez-Urbina, **Jose J. Fernandez Rodriguez**, Sara F. Santagostino, Takao Iwawaki, E. Alfonso Romero-Sandoval, Mariano Sanchez Crespo, Diana K. Morales, Iliyan D. Iliev, Tobias M. Hohl, Juan R. Cubillos-Ruiz. Inflammatory ER Stress Responses Dictate the Immunopathogenic Progression of Systemic Candidiasis. 2022.11.17.513879. *bioRxiv*.
3. Cristina Mancebo[1], **José Javier Fernández[1]**, Carmen Herrero-Sánchez, Sara Alonso, Tito A. Sandoval, Juan R. Cubillos-Ruiz, Olimpio Montero, Nieves Fernández, and Mariano Sánchez Crespo. (2021). Fungal Patterns Induce Cytokine Expression through Fluxes of Metabolic Intermediates that Support Glycolysis and Oxidative Phosphorylation. *Journal of Immunology.* SSRN-id3832997.
   (1) Equal contribution
4. Saioa Márquez[1], **José Javier Fernández[1]**, Cristina Mancebo, Carmen Herrero Sánchez, Sara Alonso, Tito A. Sandoval, Macarena Rodríguez Prados, Juan R. Cubillos-Ruiz, Olimpio Montero, Nieves Fernández and Mariano Sánchez Crespo. (2019). Tricarboxylic Acid Cycle Activity and Remodeling of Glycerophosphocholine Lipid Support Cytoline Induction in Response to Fungal Patterns. *Cell Reports*. 27, 1-12. doi: 10.1016/j.celrep.2019.03.033
   (1) Equal contribution
5. Márquez S, **Fernández JJ**, Terán-Cabanillas E, Herrero C, Alonso S, Azogil A, Montero O, Iwawaki T, Cubillos-Ruiz JR, Fernández N and Crespo MS (2017). Endoplasmic Reticulum Stress Sensor IRE1a Enhances IL-23 Expression by Human Dendritic Cells. *Front. Immunol.* 8:639. doi: 10.3389/fimmu.2017.00639.

Conference presentations

International:

11/2022 **Poster presentation.** *IRE1α-XBP1 Pathway of The Unfolded Protein Response Is Potentially Involved In COVID-19 Severity.* **UK- ICN (international coronavirus network) annual general meeting.** Cambridge (UK).

11/2022 **Poster presentation**. *Fungal Patterns Induce Cytokine Expression through Fluxes of Metabolic Intermediates That Support Glycolysis and Oxidative Phosphorylation.* **Cell Symposium: Multifaceted Mitochondria.** Seville (Spain).

03/2022 **Poster presentation. "***SARS-CoV-2 Triggers the IRE1α-XBP1 Branch of the Unfolded Protein Response during the Acute Phase of the Infection"*. **31st annual meeting of the society for virology.** German Society for Virology (GfV 2022).

09/2021 **Poster presentation.** *"Mitochondrial Complex II shapes dendritic Cell Metabolism and Cytokine Expression"*. **6th European Congress of Immunology.** (VirtualECI2021).

05/2021 **Lecturer:** *"Mitochondrial Complex II shapes dendritic Cell Metabolism and Cytokine Expression"*. **4th Conference Novel Concepts of Innate Immunity (NCII).** German Society of Immunology (DGfI).

05/2019 **Lecturer:** *"Tricarboxylic Acid Cycle and the Lands' Cycle of Phospholipid Metabolism underpin Cytokine Induction in Response to Fungal Patterns"*. **Summer school of immunology**. Porto Heli, Greece.

11/2018 **Lecturer:** *"Citrate influences mitochondrial activity and cytokine expression in human monocyte-derived Dendritic Cells (DCs)"*. I International Congress University Rey Juan Carlos (Madrid), Spain.

09/2017 **Poster Presentation:** "*Endoplasmic reticulum stress sensors IRE1a and PERK enhance IL-23 expressions by human dendritic cells"*. **31 annual conference *EMDS*** (European Macrophage and Dendritic cell Society). CNIC Madid, Spain.

National:

10/2022 **Poster presentation: "***IRE1α-XBP1 Activation Elicited by Viral Singled Stranded RNA via TLR8 May Modulate Lung Cytokine Induction in SARS-CoV-2 Pneumonia".* **II jornadas científicas de la PTI+ Salud Global.** (Valencia) Spain.

04/2021 **Poster presentation:** *"Endoplasmic Reticulum Stress and Cytokine Storm in Covid-19"*. II Covid-19 Multidisciplinary National Congress of the Spanish Scientific Societies.

09/2019 **Lecturer** *"Tricarboxylic Acid Cycle and the Lands' Cycle of Phospholipid Metabolism underpin Cytokine Induction in Response to Fungal Patterns".* II meeting of young investigators, INNOVA Salamanca.

05/2018 **Lecturer:** "*Energetic metabolism in innate immunity*", I meeting of young investigators, INNOVA Salamanca.

Support

1. **Predoctoral fellowship** of Junta de Castilla y León/Fondo Social Europeo, call 2019.
2. **Award** "yo investigo, yo soy IBGM".
3. **EFIS Short-Term Fellowship.** *University of Cambridge*, UK.
4. **EMBO Scientific Exchange Grant/Erasmus+/UVa mobility grant.** *Icahn School of Medicine at Mount Sinai.* New York, USA.
5. **Waived grant:** *European Congress of Immunology* (VirtualECI2021)
6. **Travel award** *"7th Summer School of Immunology"* Porto Heli, (Greece).
7. **Fellowship** "*Molecular Biology of the Cell*" in Pasteur institute, Paris (France).

Projects

1. **Project:** Programa Estatal De Generación de Conocimiento y Fortalecimiento Científico y Tecnológico del Sistema de I+D+I Orientada a los Retos de la Sociedad. PID2020-113751RB-I00**.**
2. **Project:** European Commission-NextGenerationEU, through CSIC's Global Health Platform (PTI Salud Global) (project SGL2103016).
3. **Project:** Junta de Castilla y León on SARS-COV-2 fund of Instituto de salud Carlos III. *Endoplasmic reticulum stress/unfolded protein response a critical trigger of cytokine storm in CoVid-19 disease*. Grant CSI035P17.
4. **Participation projet:** *Metabolism/Epigenetics axis and the modulation by diet/microbiote block in the immune response polarization* (1/10/2017-31/12/2019) BOCyL.
5. **Participation projet:** *Metabolism/Epigenomics axis in the immune response polarization* (1/01/2018-31/12/2018) MINECO.SAF2017-83079-R. PI: Mariano Sánchez Crespo and Carmen García Rodríguez, Members UIC043.

XII. Acknowledgements

Este apartado de la tesis es la más importante ya que mucha gente ha estado involucrada en este proyecto y querría dedicarle unas palabras tanto de afecto y cariño por haberme acompañado durante este camino. Sobretodo, empezar por mi padre y hermano, por haberme enseñado con honestidad valores como la tolerancia y el inconformismo, con su actitud me han dado fuerzas para afrontar este reto.

Mi laboratorio en inmunidad innata e inflamación, donde Nieves Fernández y Mariano Sánchez Crespo me han guiado en todo el camino desde que me dieron la oportunidad de formar parte de esta aventura y todas las discusiones científico-constructivas que han surgido en torno a experimentos y resultados obtenidos. Mis compañer@s de poyata, sobretodo, Sara (mis manos) y Yoli (mi supervisión), Cris Mancebo, Carmen Herrero, Saioa, Cristina Martón, Ana Yolanda, Alicia…. y tod@s los estudiantes que han pasado por el laboratorio y han dejado huella para el aprendizaje.

No me olvido de toda la tercera planta del IBGM, cada uno con su tema de investigación pero que dentro de nuestro mundo dentro de las cuatro paredes de nuestro laboratorio, nos ha dado momentos para poder enseñarnos y aprender unos de otros. De los ratos de café en el comedor que empezaban la mañana aunque fuesen días largos o duros, junto con la gente de otras plantas que te dicen buenos días al entrar al centro hasta llegar al laboratorio en la otra punta del centro que a veces ha tenido lugar conversaciones sustanciales ó simplemente ánimo con el día. Además, lo que más añoro y agradezco es el café con tortilla con mis incansables Miguel y Alberto, vosotros me habeis acompañado en todo el camino tanto en momentos de alegría como de frustración pero siempre dejando tiempo para buenos momentos y liberación.

A los colaboradores tanto del hospital Clínico Universitario de Valladolid como del Rio Hortega; sin ellos no hubiera sido posible realizar investigación básica basada en el análisis de mustras de pacientes. Muchas gracias por vuestra dedicación en tiempos de mucha presión laboral que con vuestro pundonor os dejó sacar un poco de tiempo para avanzar en este proyecto.

A mis mentores del Monte Sinai, allí aprendí lo que es la ciencia sin límites y que todo es posible si se mantienen ideas y los recursos acompañan. Especialmente gracias al equipo de antivirales, “papito” Rosales por el aprendizaje en experimentación *in vivo*, y sobretodo a los que me habeis convertido en un jugador competitivo del Jenga. Además, agradecer a

los que me enseñaron que el meta-análisis y la bioinformática también es ciencia, gracias Arturo, Enrique y Rebee por demostrarme que es posible.

A la visita a la Universidad de Cambridge, agradecer a los que formasteis parte de esta aventura enseñandome el inglés menos americano (pensaba que había desaprendido). A los que compartí poyata y me enseñasteis el punto de vista en virología en una mente inmunológica. Thanks Charlotte, Beth and Liliana, to make me stay calm when I was flustering.

Mención especial de nuevo a Sara Alonso y como no a Cristina Gómez y Noelia del Hoyo, por su comprensión y dedicación en no dejarme descarrilar aunque el viento soplara con fuerza. Con mujeres ejemplares como vosotras en la vida, he aprendido que no hay que ponerse límites siempre que se mantenga una sonrisa en la cara. Sois un ejemplo, del que me siento muy orgulloso de haber sido partícipe.

Y no olvidarme de todos los compañeros de Valladolid, tanto del equipo de balonmano, todos los picos de montaña alcanzados y todo el ocio que hemos compartido y que han hecho que genere leves raices en esta ciudad. Gracias por haber soportado mi forma de ser cambiante en cada momento desde que empecé la tesis hasta querer ser doctor. Gracias a vosotros me he convertido en quien soy a día de hoy y por haber puesto vuestro granito en intentar convertirme en buena persona y haberme ayudado en la redacción de este manuscrito.